Postelongation Strategy for the Introduction of Guanidinium Units in the Main Chain of Helical Oligourea Foldamers

Supporting Information

Karolina Pulka-Ziach,[†,‡] Stéphanie Antunes,[†,‖] Camille Perdriau,[†] Brice Kauffmann,[§] Morgane Pasco,[†] Céline Douat,[†] and Gilles Guichard*[,†]

Table of contents

1. Synthesis of oligomer intermediates.....S2

2. NMR characterizations and RP-HPLC chromatograms of hybrid oligo(thio)ureas.....S3

3. X-ray diffraction studies S17

4. RP-HPLC chromatograms, ES-MS analyses and NMR characterizations of the guanidinylated products synthesized in solution..... S20

5. NMR characterizations, RP-HPLC chromatograms, ESI-MS analyses and CD spectra of oligomers 20 and 22..... S54

6. Study of backbone NH H/D exchange rates S58

1. Synthesis of oligomer intermediates

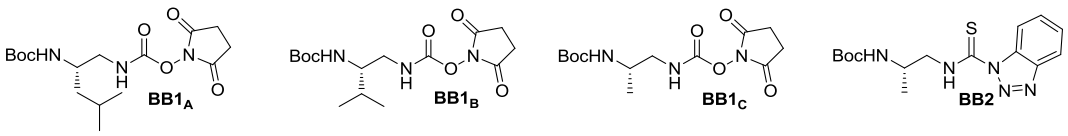

Figure S1. Different activated ethylene diamine building blocks **BB1$_{A-C}$** and **BB2** used to perform the hybrid oligo(thio)urea synthesis in solution.

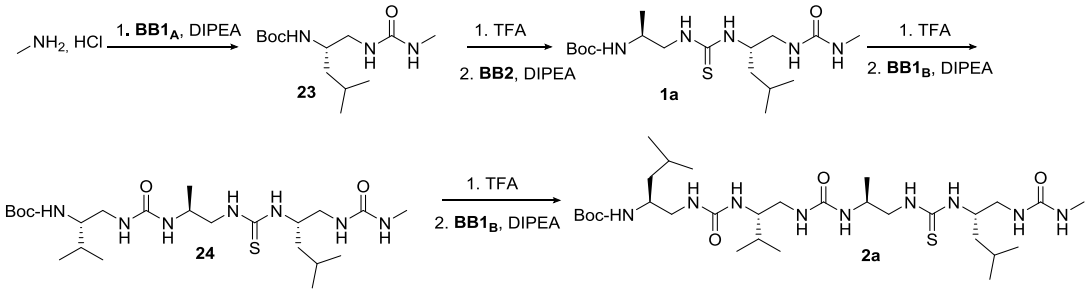

Scheme S1. Convergent synthesis of hybrid dimer **1a** and related tetramer **2a** with corresponding intermediates **23** and **24**.

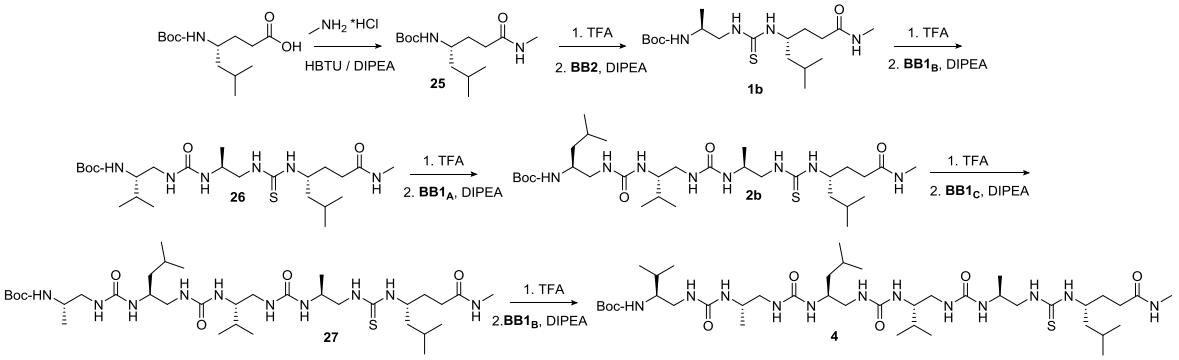

Scheme S2. Convergent syntheses of dimer **1b,** tetramer **2b** and hexamer **4** from intermediates **25-27.**

2. *NMR characterizations and RP-HPLC chromatograms of hybrid oligo(thio)ureas*

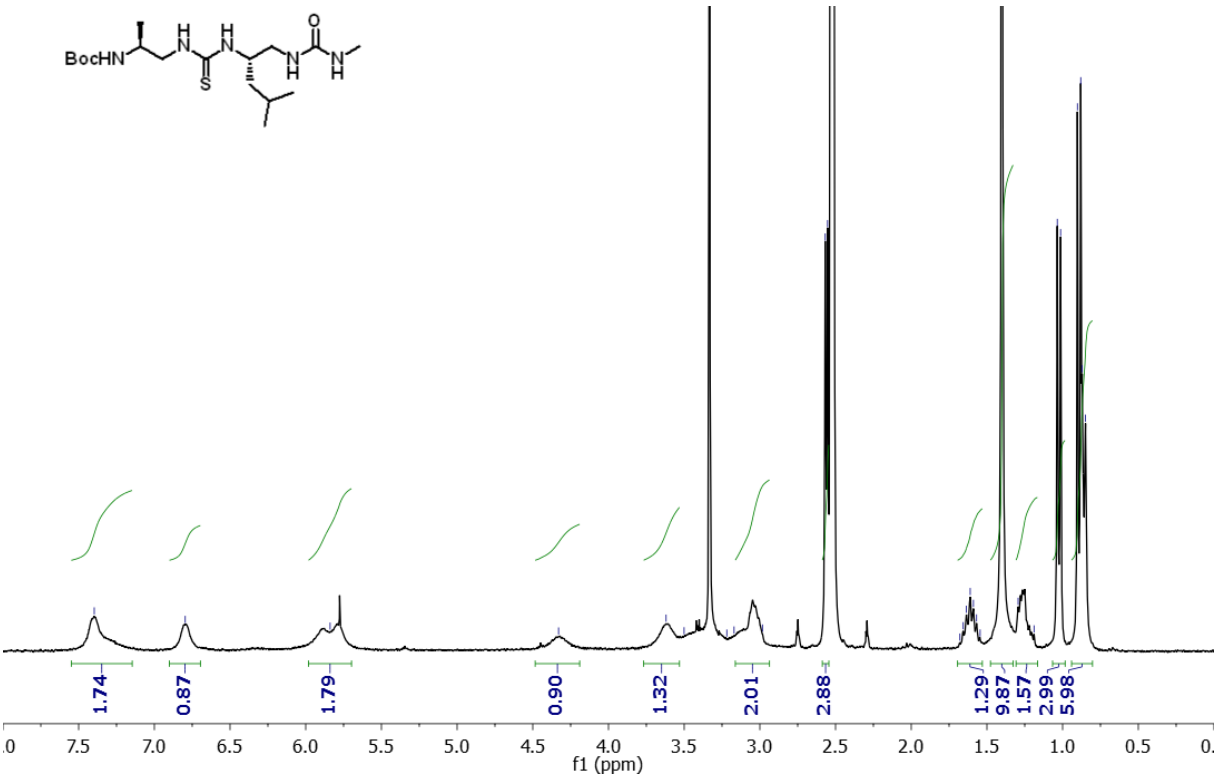

Figure S2. ^{1}H-NMR spectrum of **1a** in DMSO-d_6 (300 MHz)

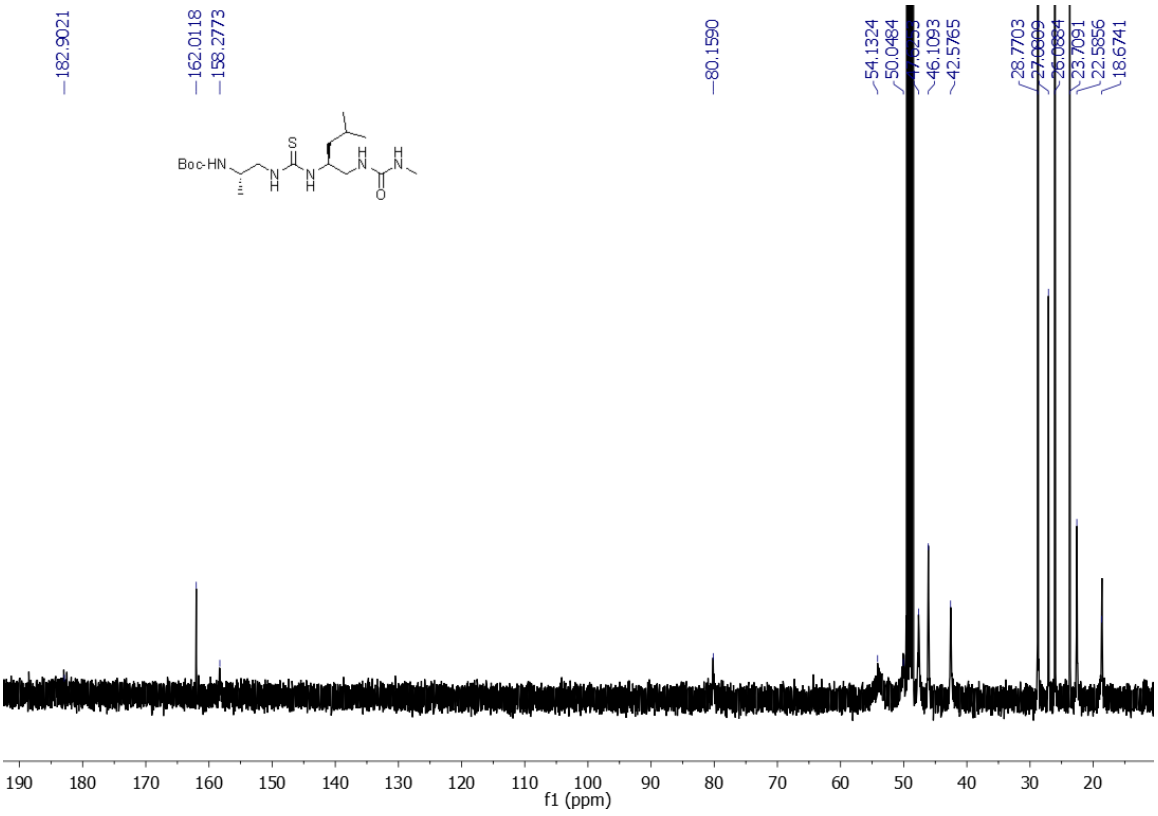

Figure S3. ^{13}C-NMR spectrum of **1a** in CD_3OD (125 MHz)

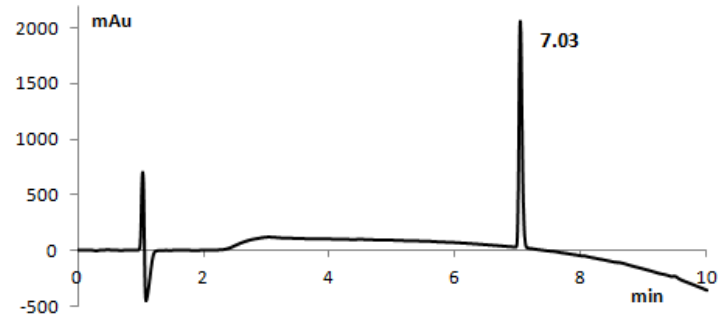

Figure S4. RP-HPLC chromatogram of **1a** (λ = 200nm, 10−100% B in 10 min)

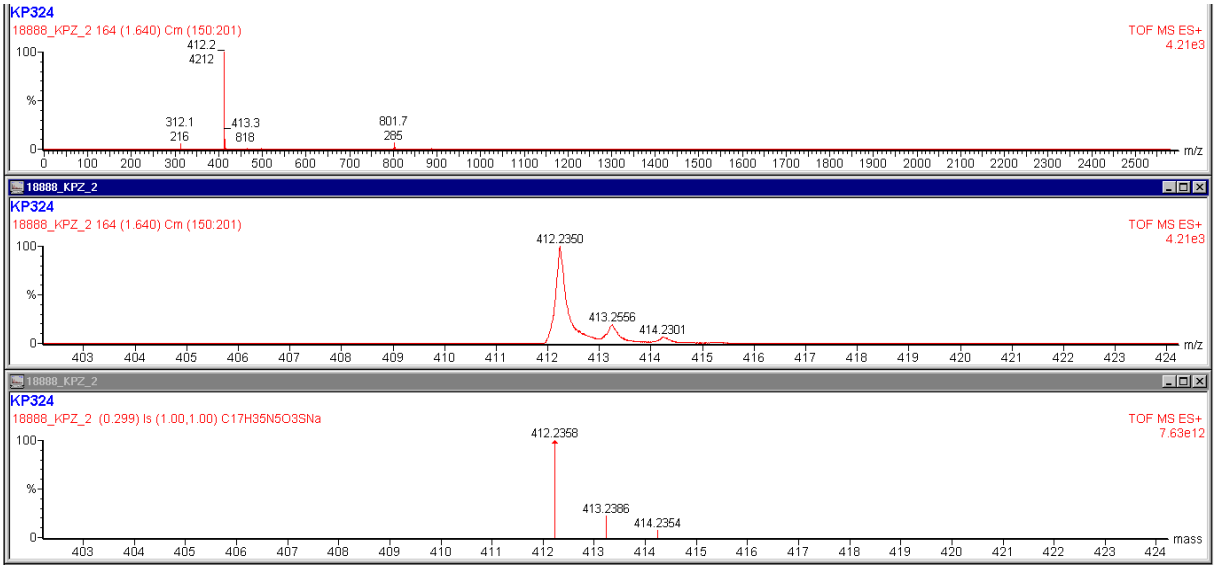

Figure S5. HRMS (ESI-TOF) spectra of compound **1a**

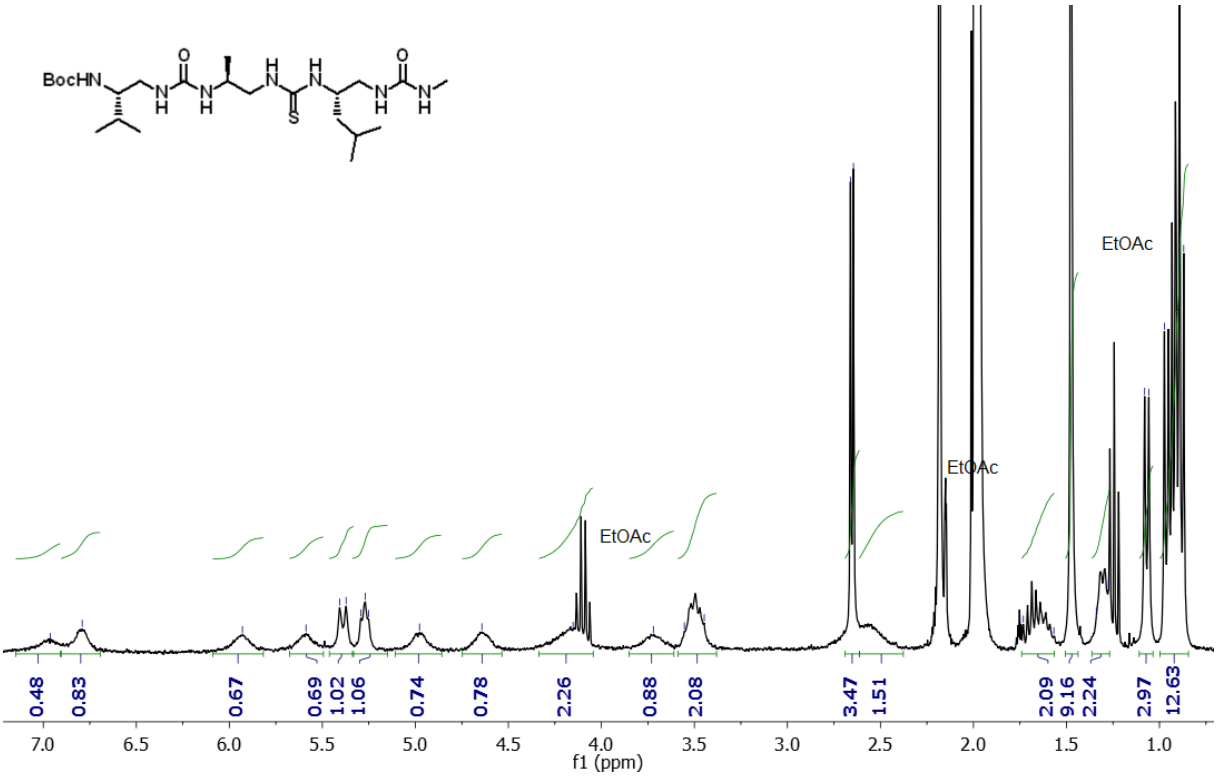

Figure S6. ^{1}H-NMR spectrum of intermediate **24** in CD_3CN (300 MHz)

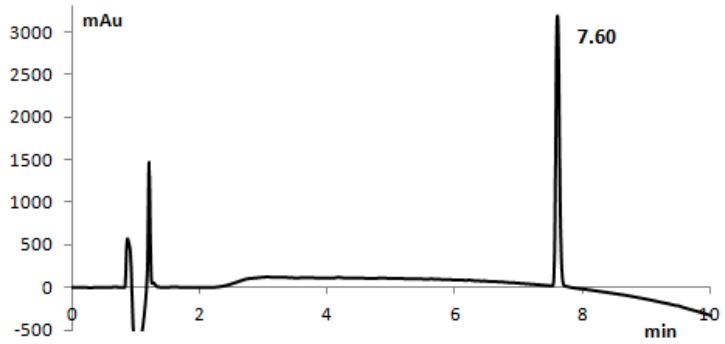

Figure S7. RP-HPLC chromatogram of intermediate **24** (λ = 200nm, 10−100% B in 10 min)

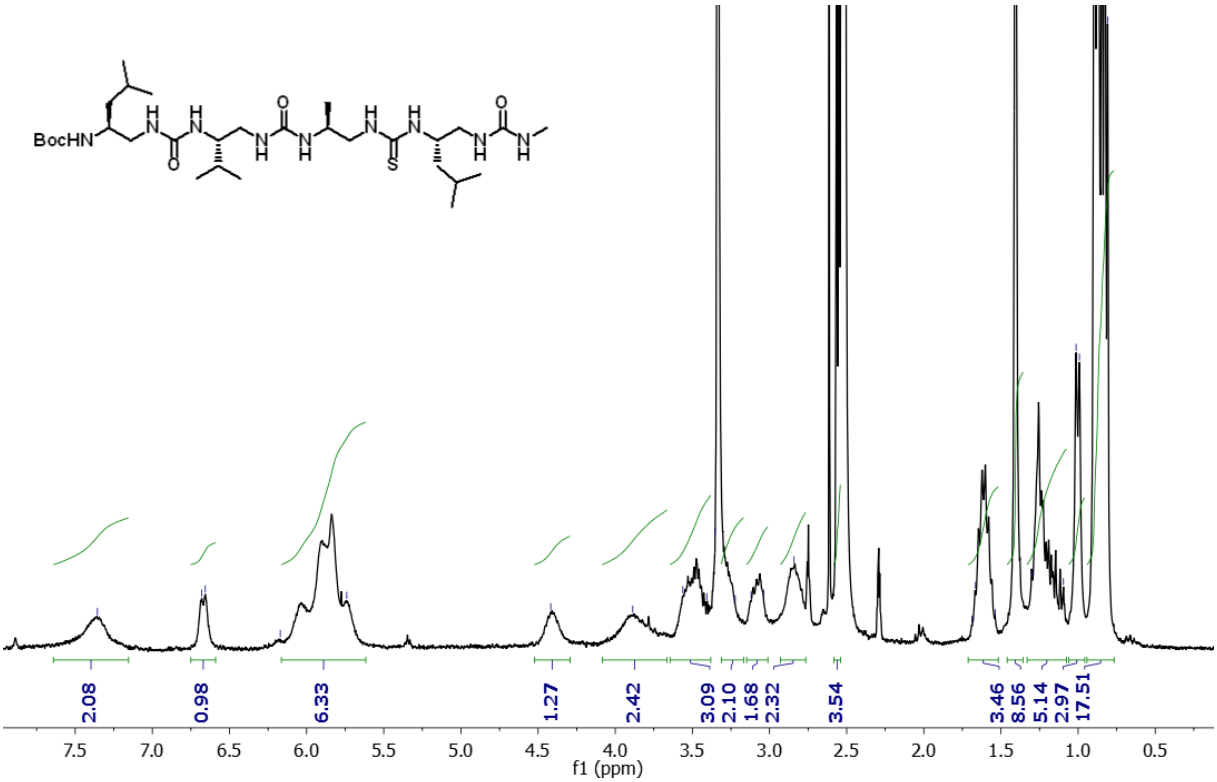

Figure S8. ^{1}H-NMR spectrum of **2a** in DMSO-d_6 (300 MHz)

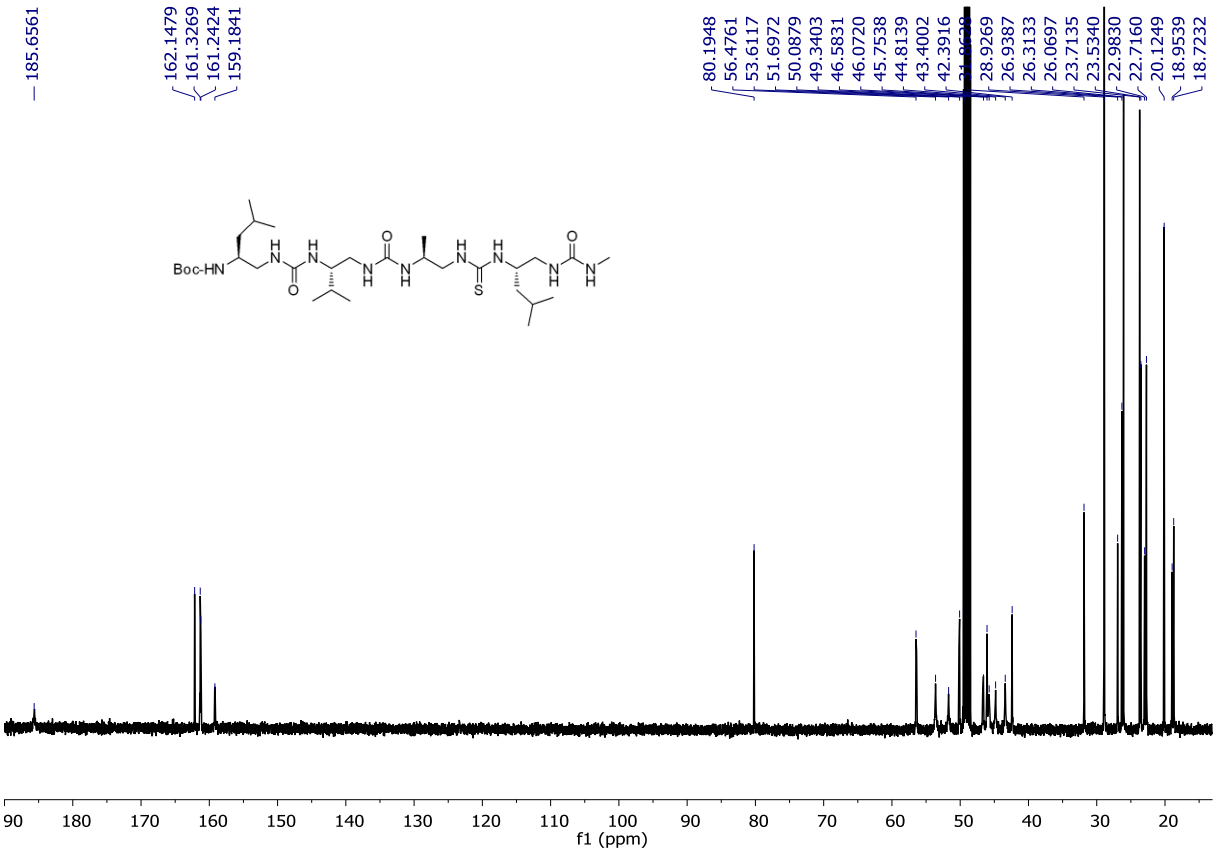

Figure S9. ^{13}C-NMR spectrum of **2a** in CD_3OD (125 MHz)

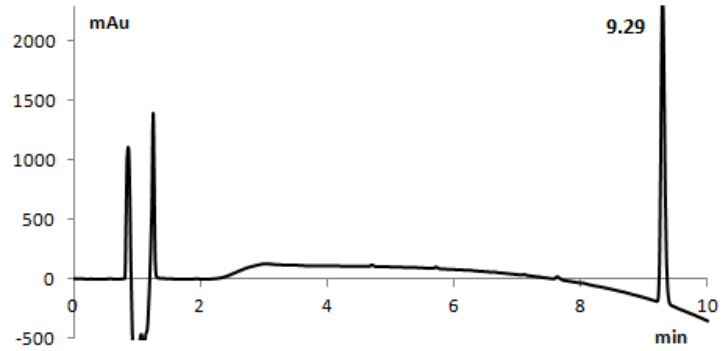

Figure S10. RP-HPLC chromatogram of tetramer **2a** (λ = 200nm, 10−100% B in 10 min)

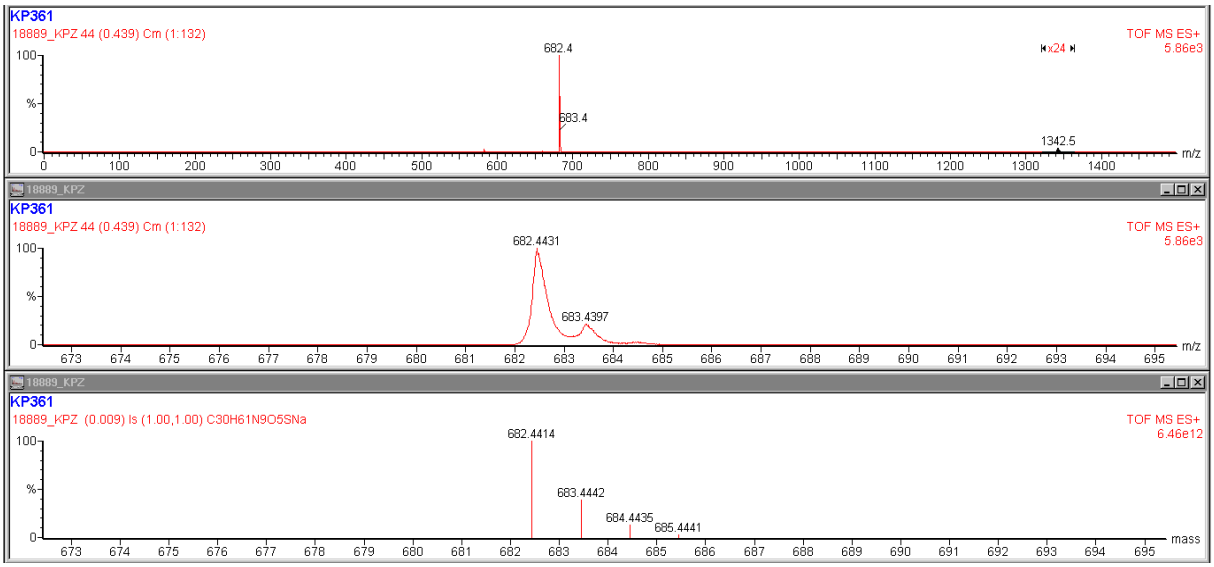

Figure S11. HRMS (ESI-TOF) spectra of compound **2a**

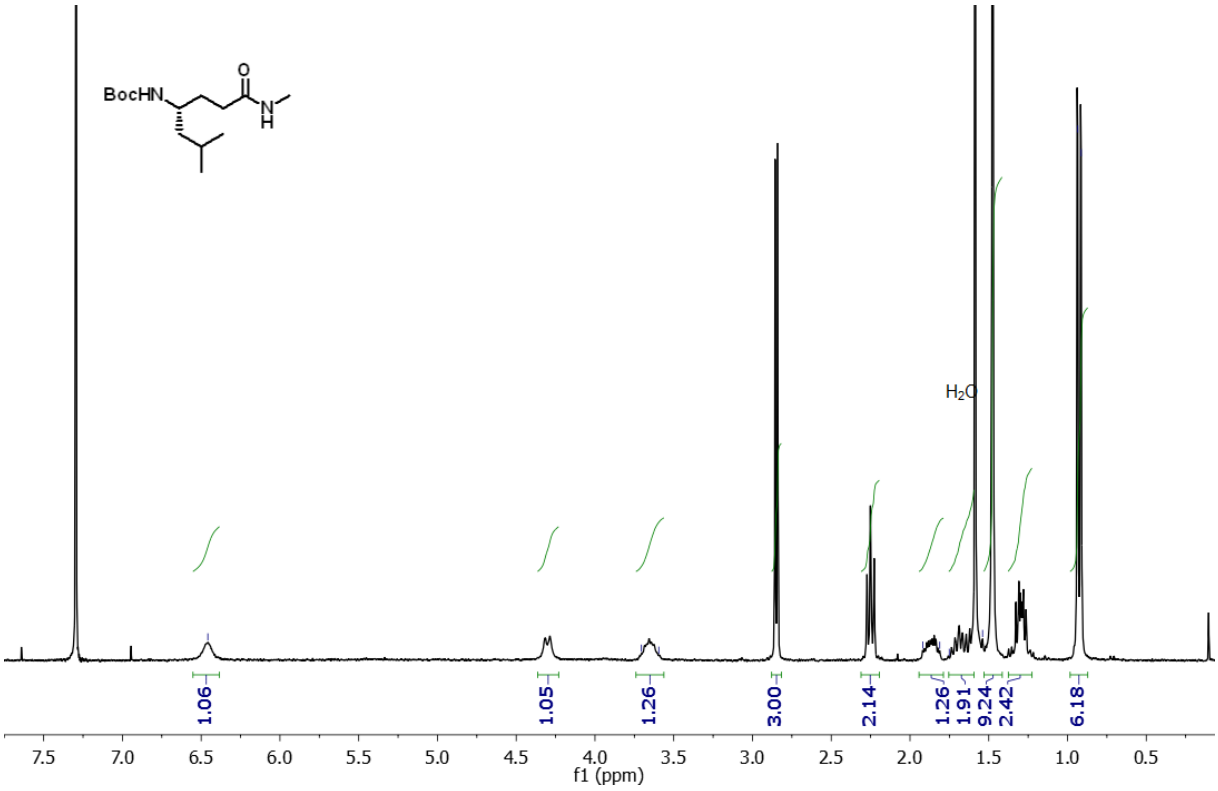

Figure S12. ^{1}H-NMR spectrum of intermediate **25** in $CDCl_3$ (300 MHz)

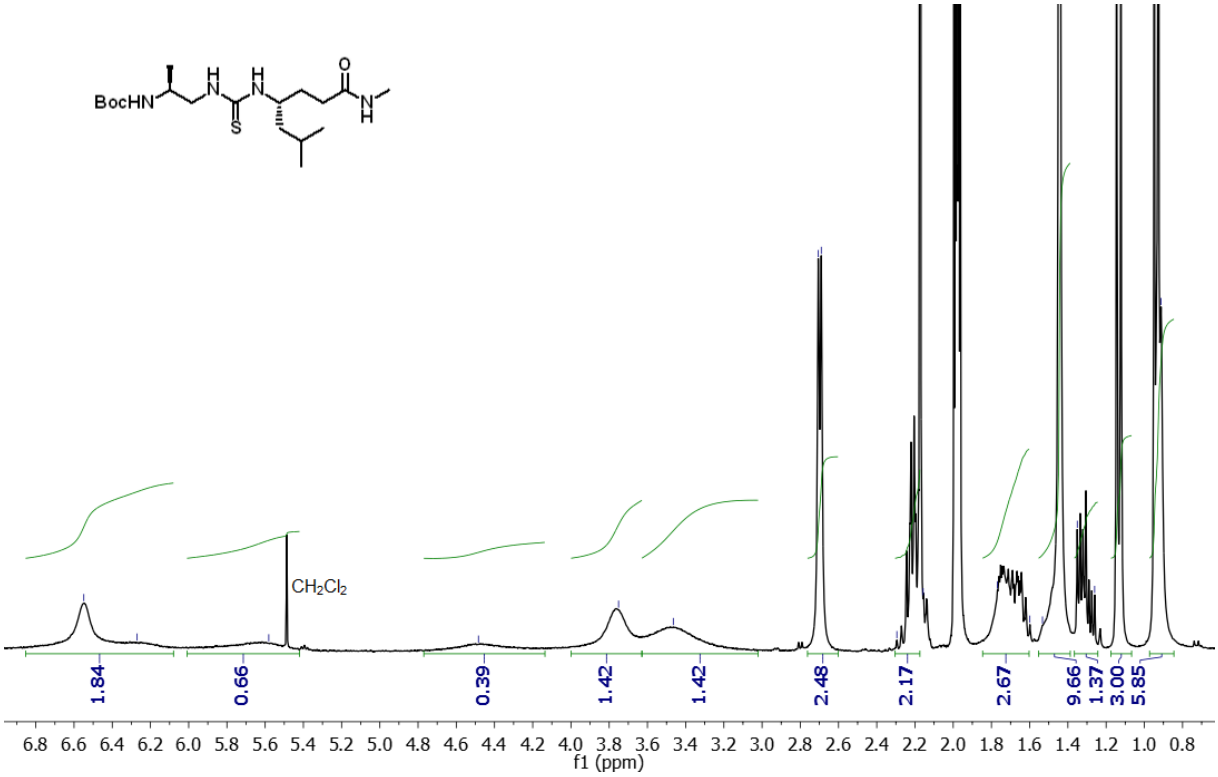

Figure S13. ^{1}H-NMR spectrum of **1b** in CD_3CN (300 MHz)

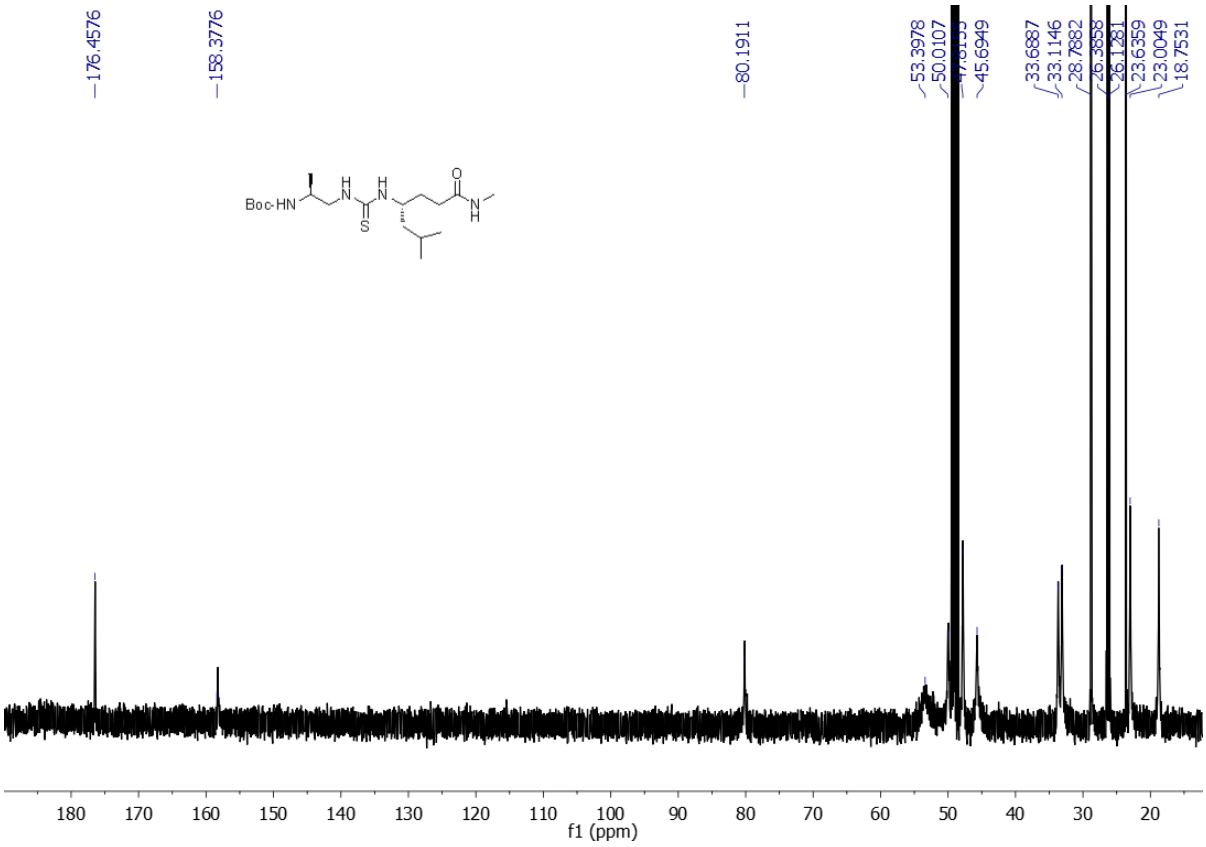

Figure S14. ^{1}H-NMR spectrum of **1b** (125MHz, CD3OD)

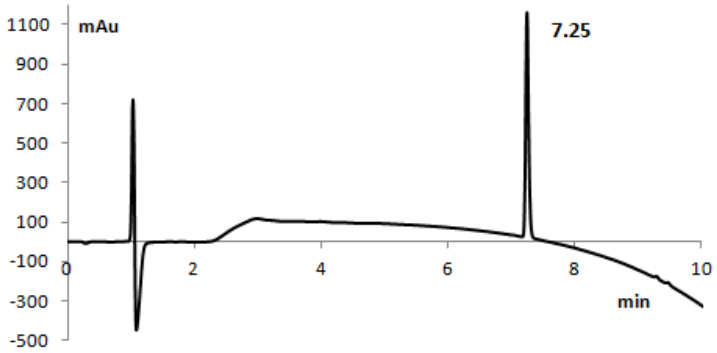

Figure S15. RP-HPLC chromatogram of **1b** (λ = 200nm, 10−100% B in 10 min)

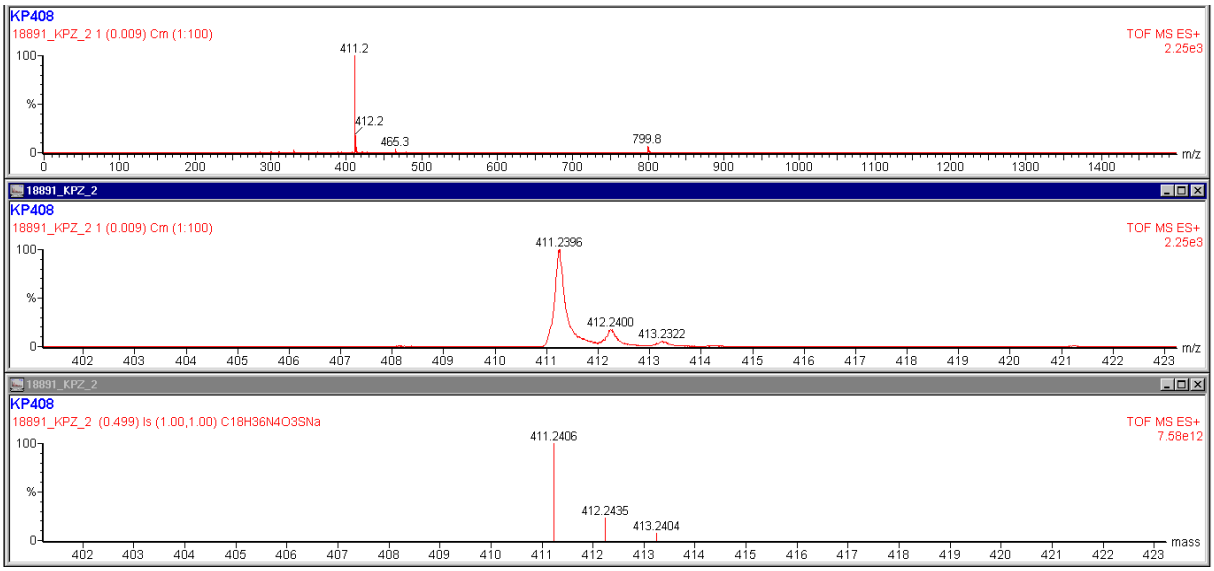

Figure S16. HRMS (ESI-TOF) spectra of compound **1b**

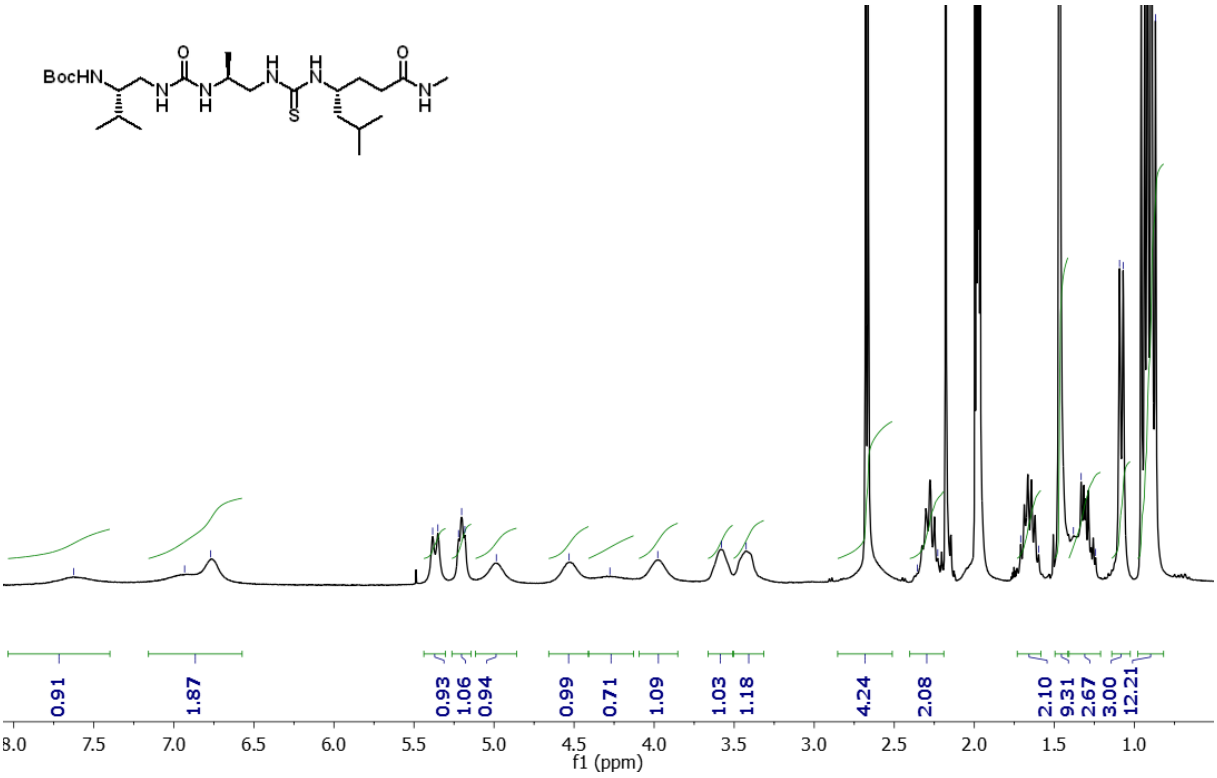

Figure S17. ^{1}H-NMR spectrum of intermediate **26** in CD_3CN (300 MHz)

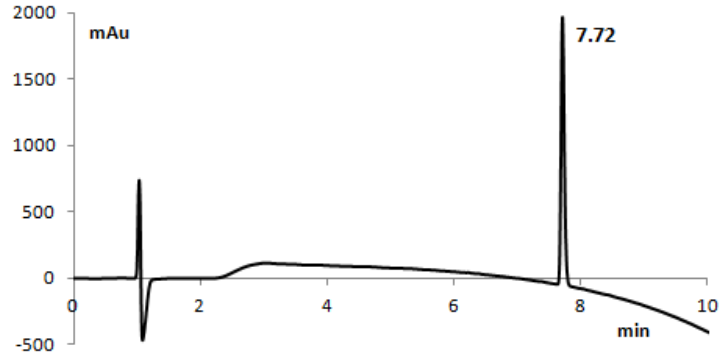

Figure S18. RP-HPLC chromatogram of trimer intermediate **26** (λ = 200nm, 10−100% B in 10 min)

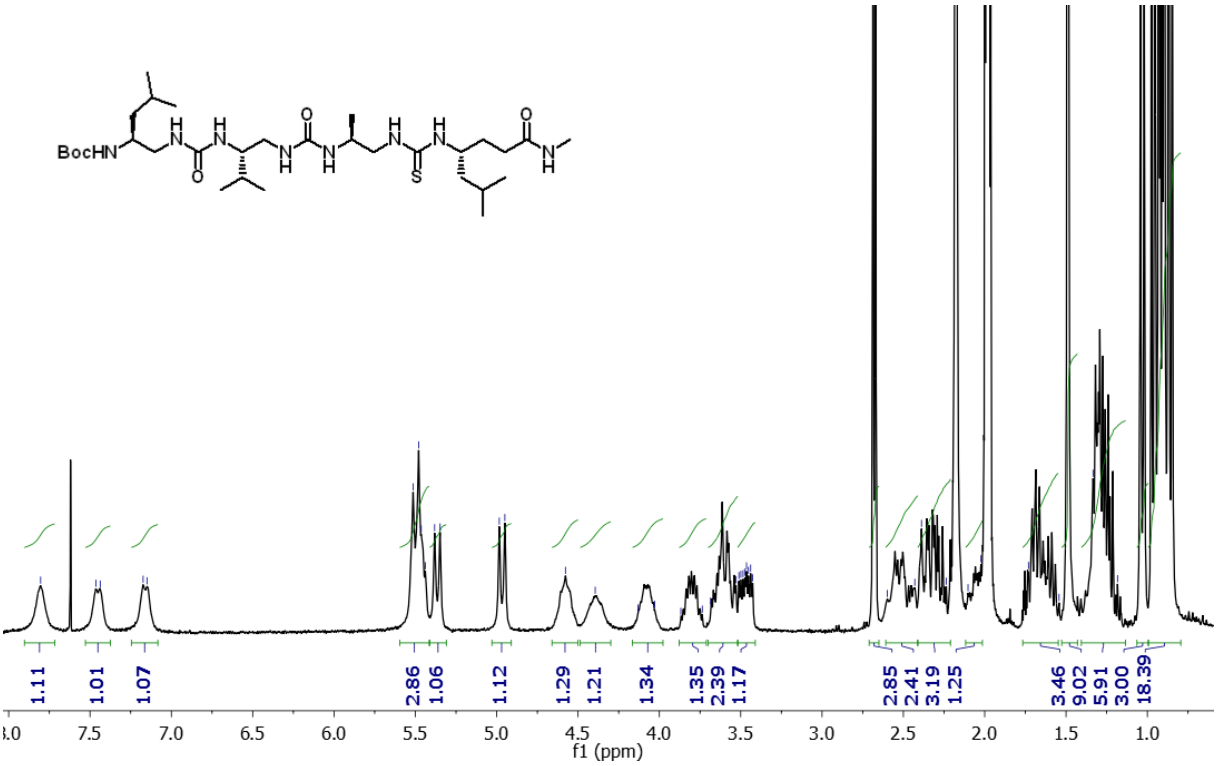

Figure S19. ^{1}H-NMR spectrum of **2b** in CD_3CN (300 MHz)

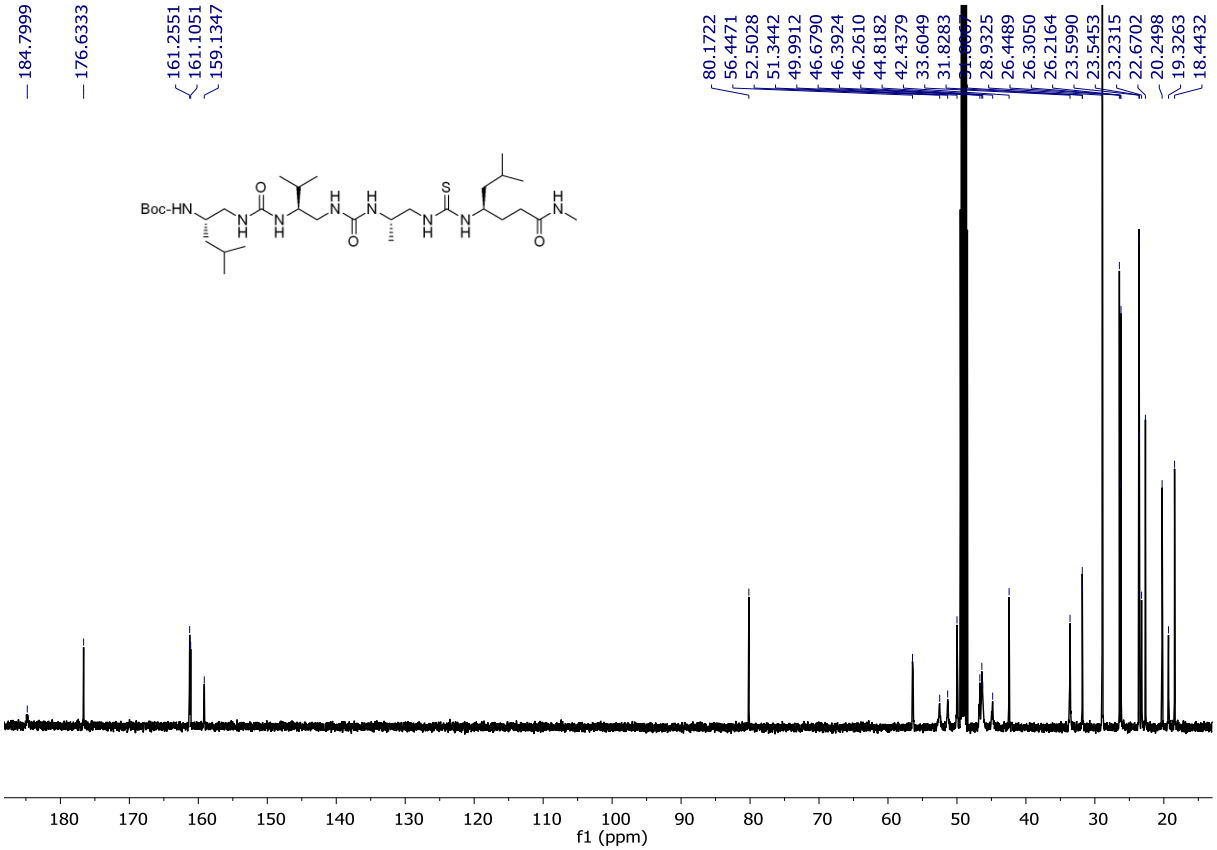

Figure S20. ^{13}C-NMR spectrum of **2b** in CD_3OD (125 MHz)

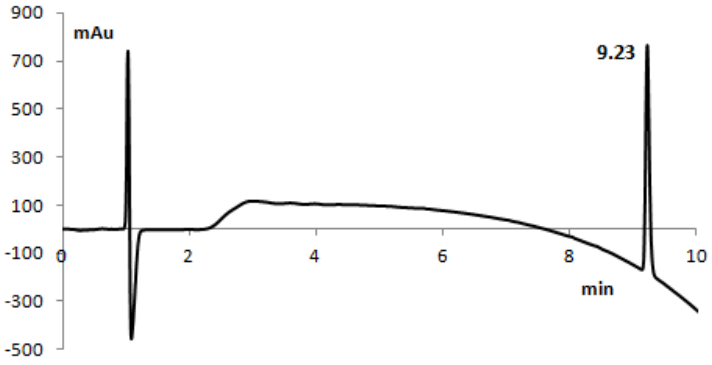

Figure S21. RP-HPLC chromatogram of **2b** (λ = 200nm, 10−100% B in 10 min)

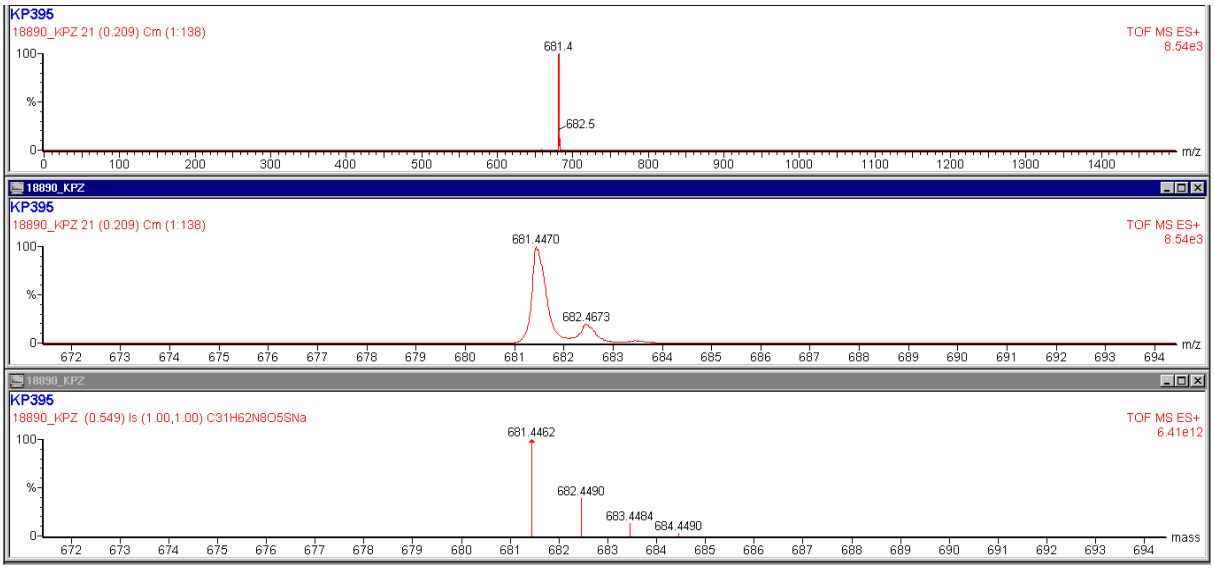

Figure S22. HRMS (ESI-TOF) spectra of compound **2b**

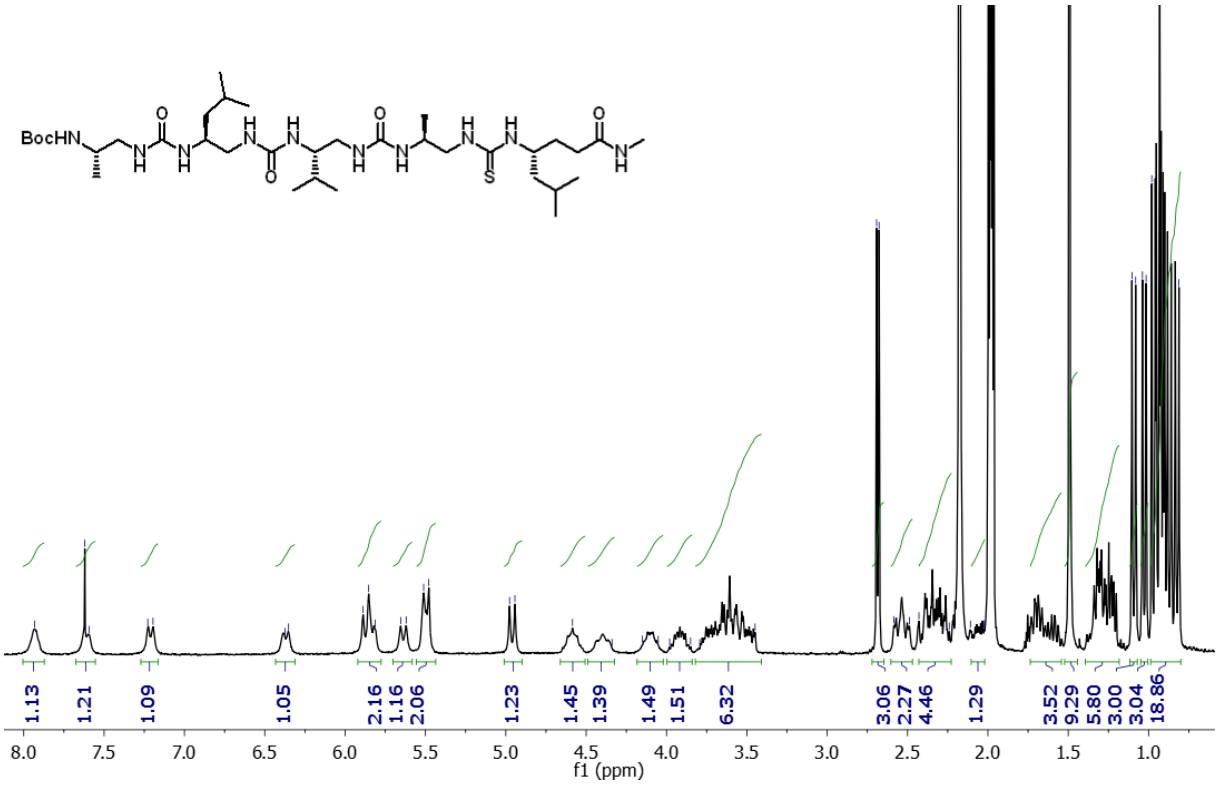

Figure S23. ^{1}H-NMR spectrum of intermediate **27** in CD_3CN (300 MHz)

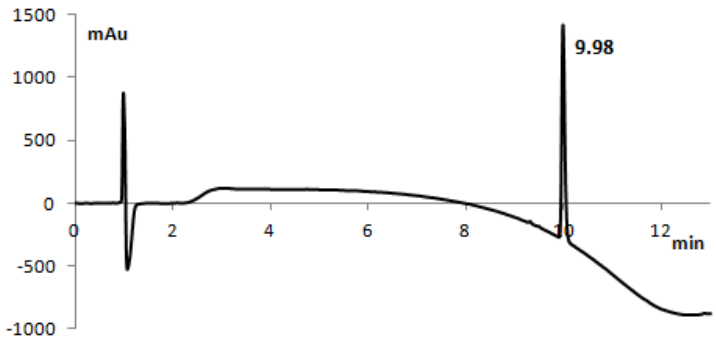

Figure S24. RP-HPLC chromatogram of intermediate **27** (λ = 200nm, 10−100% B in 10 min then 100% B for 3 min)

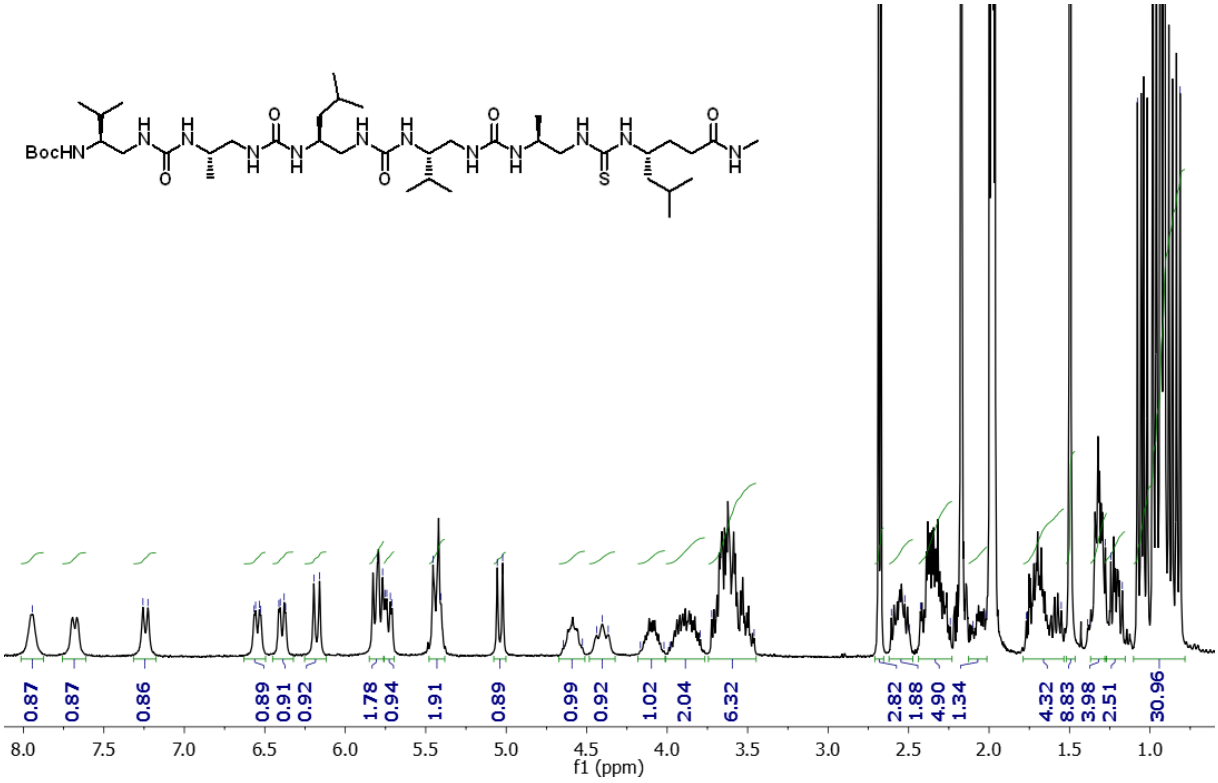

Figure S25. ^{1}H-NMR spectrum of **4** in CD_3CN (300 MHz)

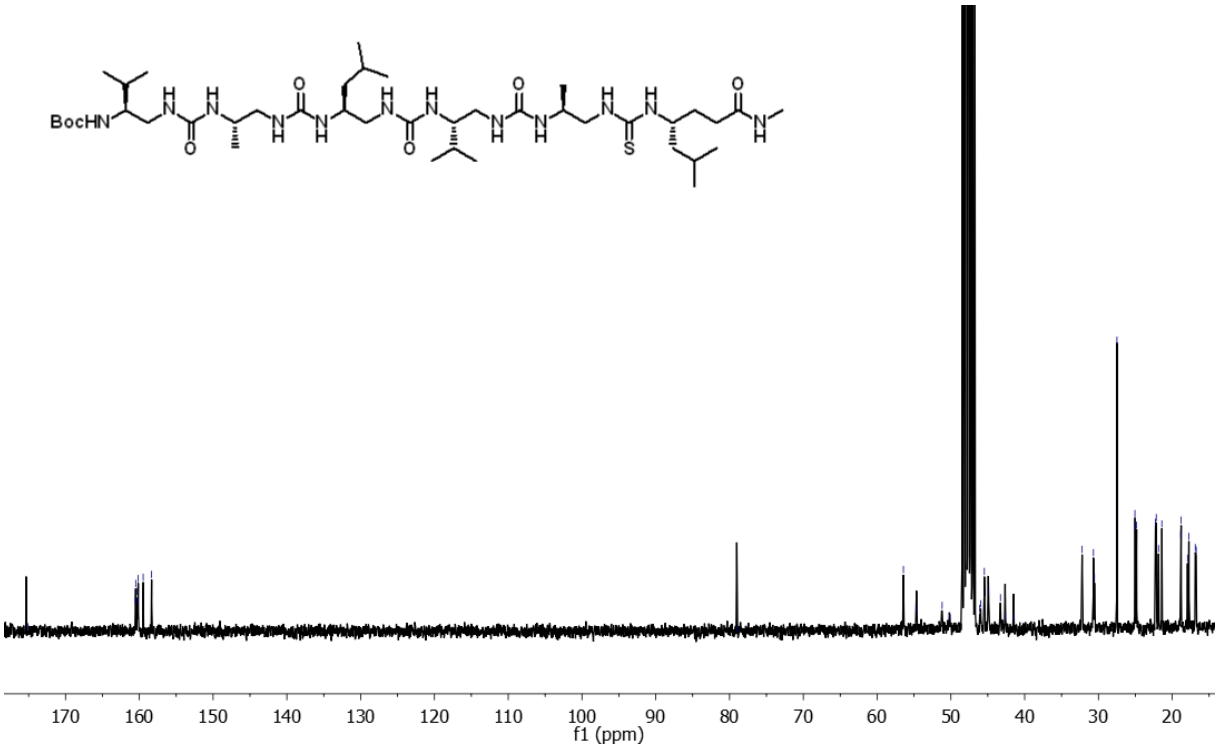

Figure S26. ^{13}C-NMR spectrum of **4** in CD_3CN (75 MHz)

Table S1. ^{1}H-NMR chemical shifts (ppm) of **4** recorded in CD_3CN (3mM, 300MHz)

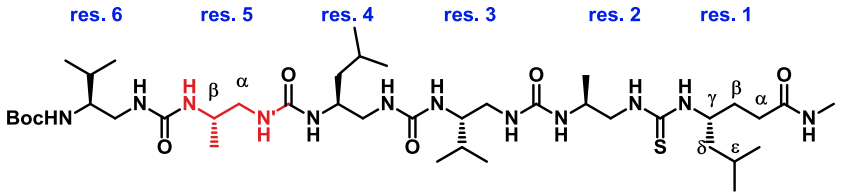

Residue	HN	HN'	$^{\alpha}$CH^{1}	$^{\alpha}$CH^{2}	$^{\beta}$CH	$^{\gamma}$CH	$^{\delta}$CH	$^{\varepsilon}$CH	Other
HNMe	7.94	-	-	-	-	-	-	-	2.68
γLeu	7.24 (*J* = 9.3)	-	2.28	-	2.05 $^{\beta}$CH^{1} 1.31 $^{\beta}$CH^{2}	4.59	1.28	1.69	0.97/0.92
Ala^{T}	5.78 (*J* = 9.7)	7.68 (*J* = 7.5)	4.40	2.54	4.09	1.03	-	-	-
Val^{U}	6.18 (*J* = 10.7)	6.31 (*J* = 9.6, 2.1)	3.58	2.37	3.65	1.57	0.89	-	-
Leu^{U}	5.81 (*J*=10.2)	6.55 (*J*=9.7, 2.6)	3.67	2.28	3.91	1.20	1.70	0.97/ 0.92	-
Ala^{U}	5.04 (*J*=10.0)	5.73 (*J*=9.9, 3.3)	3.61	2.32	3.84	1.07	-	-	-
Val^{U}	5.44	5.42	3.64	2.55	3.52	1.68	0.91	-	-
Boc	-	-	-	-	-	-	-	-	1.49

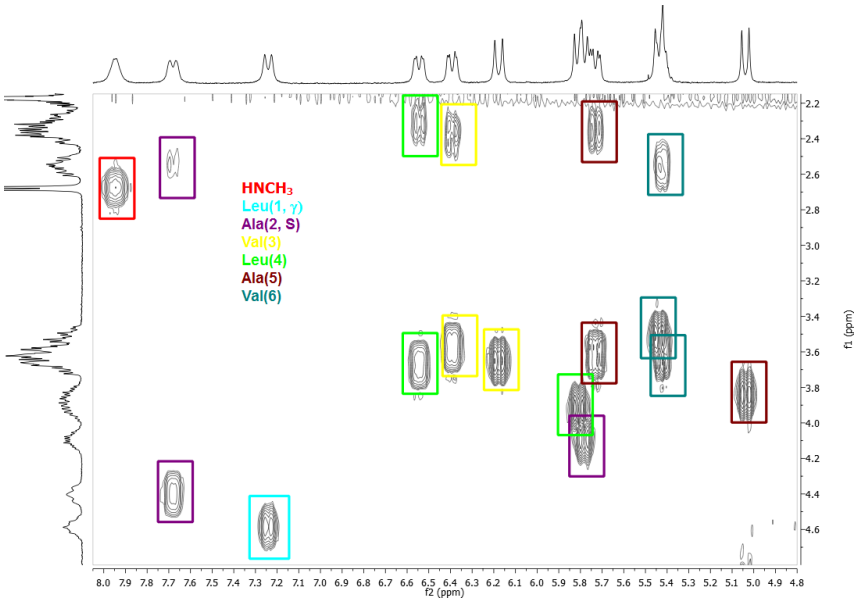

Figure S27. Zoom of the 2D-COSY NH/CH region of **4** recorded in CD_3CN (3mM, 300MHz)

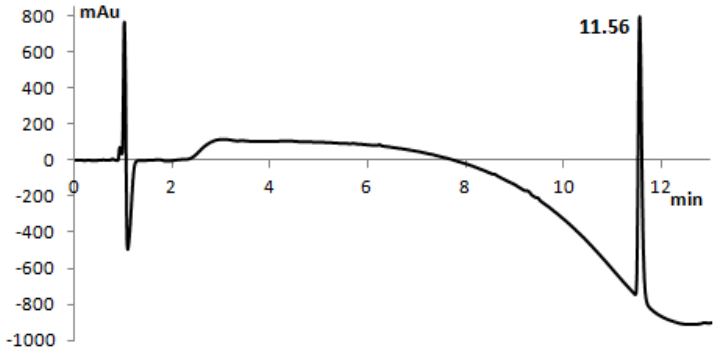

Figure S28. RP-HPLC chromatogram of hexamer **4** (λ = 200nm, 10−100% B in 10 min then 100% B for 3 min)

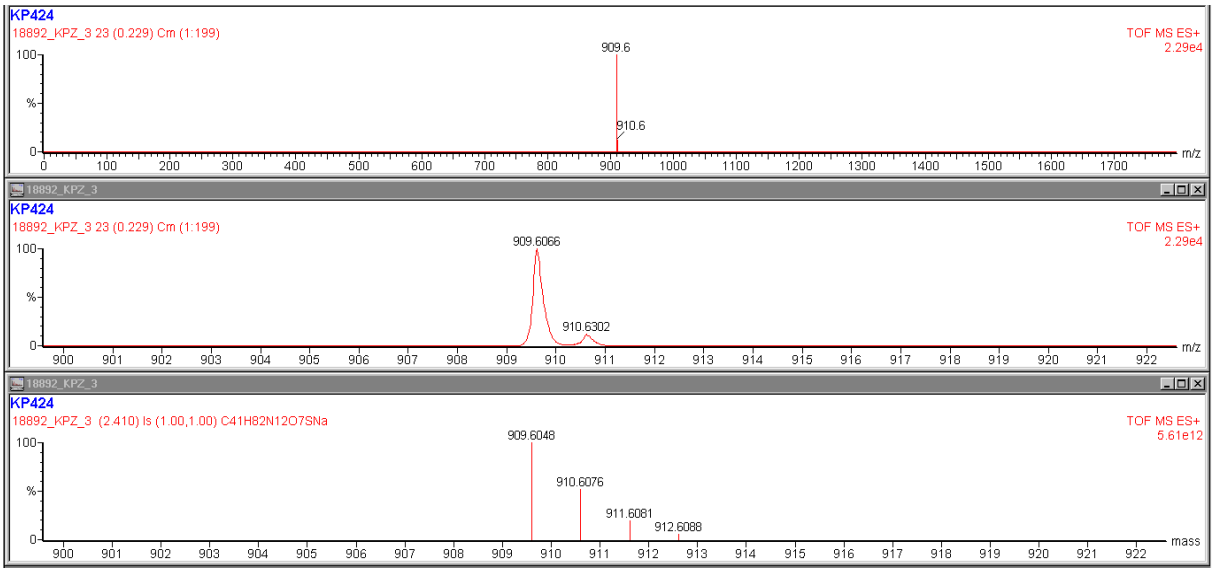

Figure S29. HRMS (ESI-TOF) spectra of compound **4.**

3. X-ray diffraction studies

Data collections were performed at the IECB X-ray facility (UMS3033) on two different high flux microfocus Rigaku rotating anodes at the copper k_α wavelength. Data for compound **4** were collected on a micromax MM07 (800W) equipped with osmic Varimax mirrors and semi-cylindrical R-Axis spider IP detector. Data for compound **2b** were colllected on a FRX (2.7kW) equipped with osmic Varimax mirrors and a Dectris Pilatus 200K hybrid detector. The crystals were mounted on cryo-loops after quick soaking on Paratone—N oil from Hampton research and flash-frozen. Both diffractometers have partial chi geometry goniometer allowing omega-scan data collections. The data were processed with the CrystalClear suite version 1.36 and 2.1b25.[1] All crystal structures were solved using direct methods implemented in SHELXT[2] and were refined using SHELXL 2013 version. Full-matrix least-squares refinement were performed on F^2 for all unique reflections, minimizing $w(Fo^2- Fc^2)^3$, with anisotropic displacement parameters for non-hydrogen atoms. Hydrogen atoms were positioned in idealized positions and refined with a riding model, with Uiso constrained to 1.2 Ueq value of the parent atom (1.5 Ueq when CH_3). The positions and isotropic displacement parameters of the remaining hydrogen atoms were refined freely. DFIX, RIGU commands were used to restrain some side chains as rigid groups and restrain their displacement parameters. Data statistics are presented in table S2 and in the cif files.

Checkcif Alert level A remain for compound **4**. SHFSU01_ALERT_2_A, THETM01_ALERT_3_A and PLAT080_ALERT_2_A. These Alerts concern the low diffraction power of the small crystal and the residual electron density remaining close to the sulphur atom of the thiourea unit.

1. CrystalClear-SM Expert 2.1 (Rigaku, Jun 7th 2013) Software, Version 5.6.2.0, Tokyo, Japan.
2. G.M. Sheldrick, *Acta Cryst.* **2015**. *A71*, 3-8.
3. G.M. Sheldrick, *Acta Cryst.* **2015** *C71*, 3-8.

Table S2: Crystallographic data statistics for compounds **2b** and **4.**

Compounds	**2b**	**4**
Crystal System	triclinic	monoclinic
Space Group	P1	$P2_1$
Z	1	2
Unit Cell Parameters a, Å	9.5027(7)	9.6558(19)
Unit Cell Parameters b, Å	10.5139(7)	20.213(4)
Unit Cell Parameters c, Å	11.4874(8)	14.022(3)
Unit Cell Parameters α, °	74.736 (6)	90
Unit Cell Parameters β, °	66.148(6)	97.03(3)
Unit Cell Parameters γ, °	81.699(6)	90
Temperature, K	120	150
Volume, Å3	1011.72(13)	2716.2(9)
FW, g.mol-1	690.98	887.24
ρ, g.cm-3	1.134	1.085
λ, E	1.097	0.923
θ min	4.320	6.729
θ max	68.245	49.077
Radiation	Cu	Cu
Reflections Measured	12834	28691
Reflections Unique ([*Fo* > 2σ*Fo*)])	5659	5101
Parameters/restraints	439/5	564/40
GOF	1.078	1.070
R1 (I>2σ(I))	0.0480	0.0773
wR2 (all data)	0.1357	0.1939
CCDC#	CCDC 1563646	CCDC 1563645

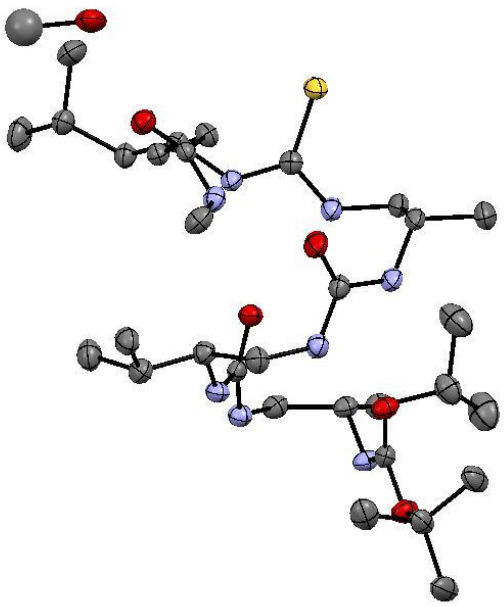

Figure S30: ORTEP representation of compound **2b** along the crystallographic a axis. Displacement ellipsoids are plotted at the 50% probability level, H atoms have been removed for clarity.

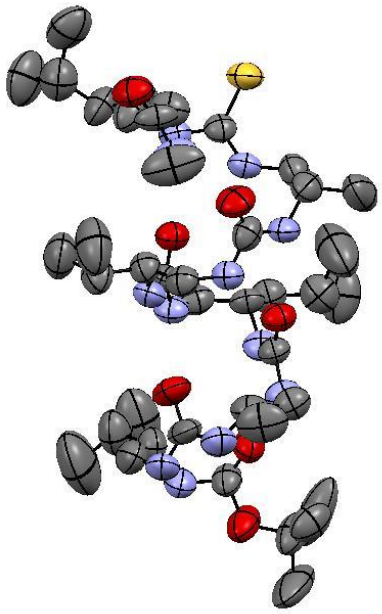

Figure S31: ORTEP representation of compound **4** along the crystallographic a axis. Displacement ellipsoids are plotted at the 50% probability level, H atoms have been removed for clarity.

4. RP-HPLC chromatograms, ES-MS analyses and NMR characterizations of the guanidinylated products synthesized in solution

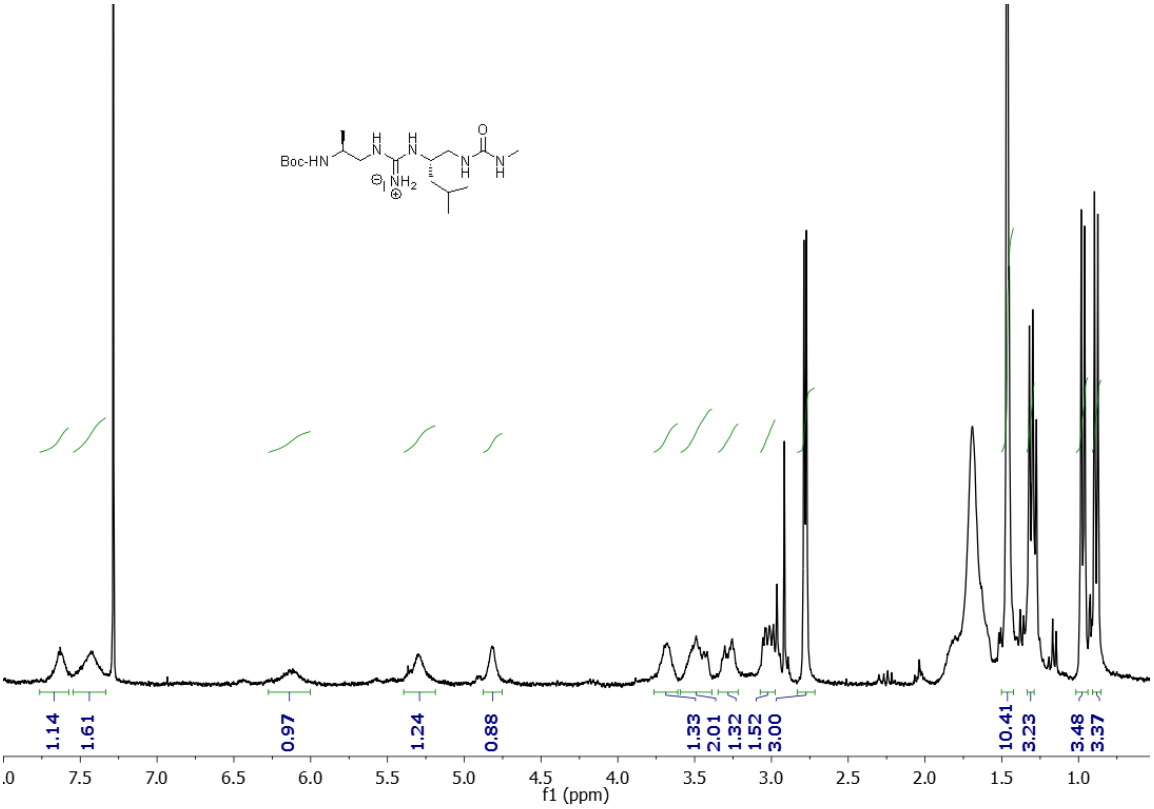

Figure S32. ^{1}H-NMR spectrum of compound **5** in $CDCl_3$ (300 MHz)

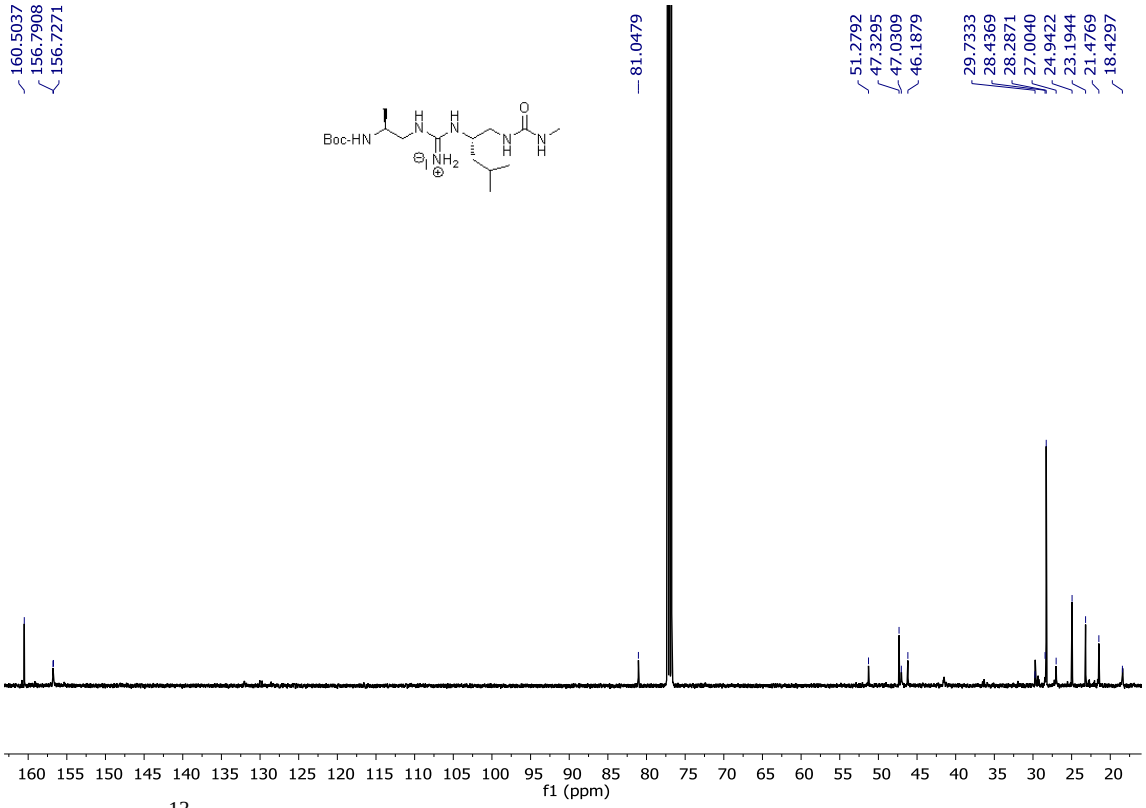

Figure S33. ^{13}C-NMR spectrum of compound **5** in (125 MHz, $CDCl_3$, cryoprobe)

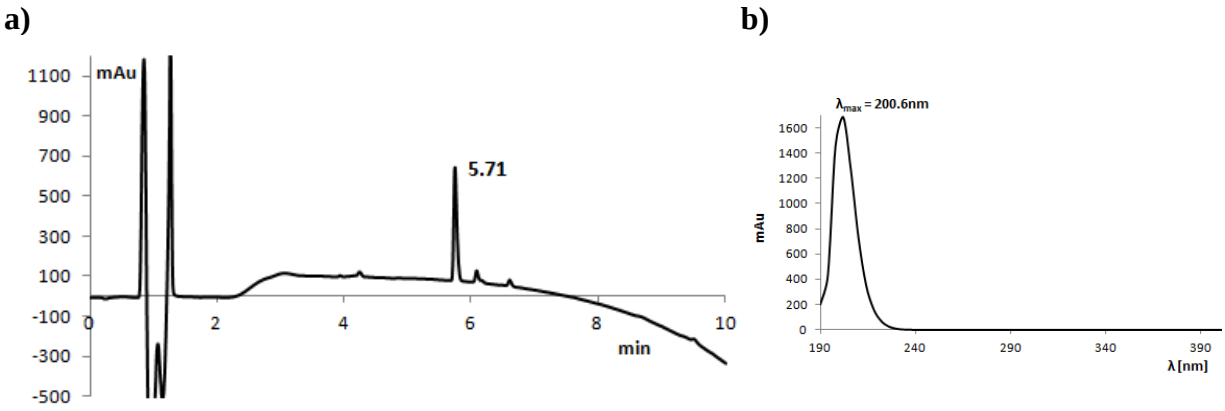

Figure S34. a) Chromatogram of linear guanidylated dimer **5** (λ = 200nm); b) UV spectrum of dimer **5.**

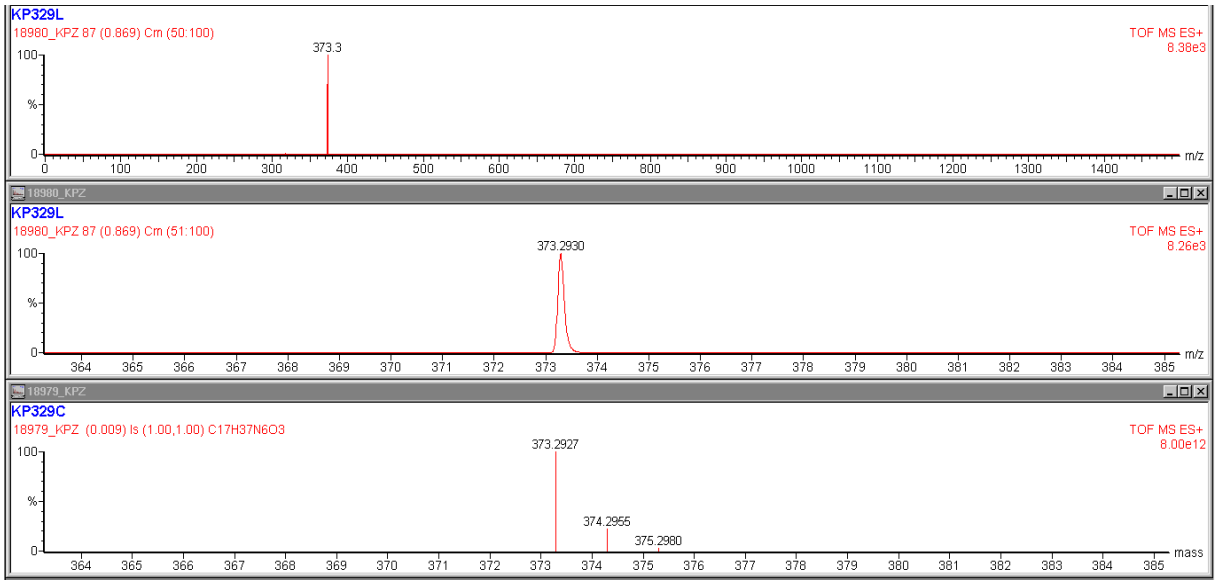

Figure S35. HRMS (ESI-TOF) spectra of compound **5.**

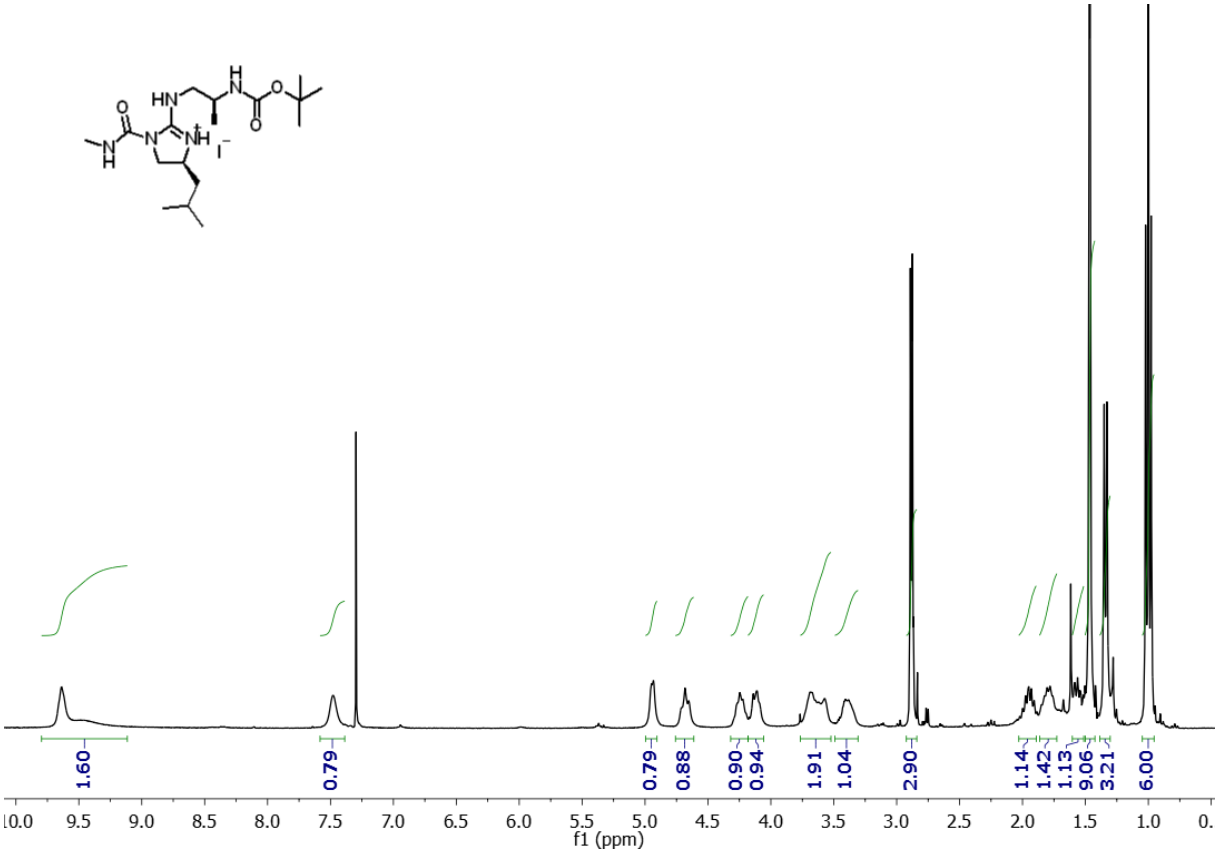

Figure S36. ^{1}H-NMR spectrum of cyclic compound **7** in $CDCl_3$ (300 MHz)

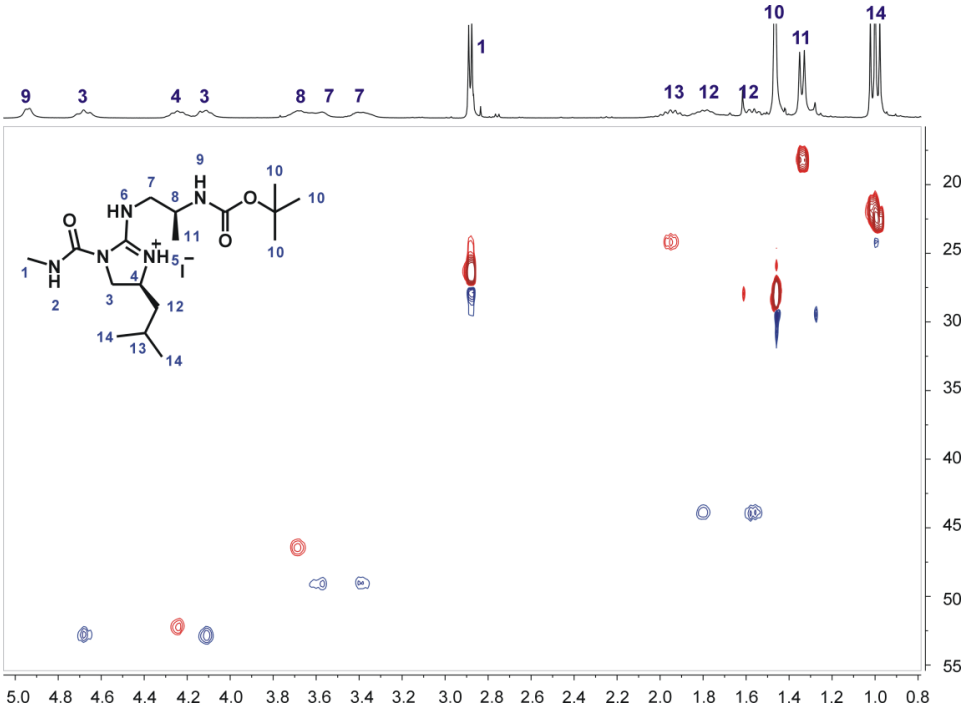

Figure S37. 2D-HSQC-NMR spectrum of cyclic compound **7** in $CDCl_3$ (75 MHz) with signal assignments

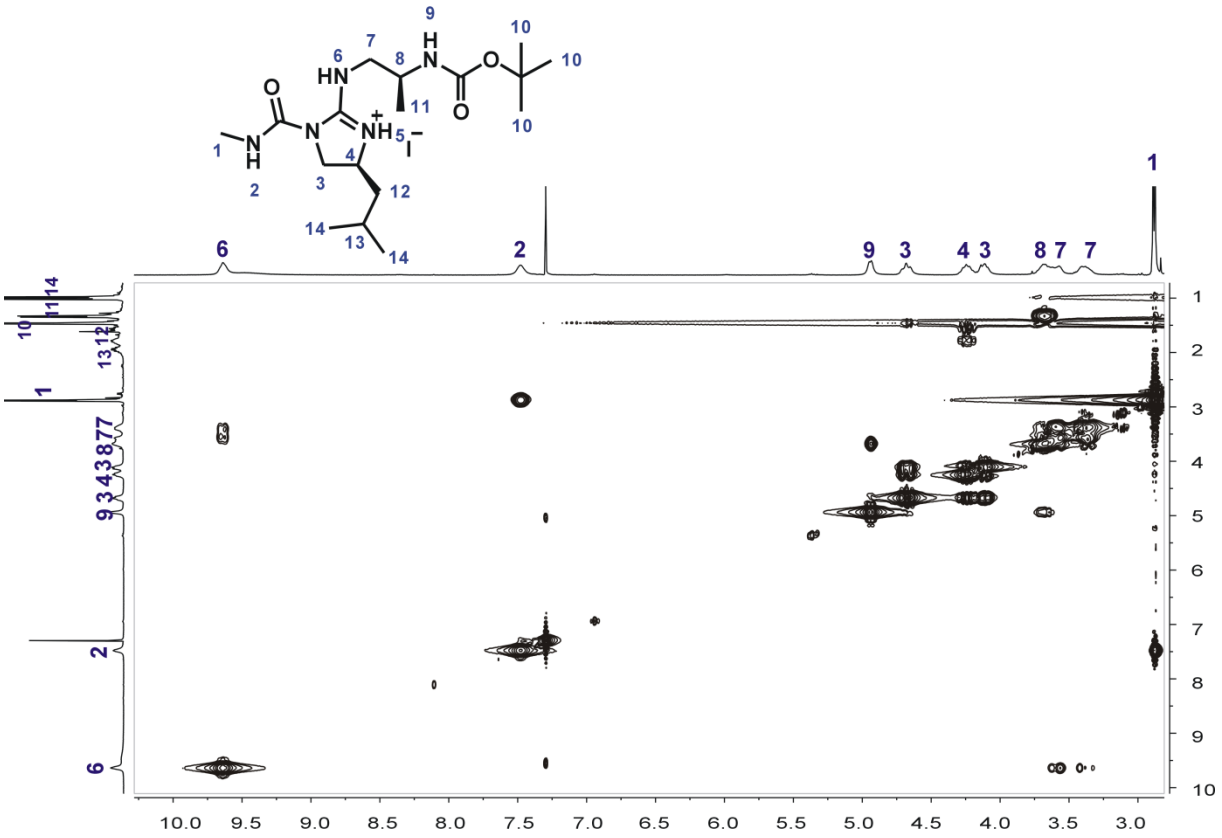

Figure S38. Part of the 2D-COSY spectrum of compound **7** in $CDCl_3$ (300 MHz)

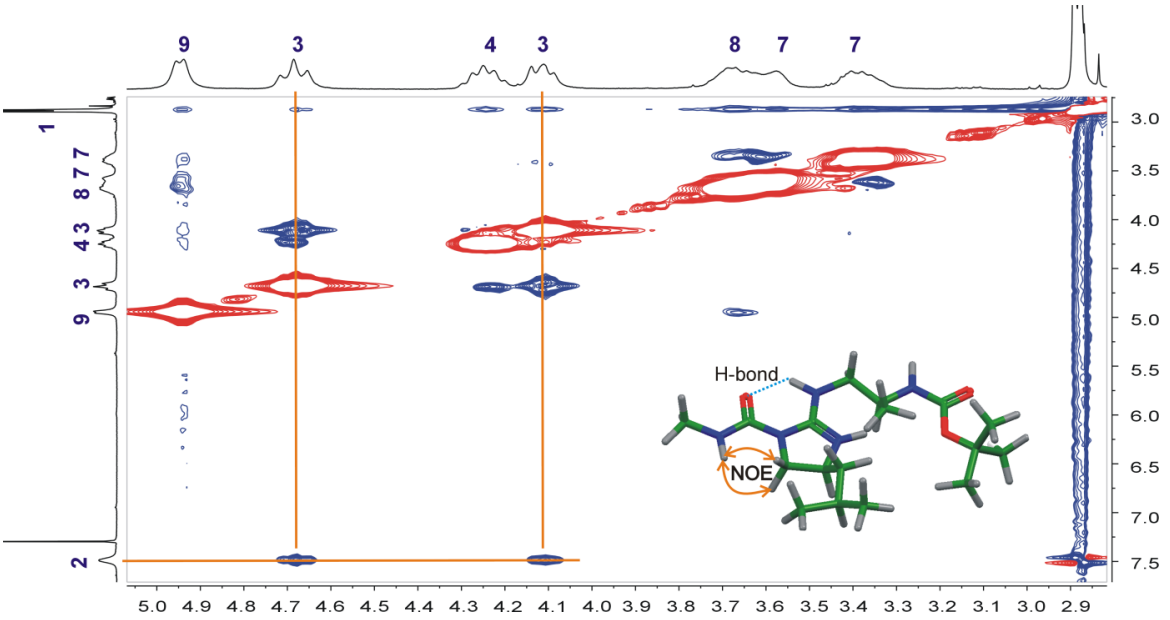

Figure S39. Zoom of the 2D-NOESY CH/NH region of compound **7** in $CDCl_3$ (300 MHz) with signal attributions. The orange arrows show NOE connectivities between NH and the diastereotopic protons of the CH_2[3].

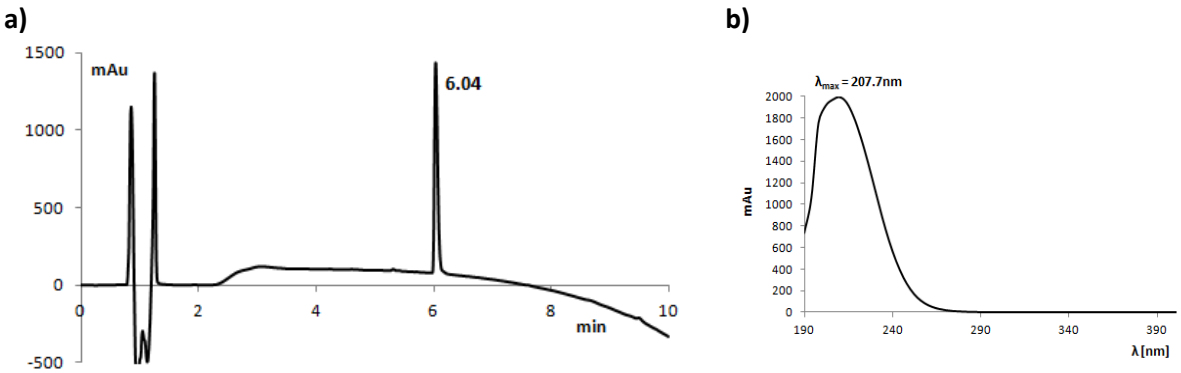

Figure S40. a) RP-HPLC chromatogram (λ = 200nm, 10−100% B in 10 min) and b) UV spectrum of compound **7.**

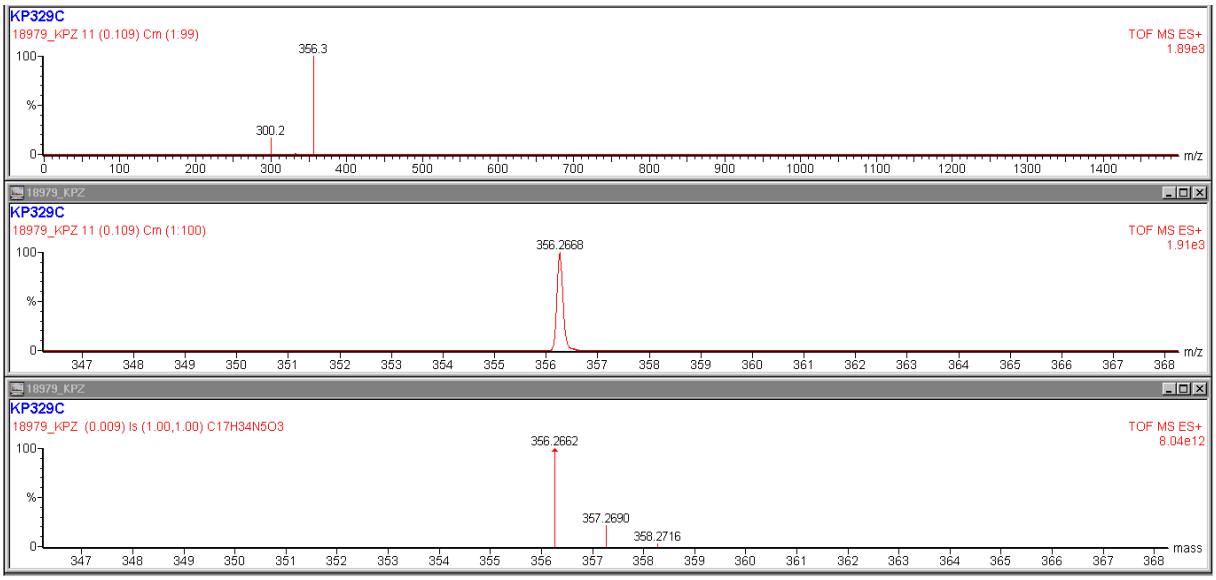

Figure S41. HRMS (ESI-TOF) spectra of compound **7.**

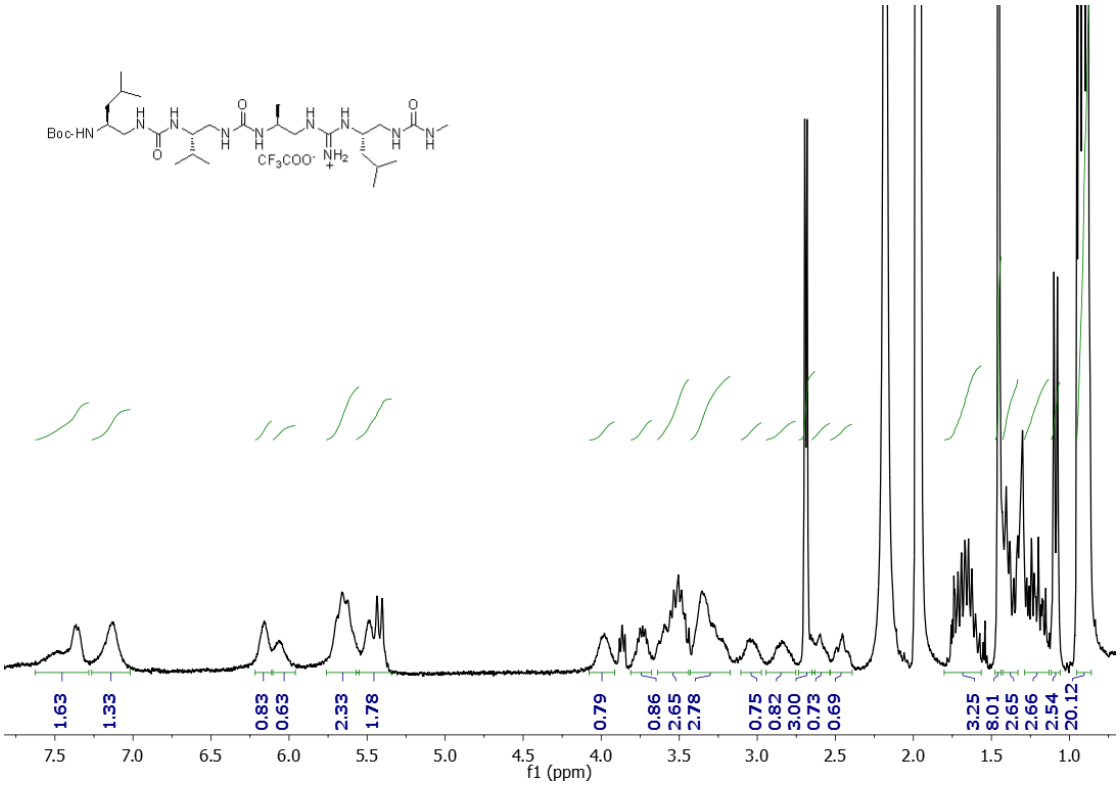

Figure S42. ^{1}H-NMR spectrum of compound **8** in CD_3CN (300 MHz)

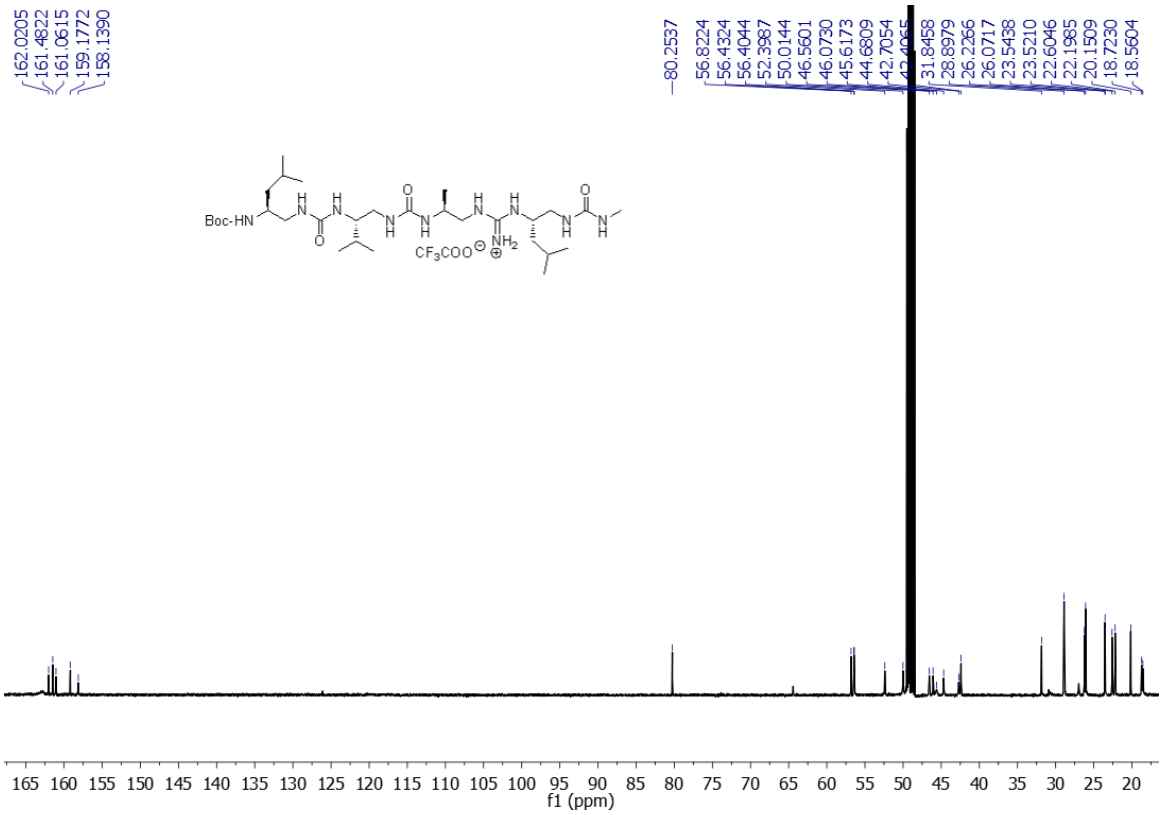

Figure S43. ^{13}C-NMR spectrum of compound **8** in CD_3OD (125MHz, CD_3OD, cryoprobe)

a) **b)**

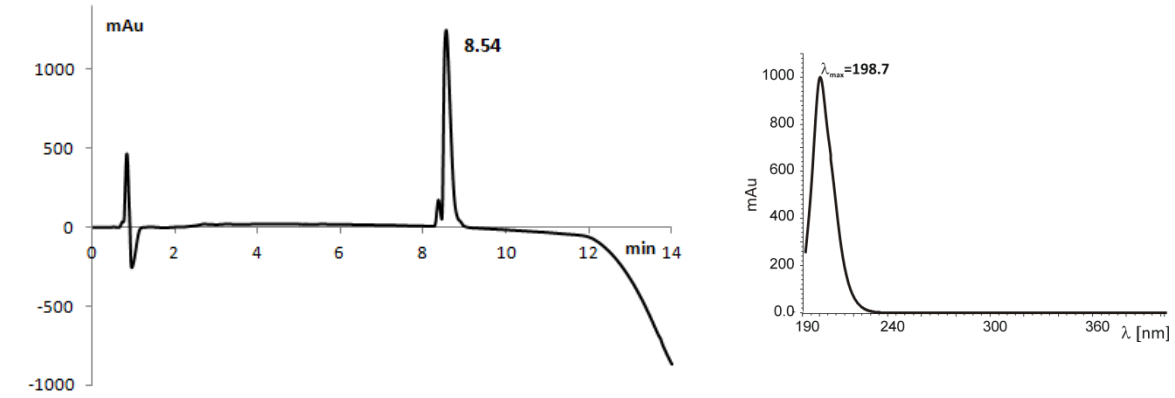

Figure S44. a) Chromatogram of linear guanidinylated tetramer **8** (λ = 200nm); b) UV spectrum of tetramer **8.**

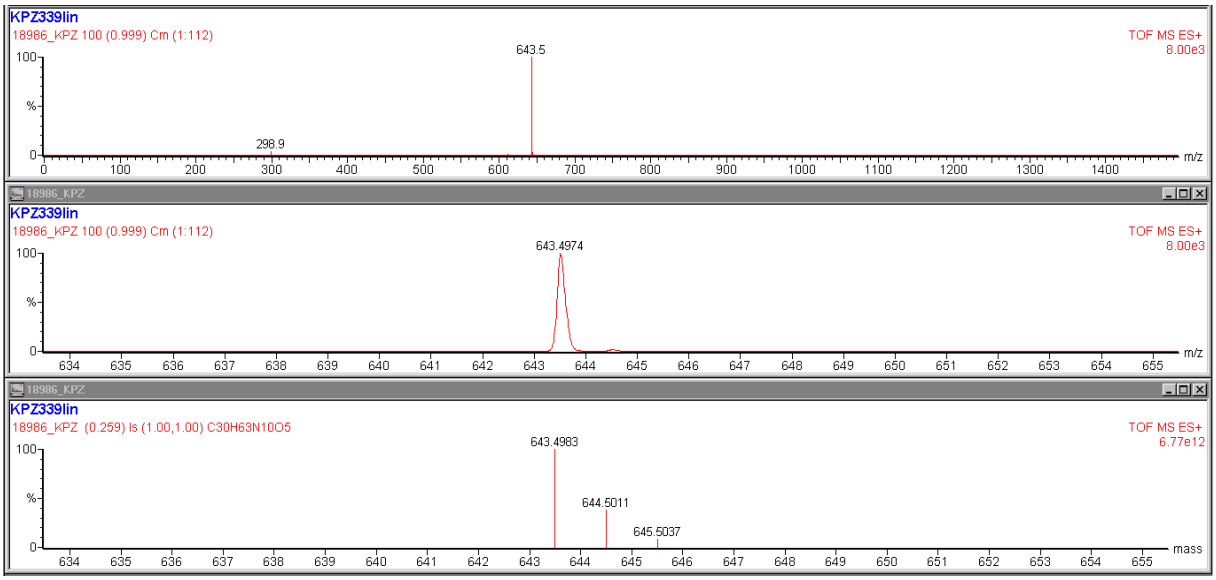

Figure S45. HRMS (ESI-TOF) spectra of compound **8.**

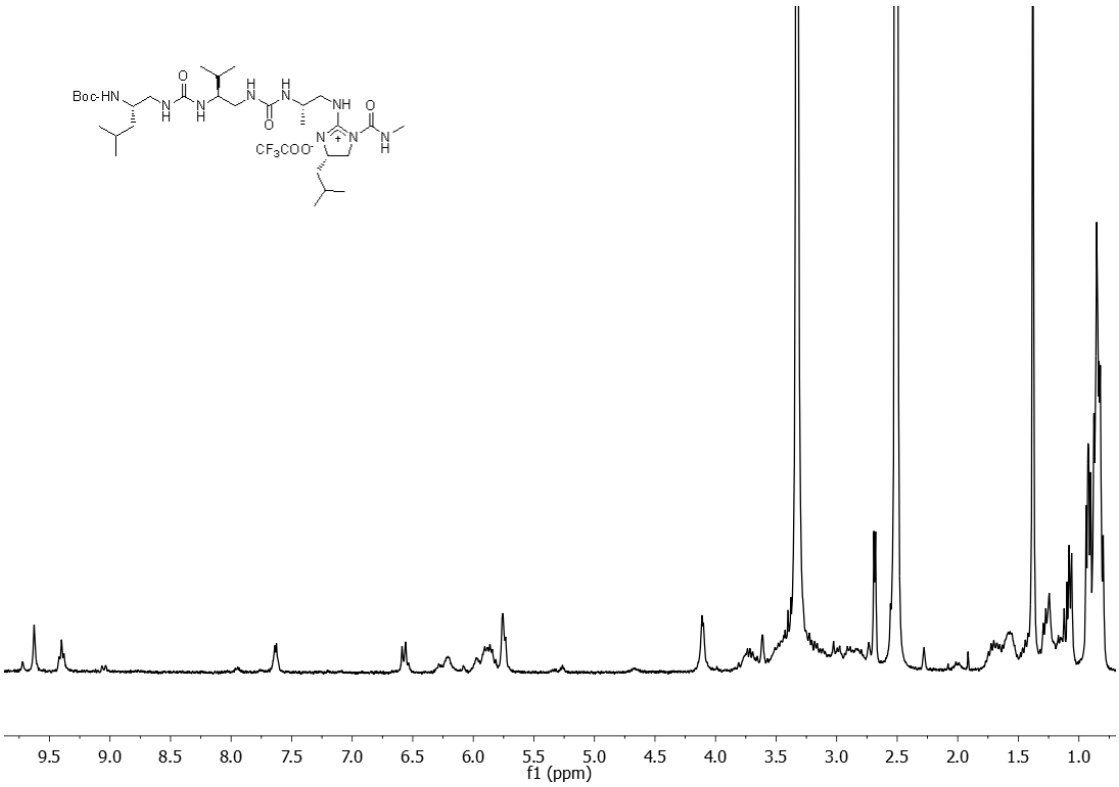

Figure S46. ^{1}H-NMR spectrum of cyclic compound **9** in DMSO d_6 (300 MHz)

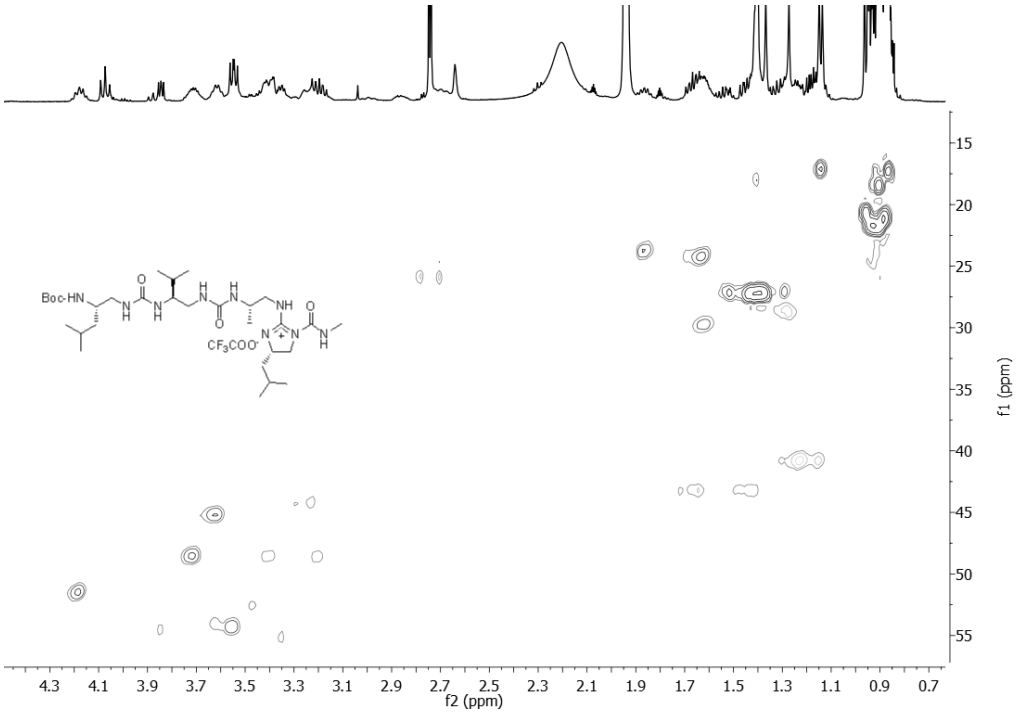

Figure S47. 2D-HSQC-NMR spectrum of cyclic compound **9** (125/500MHz, CD_3CN)

a) **b)**

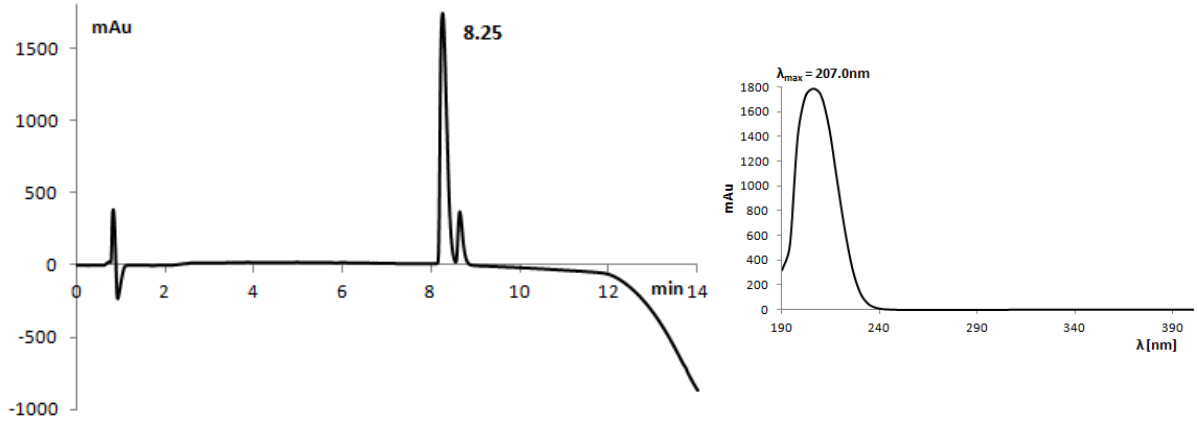

Figure S48. a) Chromatogram of cyclic tetramer **9** (λ = 200 nm,); b) UV spectrum of **9**

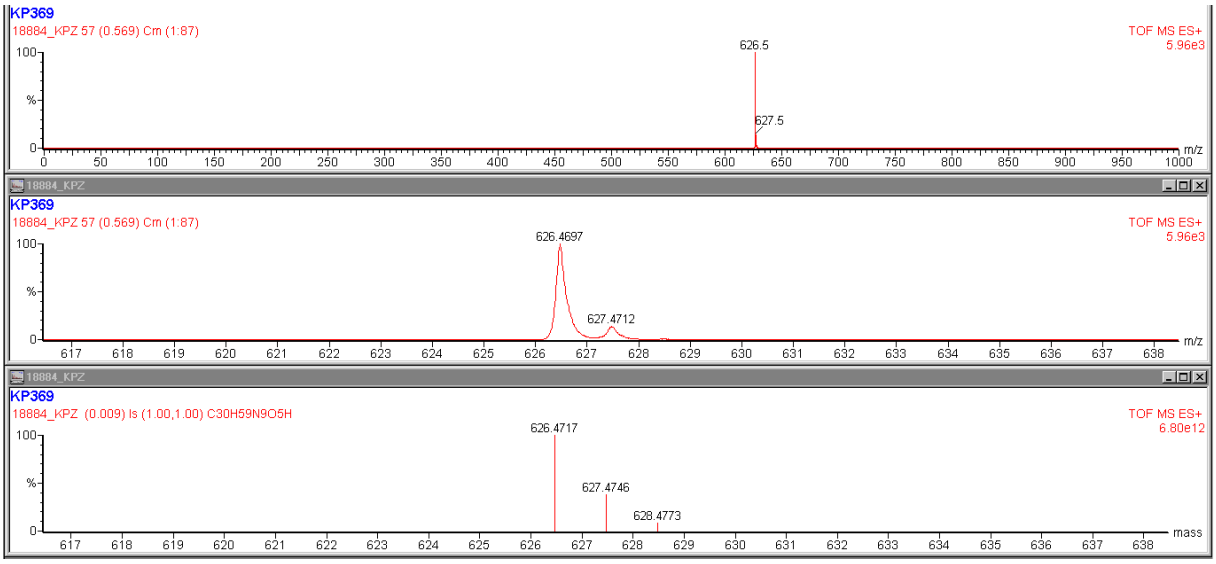

Figure S49. HRMS (ESI-TOF) spectra of cyclic tetramer **9**

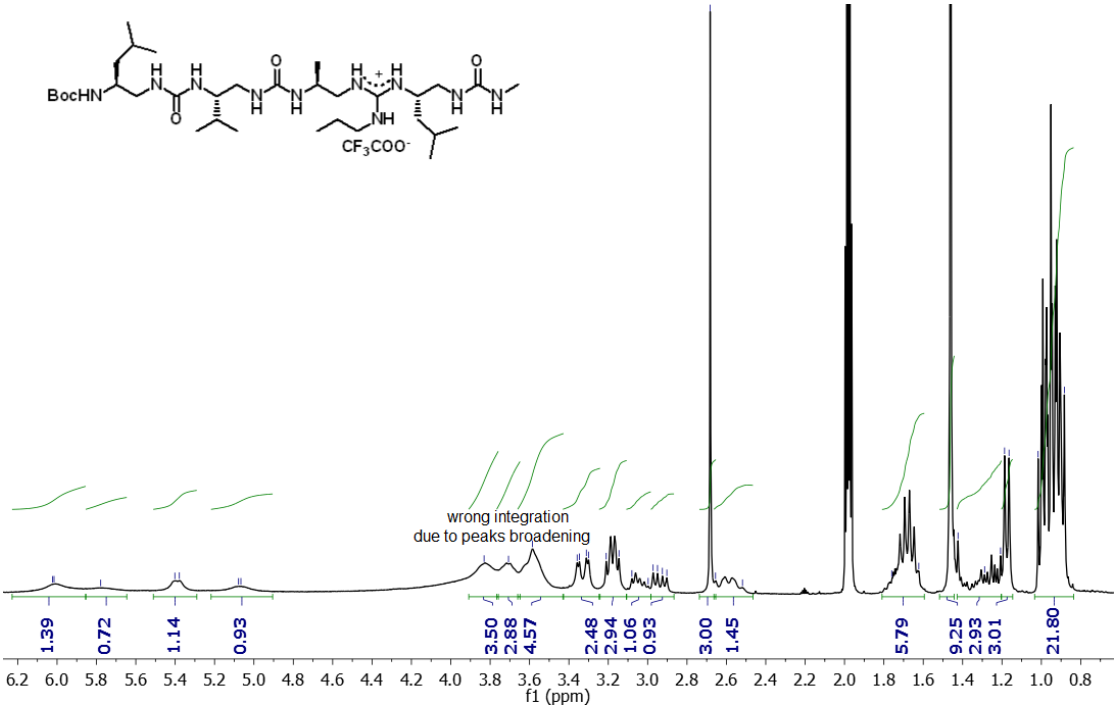

Figure S50. ^{1}H-NMR spectrum of linear compound **11** in CD_3CN (300 MHz)

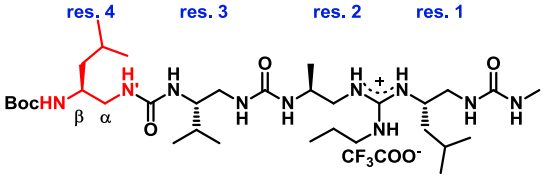

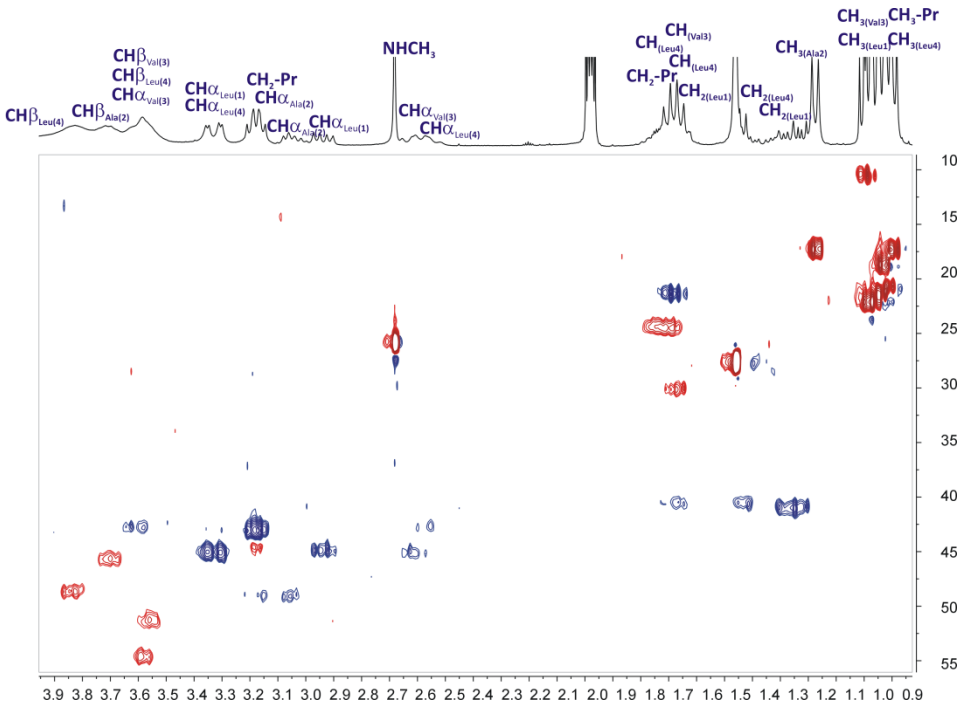

Figure S51. 2D-HSQC-NMR spectrum of **11** (75 MHz)

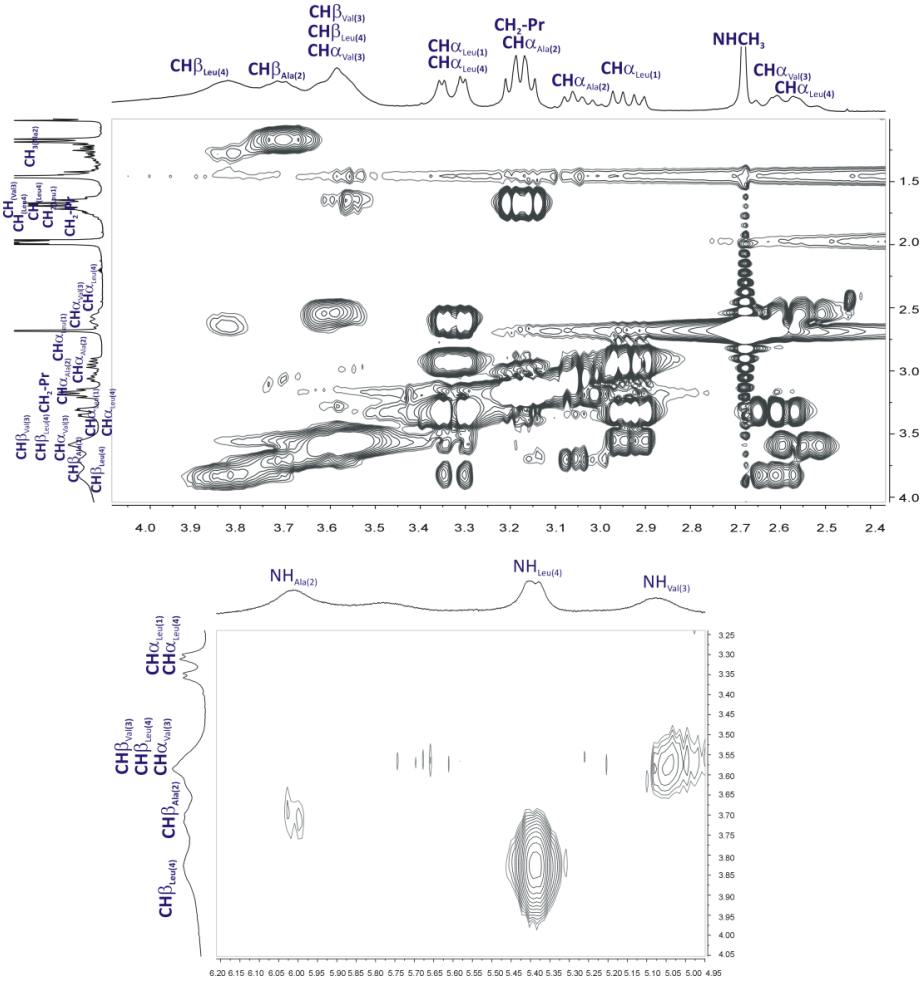

Figure S52. Zoom of the 2D-COSY CH/CH region of **11** in CD_3CN (300 MHz) with signal assignments

Table S3. ^{1}H-NMR chemical shifts (ppm) of compound **11** in CD_3CN (3 mM, 300MHz**)**

Residue	HN	HN'	$^{\alpha}CH^{1}$	$^{\alpha}CH^{2}$	$^{\beta}CH$	$^{\gamma}CH$	$^{\delta}CH$	$^{\varepsilon}CH$	Other
HN-Me	not visible	-	-	-	-	-	-	-	2.68
Leu^{U}	not visible	not visible	3.33	2.94	3.55	1.66/1.44	1.70	signals. overlap.	-
Ala^{G}	6.02	not visible	3.15	3.05	3.71	1.18	-	-	-
Val^{U}	5.08	not visible	3.61	2.58	3.57	1.66	signals overlap	-	-
Leu^{U}	5.39	not visible	3.33	2.62	3.83	1.29/1.22	1.69	signals. overlap.	
***n*PrNH**	not visible								0.99 1.67 3.18
Boc	-	-	-	-	-	-	-	-	1.46

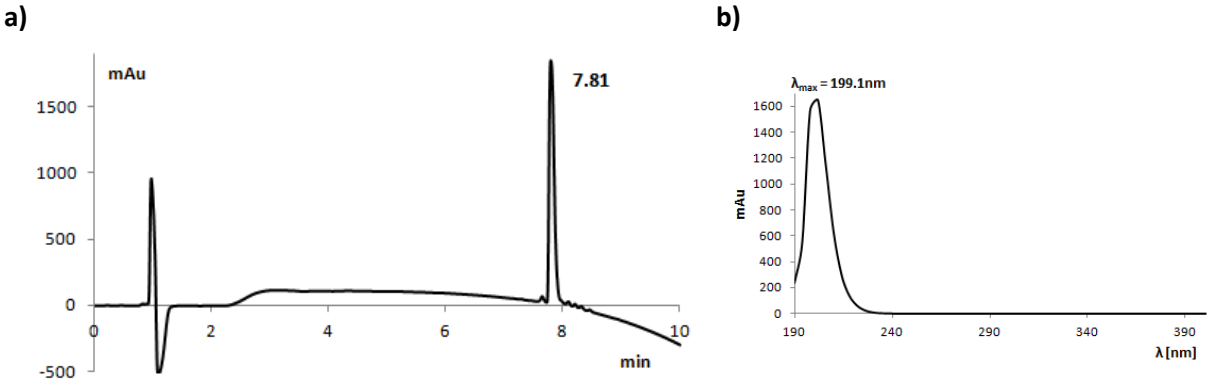

Figure S53. a) RP-HPLC chromatogram (λ = 200nm, 10−100% B in 10 min) of **11** and b) UV spectrum of **11**

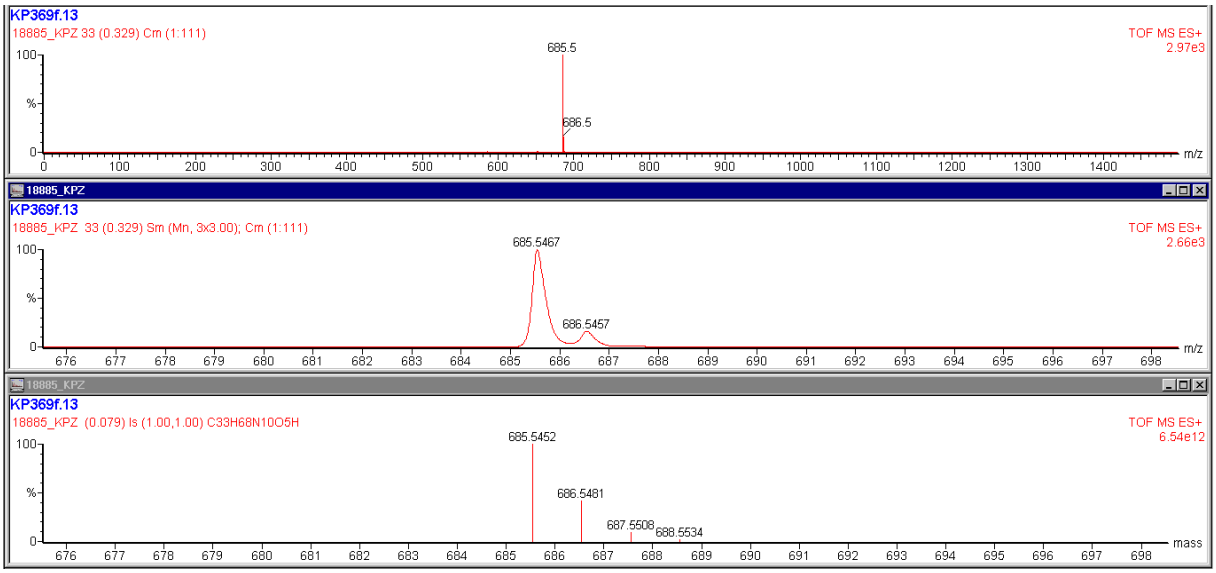

Figure S54. HRMS (ESI-TOF) spectra of linear tetramer **11**

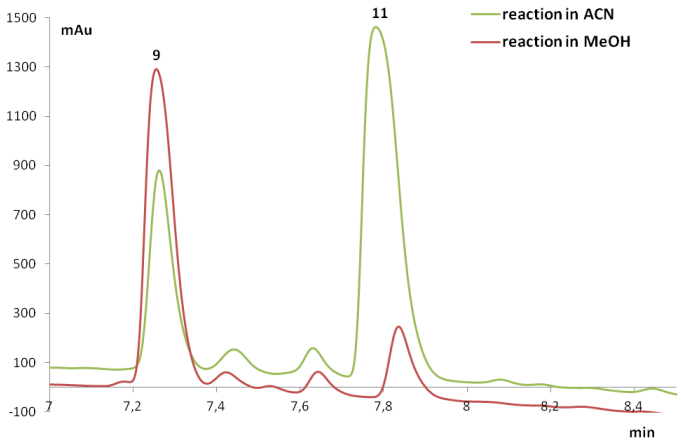

Figure S55. Comparison of RP-HPLC chromatograms of the reaction of **2a** in the presence of *n*-$PrNH_2$ performed either in CH_3OH or CH_3CN to give rise to expected oligomer **11** and cyclic guanidinium **9**.

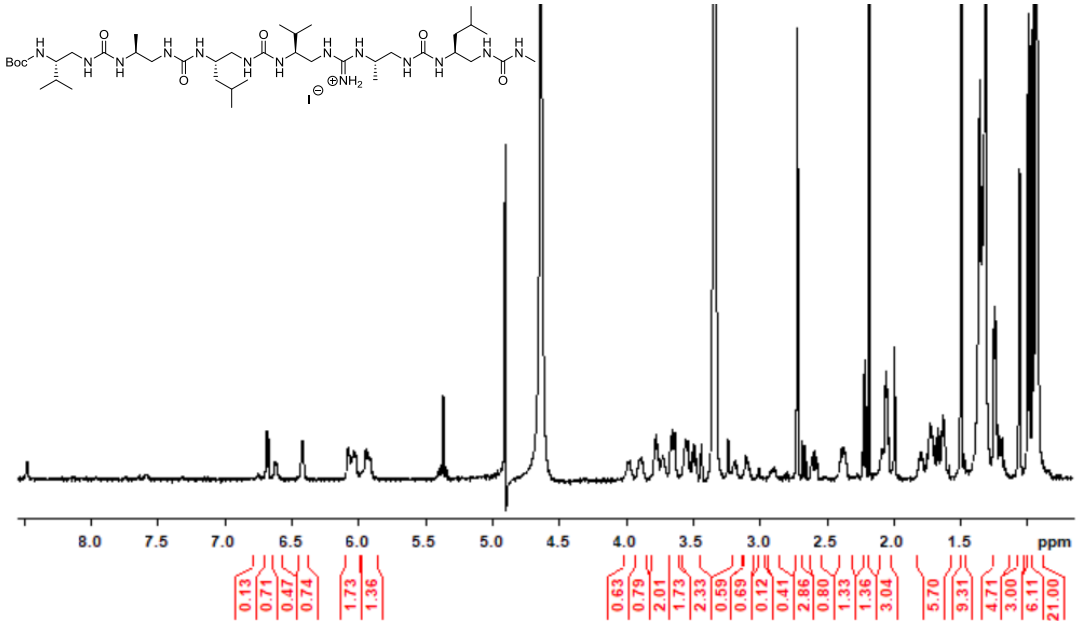

Figure S56: ^{1}H-NMR spectrum of **12** in CD_3OH (700 MHz).

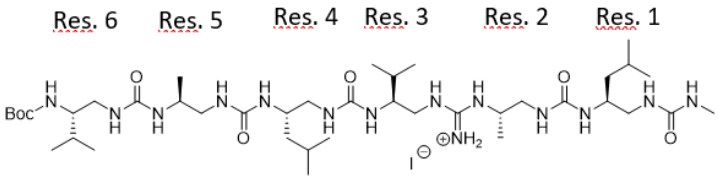

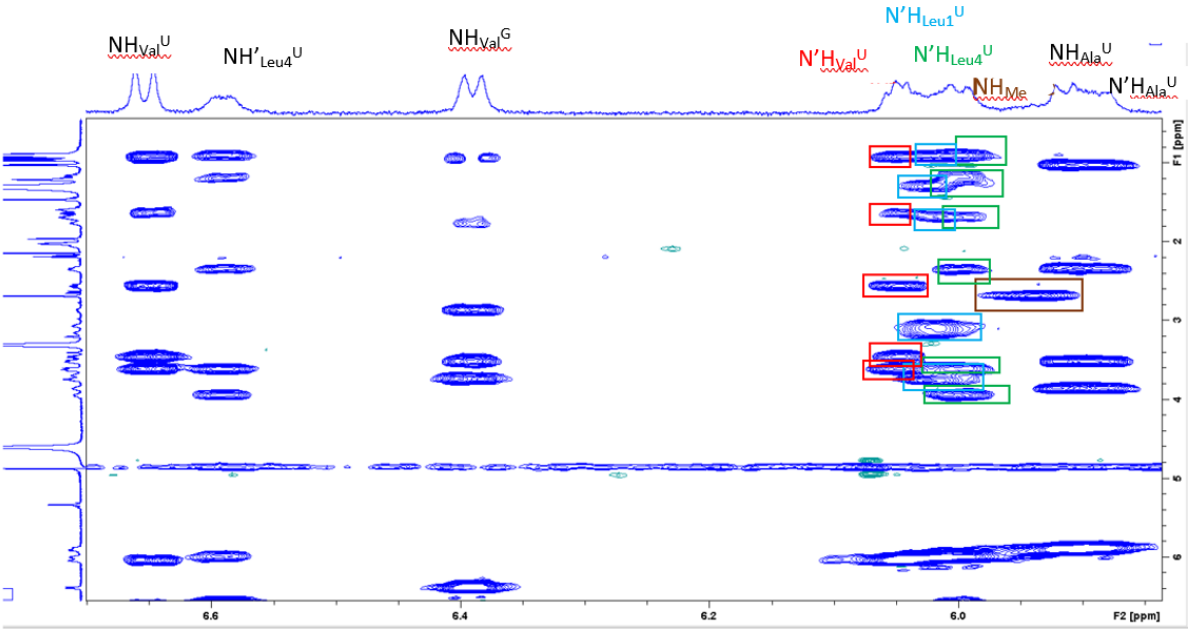

Figure S57. Zoom of the 2D-TOCSY NH and N'H regions of **12** recorded in CD_3OH (700MHz).

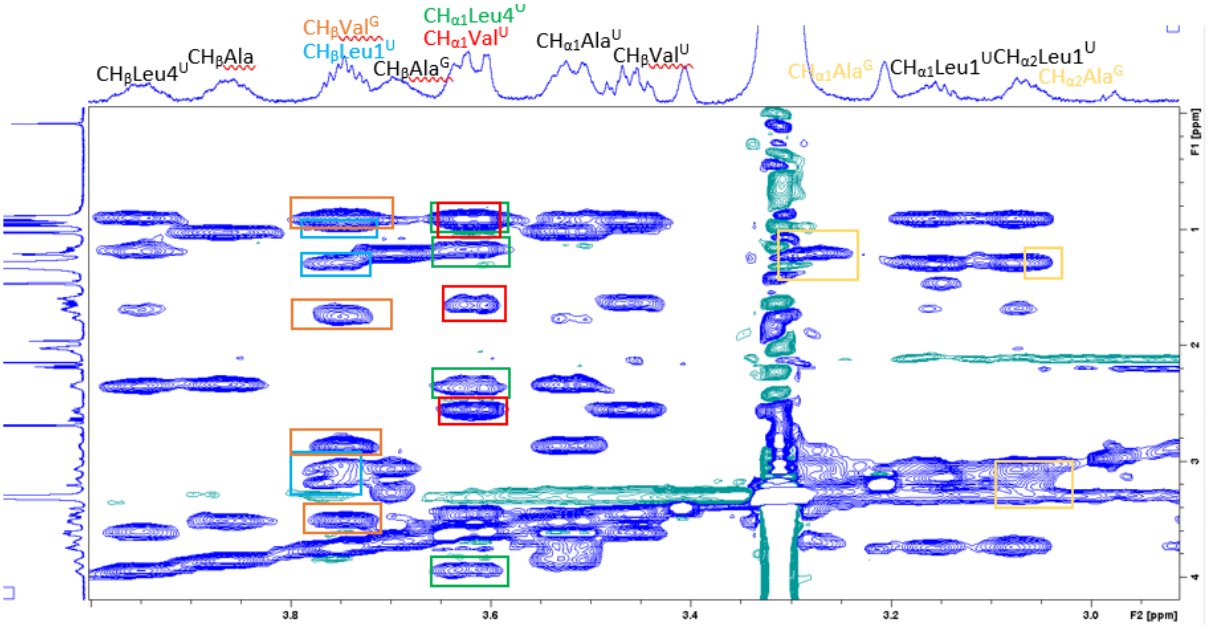

Figure S58. Zoom of the 2D-TOCSY β-CH and α-CH regions of **12** recorded in CD_3OH (700MHz).

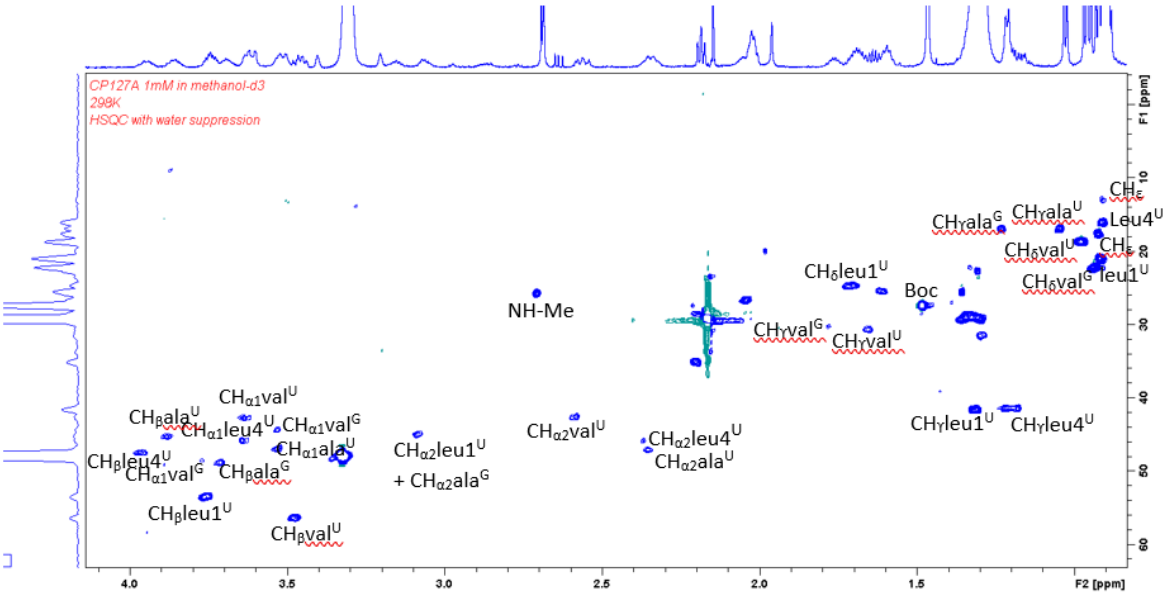

Figure S59. 2D-HSQC-NMR spectrum of **12** recorded in CD_3OH (700MHz).

Table S4. ^{1}H-NMR chemical shifts (ppm) of **12** in CD_3OH (1mM, 700MHz).

Residue	HN	HN'	$^{\alpha}CH^{1}$	$^{\alpha}CH^{2}$	$^{\beta}CH$	$^{\gamma}CH$	$^{\delta}CH$	$^{\varepsilon}CH$	Other	$\Delta\delta$ ($^{\alpha}CH$)
HNMe	5.95	-	-	-	-	-	-	-	2.69	
Leu^{U}	6.39	6.01	3.16	3.07	3.74	1.30	1.68	0.91		0.09
Ala^{G}	6.40	not visible	3.27	3.06	3.69	1.20	-	-	-	0.21
Val^{G}	6.37	7.30	3.52	2.87	3.75	1.75	0.92	-	-	0.65
Leu^{U}	6.00	6.58	3.62	2.34	3.94	1.18	1.70	0.89	-	1.28
Ala^{U}	5.90	5.87	3.55	2.33	3.87	1.03	-	-	-	1.22
Val^{U}	6.65	6.05	3.65	2.56	3.46	1.63	0.95	-	-	1.09
Boc	-	-	-	-	-	-	-	-	1.47	

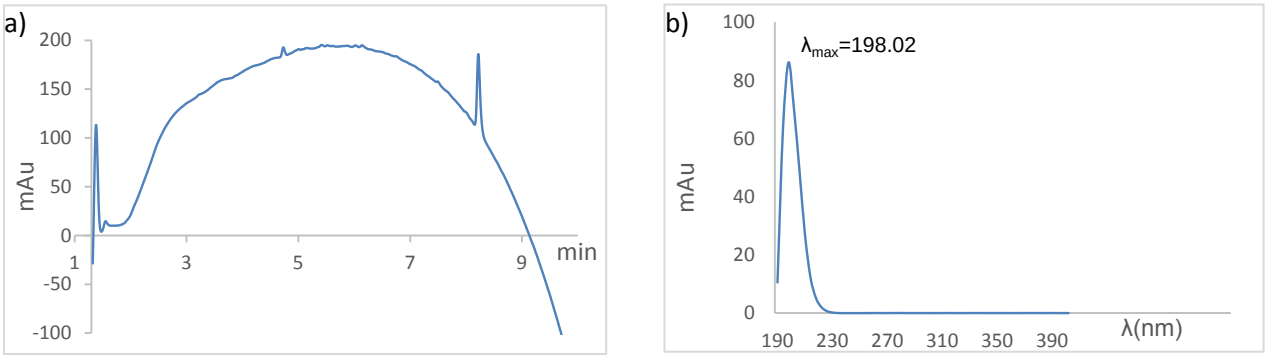

Figure S60. a) RP-HPLC chromatogram of compound **12** (λ = 200nm, 10−100% B in 10 min). b) UV-spectrum of **12**.

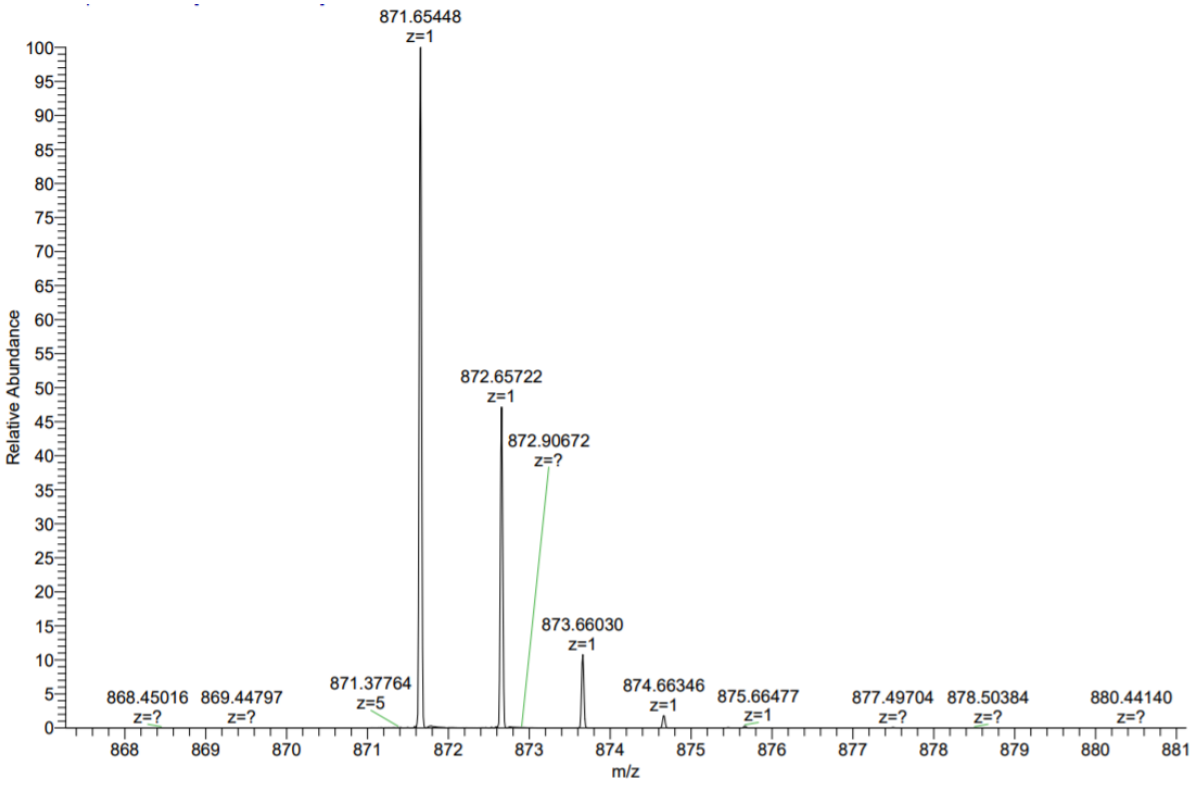

Figure S61. HRMS (ESI-TOF) spectra of compound **12.**

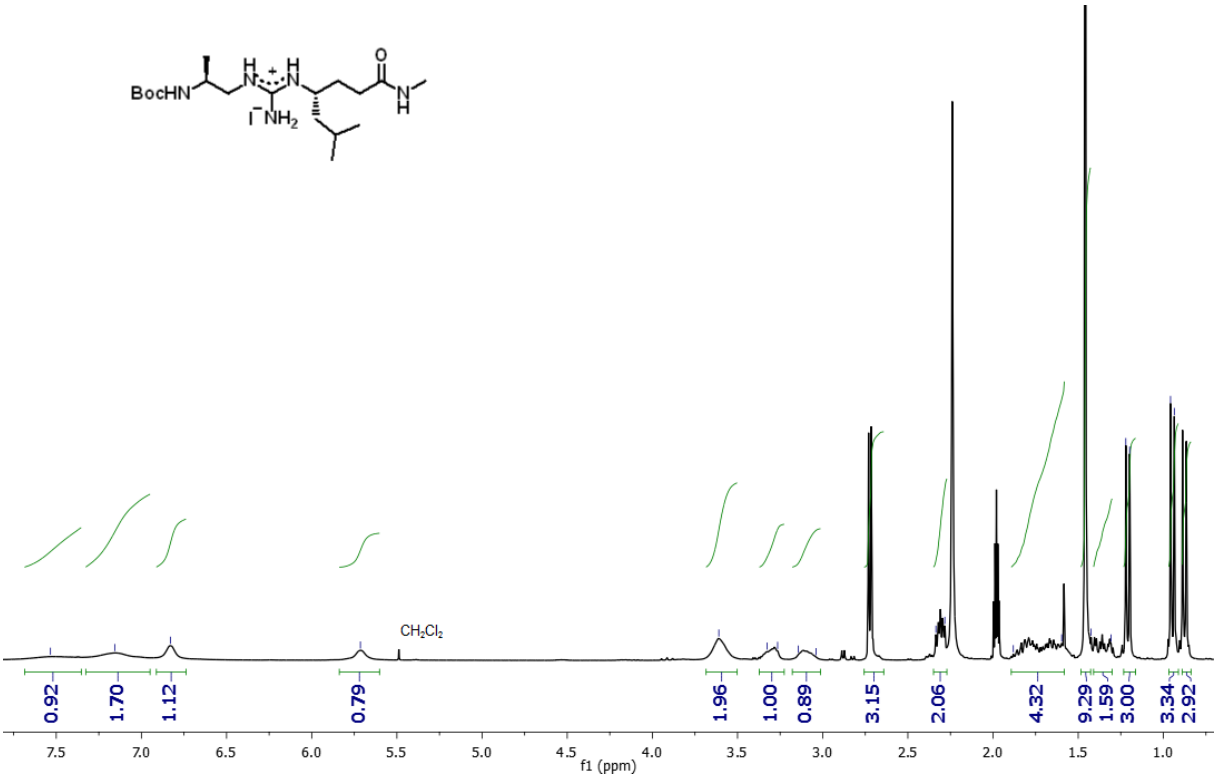

Figure S62. ^{1}H-NMR spectrum of guanidinylated dimer **15** in CD_3CN (300 MHz)

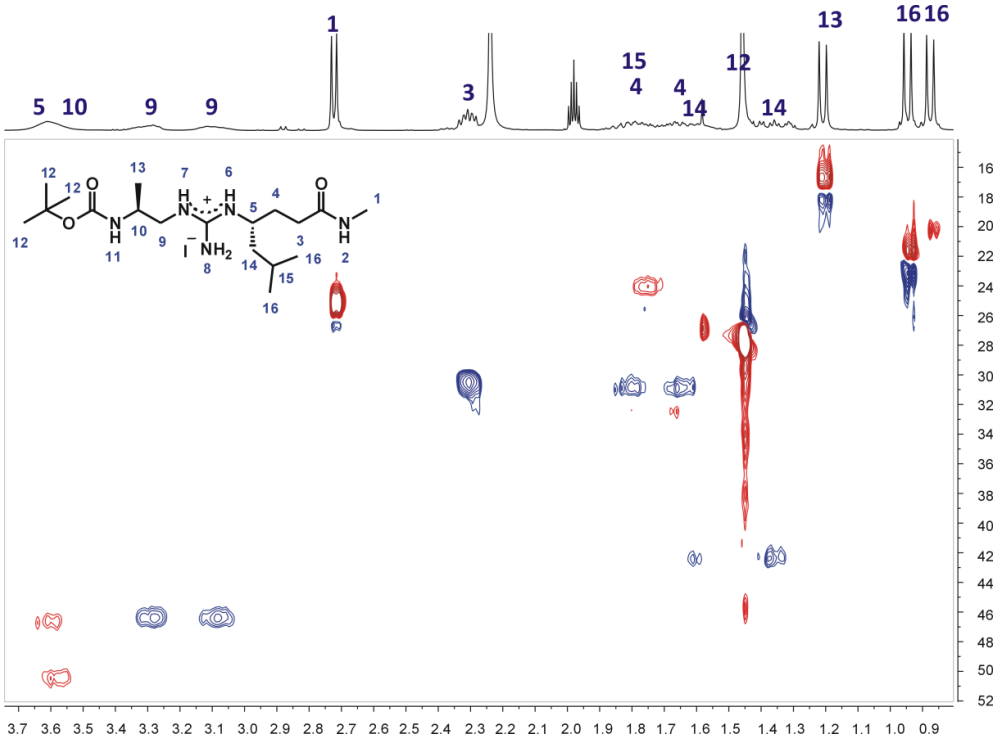

Figure S63. 2D-HSQC-NMR spectrum of **15** in CD_3CN (75 MHz) with signal assignments

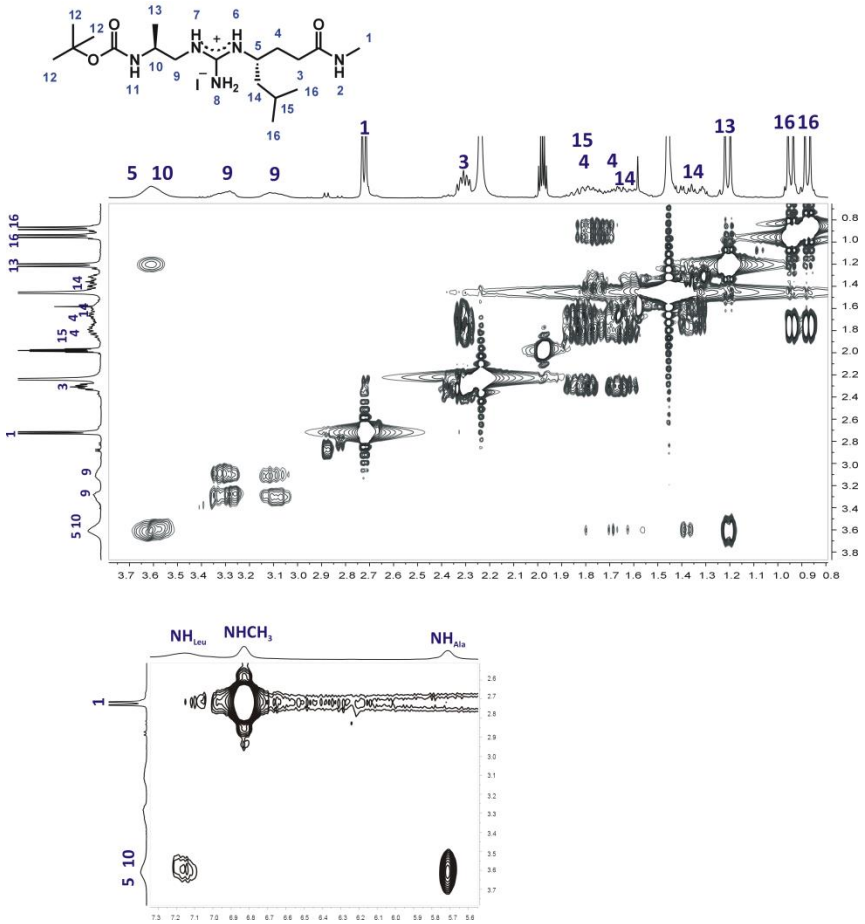

Figure S64. Zoom of the 2D-COSY CH/CH and NH/CH regions of **15** (300 MHz) with signal assignments

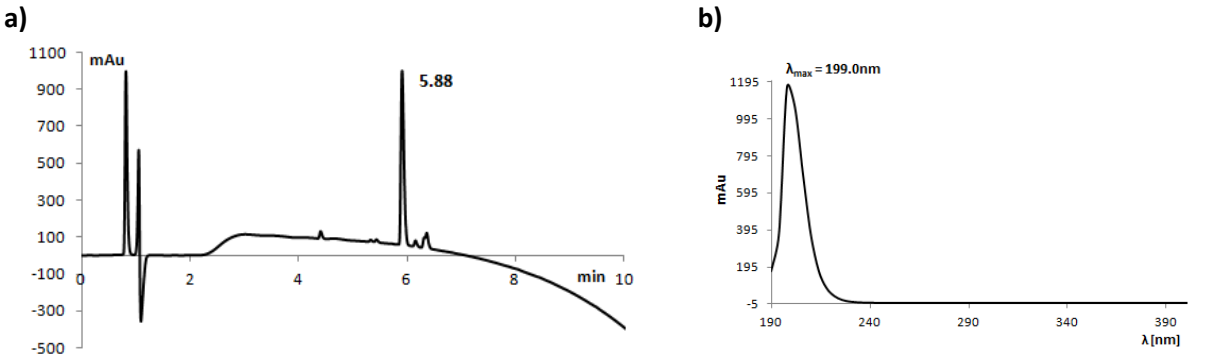

Figure S65. a) RP-HPLC chromatogram (λ = 200nm, 10−100% B in 10 min) and b) UV spectrum of **15**

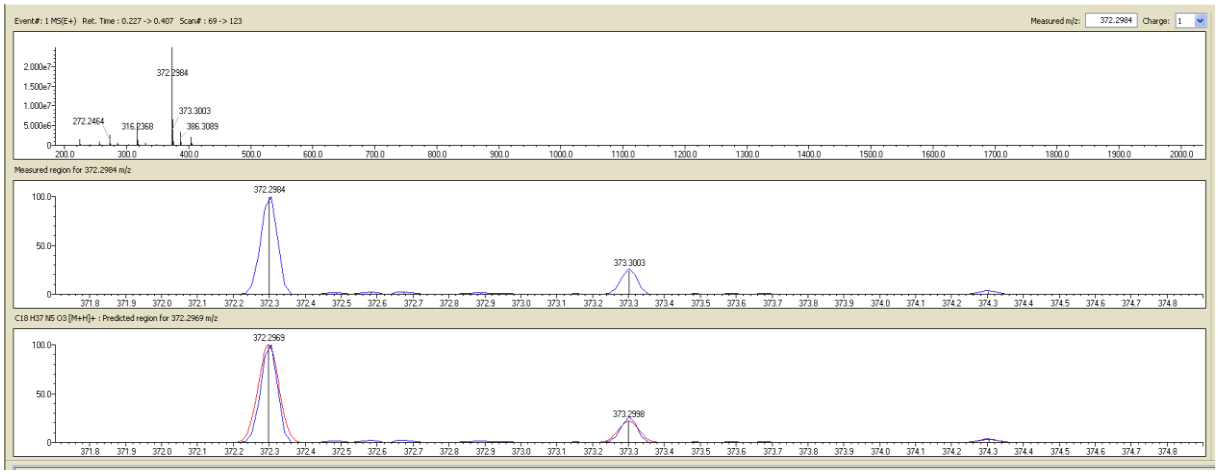

Figure S66. HRMS (ESI-TOF) spectra of compound 15.

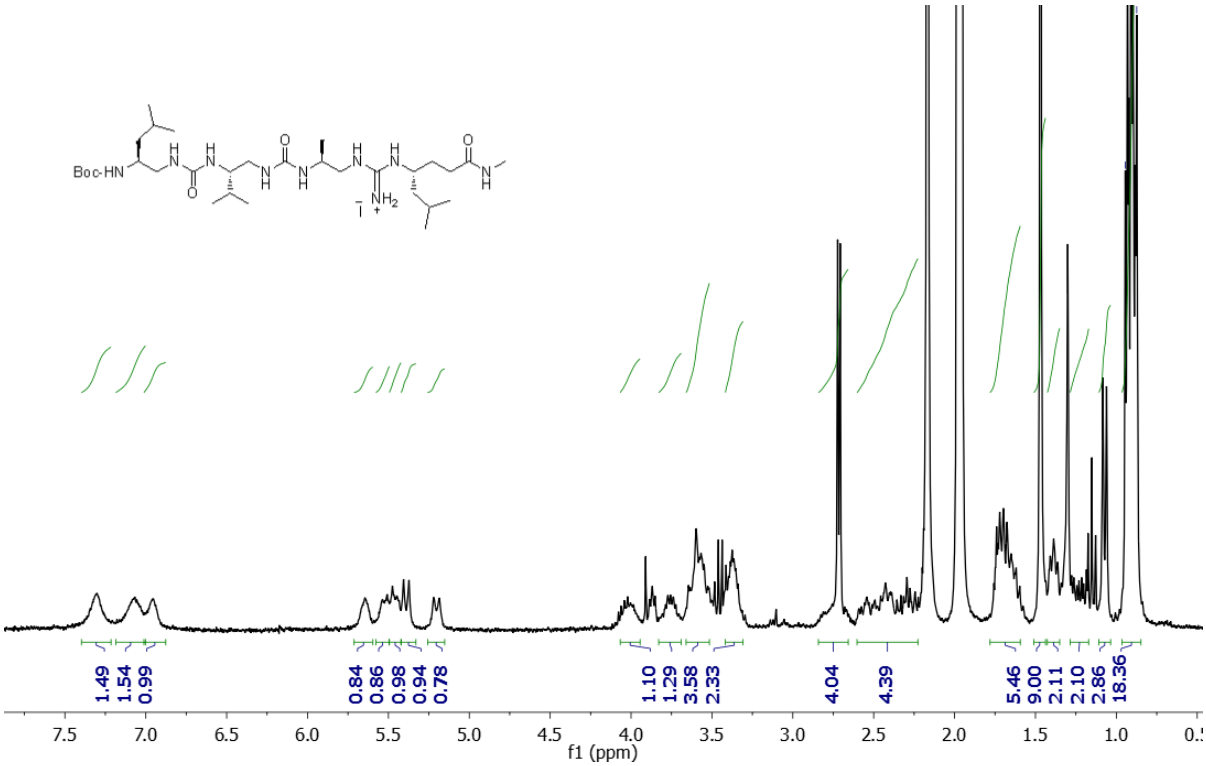

Figure S67.[1]H-NMR spectrum of compound **16** in CD_3CN (300 MHz)

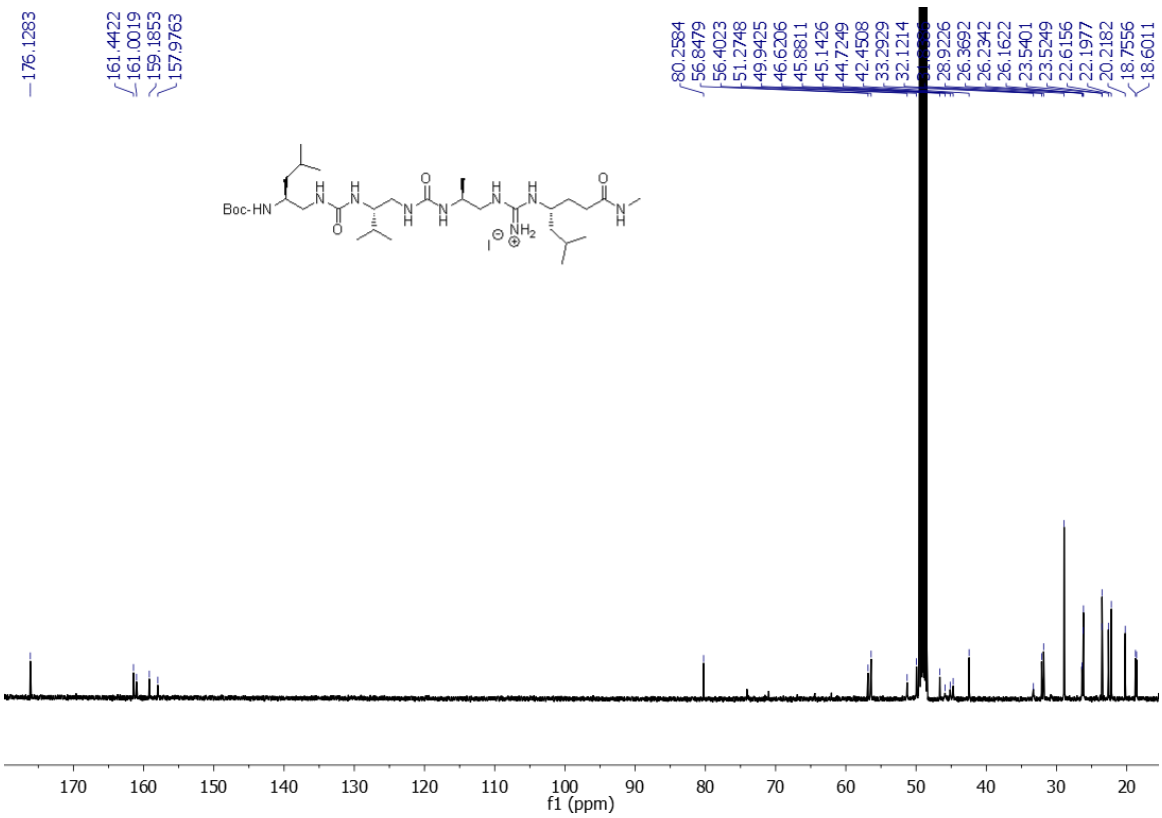

Figure S68.[13]C-NMR spectrum of compound **16** (125MHz, CD_3OD, cryoprobe)

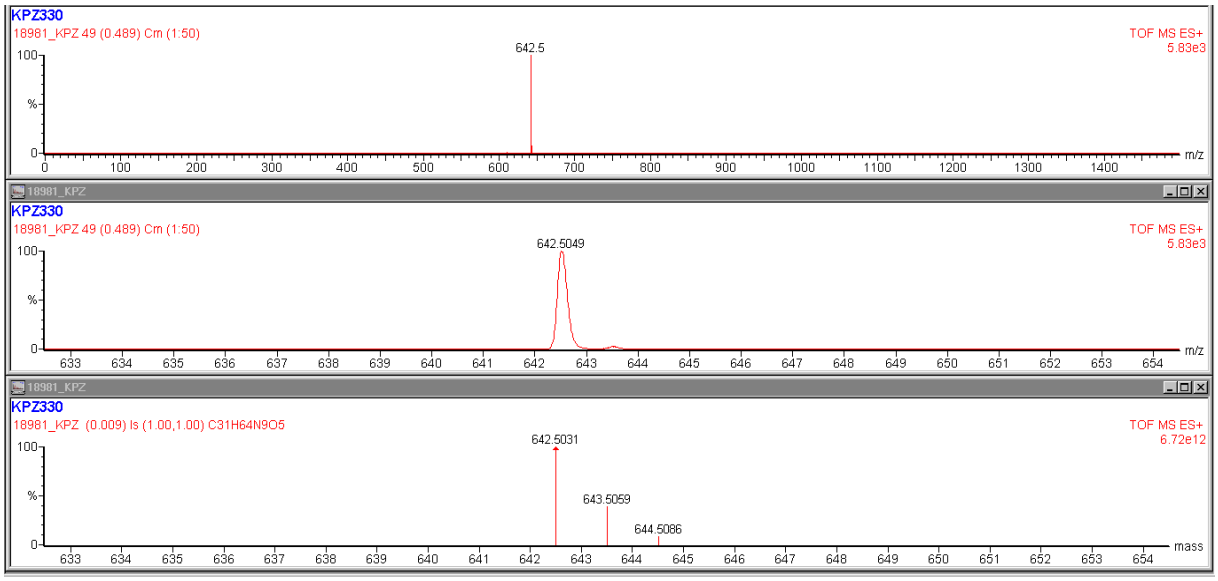

Figure S69. HRMS (ESI-TOF) spectra of compound **16**

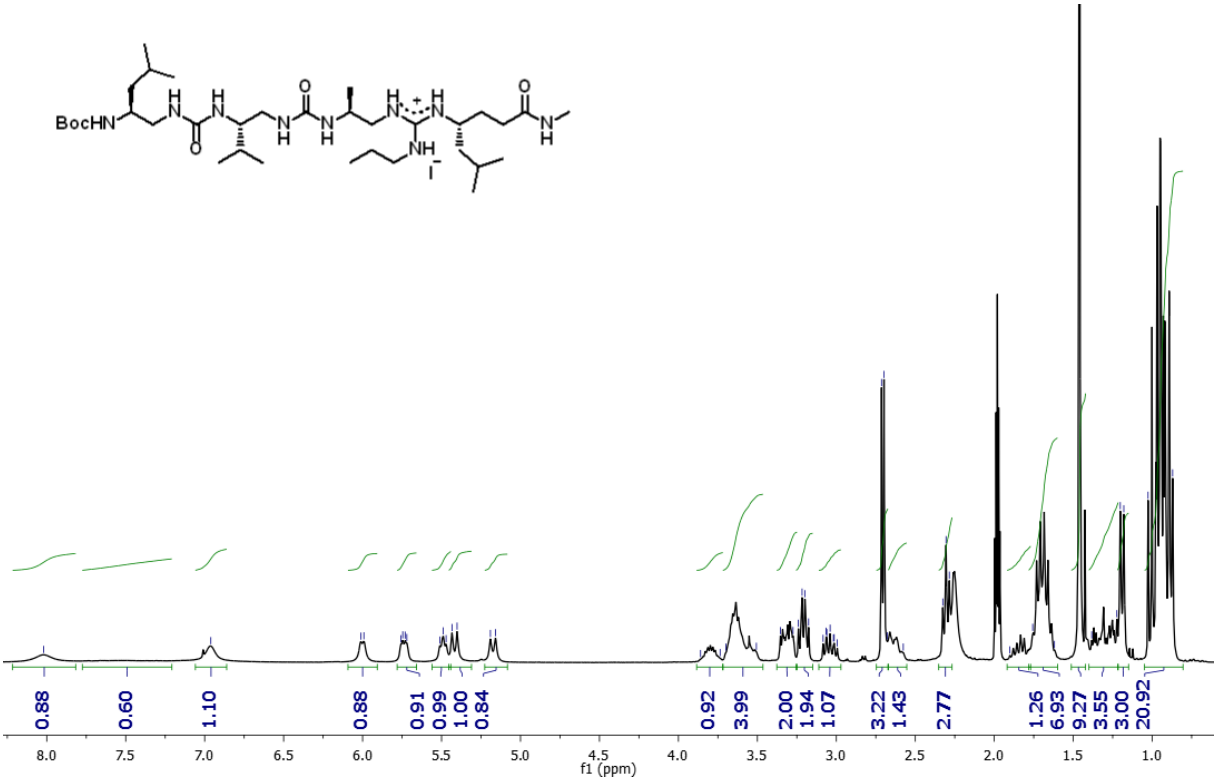

Figure S70. ^{1}H-NMR spectrum of **17** in CD_3CN (300 MHz)

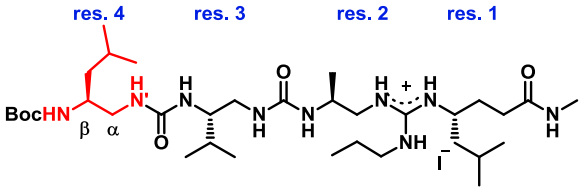

Table S5. ^{1}H-NMR chemical shifts (ppm) of **17** in CD_3CN (300MHz)

Residue	HN	HN	$^{\alpha}CH^{1}$	$^{\alpha}CH^{2}$	$^{\beta}CH$	$^{\gamma}CH$	$^{\delta}CH$	$^{\varepsilon}CH$	other
$HNCH_3$	6.96	-	-	-	-		-	-	2.71
γLeu	not visible		2.31		1.83 **$^{\beta}CH^{1}$** 1.71 **$^{\beta}CH^{2}$**	3.65	1.36/1.72	1.73	0.97/ 0.95-
Ala^{G}	6.00 (*J*=6.0)	-	3.32	3.04	3.65	1.19	-	-	-
Val^{U}	5.74 (*J*=8.0, 3.4)	5.17 (*J*=9.6)	3.54	2.62	3.67	1.74	0.91	-	-
Leu^{U}	5.42 (*J*=9.7)	5.49 (*J*=6.0)	3.32	2.66	3.80	1.25 /1.30	1.65	0.97/0.92	-
***n*PrNH**	8.02	-	-	-	-	-	-	-	0.99 1.70 3.20
Boc	-	-	-	-	-	-	-	-	1.46

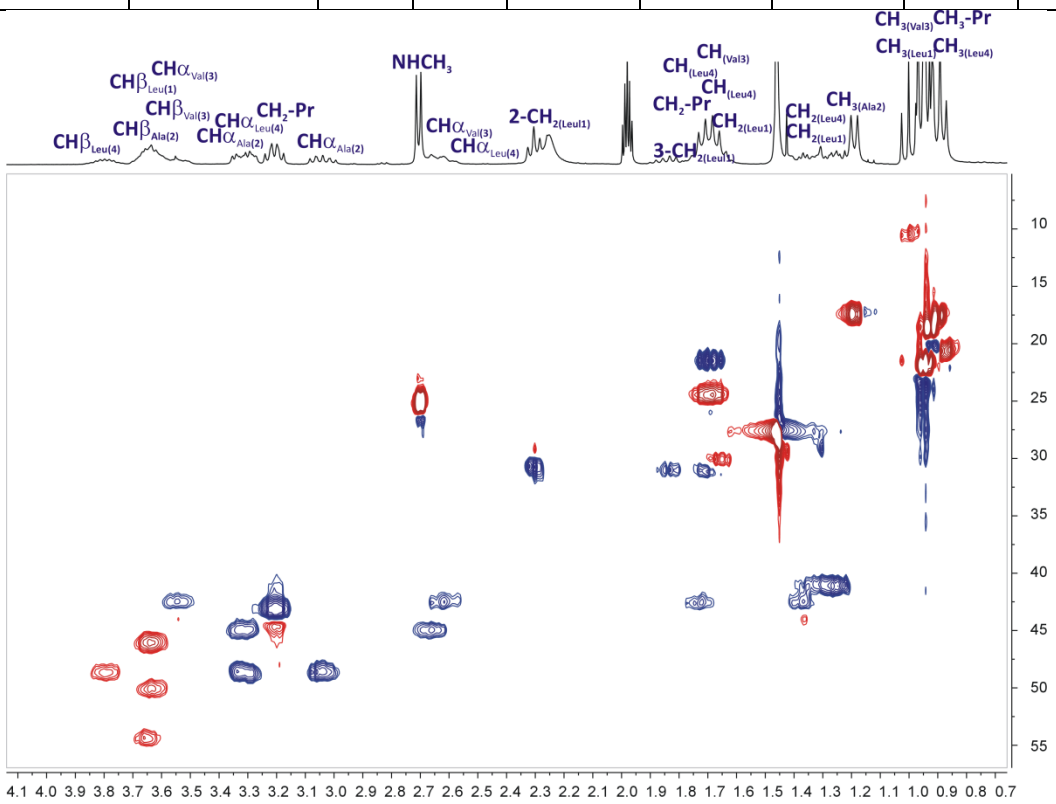

Figure S71. 2D-HSQC-NMR spectrum of **17** in CD_3CN (75 MHz) with signal assignments

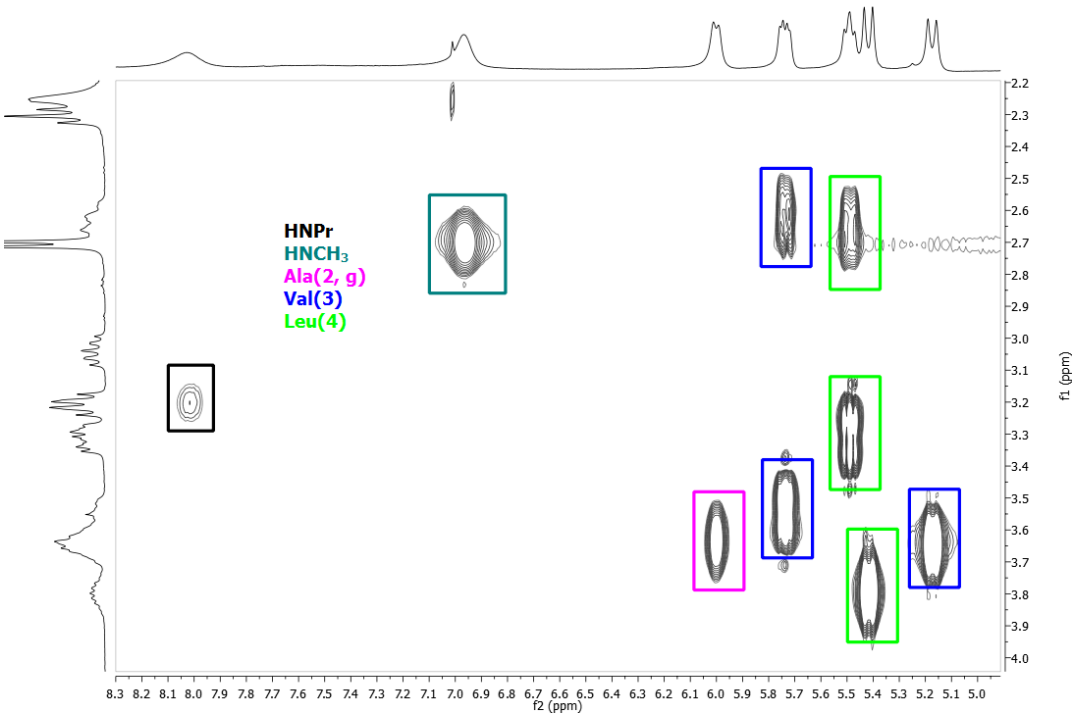

Figure S72. Zoom of the 2D-COSY NH/β-CH and N'H/α-CH regions of **17** recorded in CD_3CN (3mM, 300MHz)

a) b)

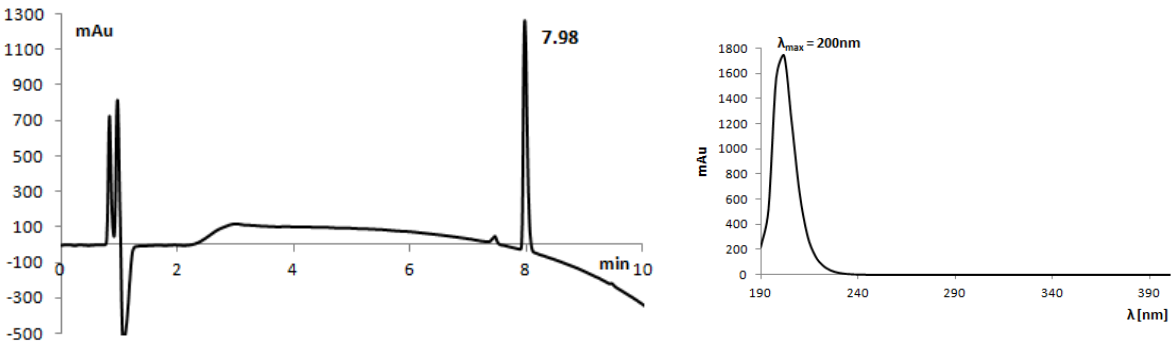

Figure S73 a) RP-HPLC chromatogram (λ = 200nm, 10−100% B in 10 min) and b) UV spectrum of **17**

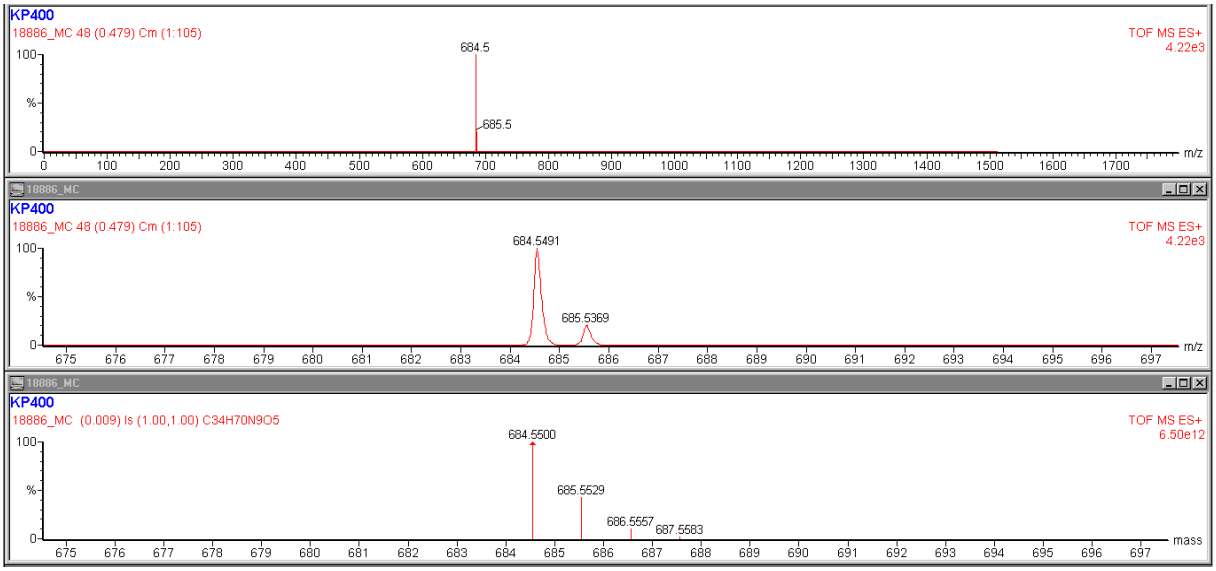

Figure S74. HRMS (ESI-TOF) spectrum of **17**

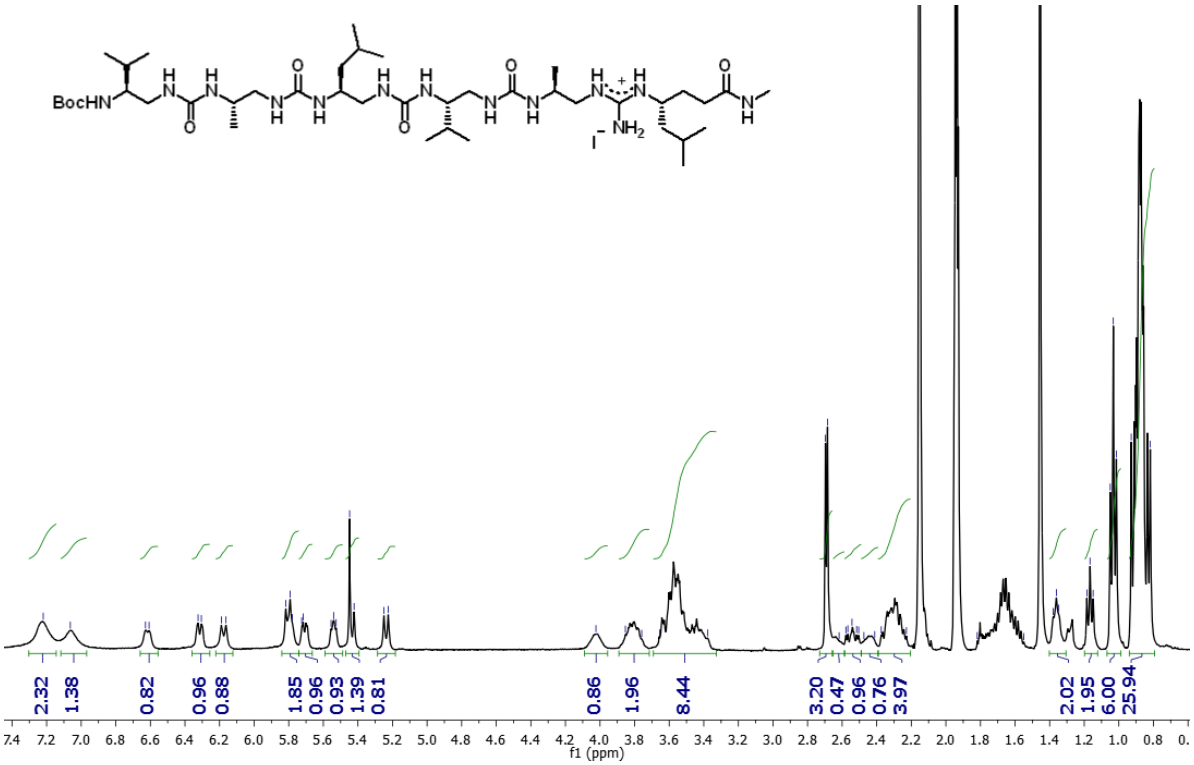

Figure S75. ^{1}H-NMR spectrum of **18** in CD_3CN (300 MHz)

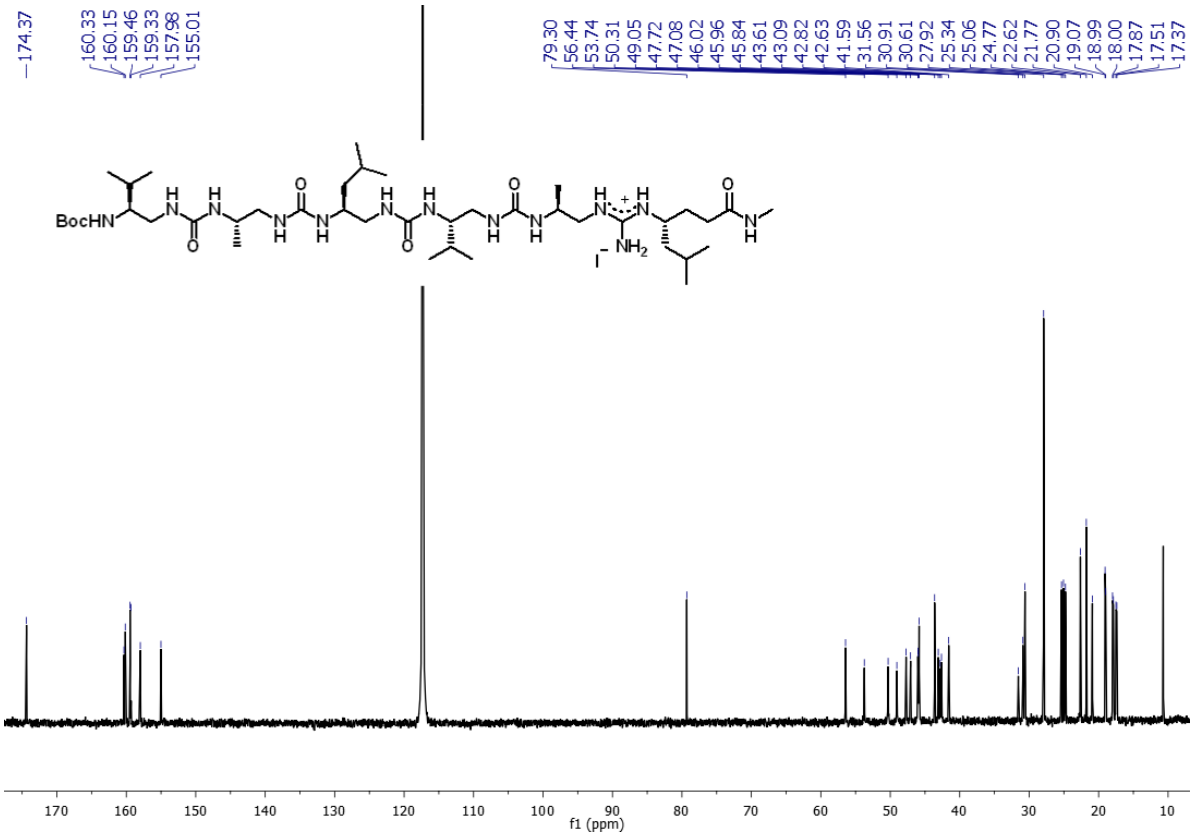

Figure S76. ^{13}C-NMR spectrum of **18** in CD_3CN (75 MHz)

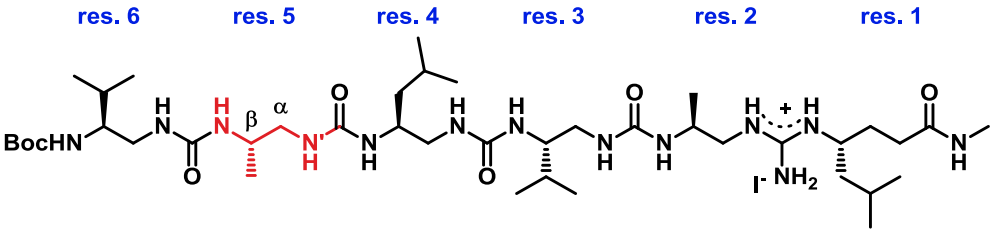

Table S6. ^{1}H-NMR chemical shifts (ppm) of **18** in CD_3CN (3mM, 400MHz)

Residue	HN	HN'	$^{\alpha}CH^{1}$	$^{\alpha}CH^{2}$	$^{\beta}CH$	$^{\gamma}CH$	$^{\delta}CH$	$^{\varepsilon}CH$	other CH
HNMe	7.06	-	-	-	-	-	-		2.72
γLeu	-		2.45	2.25	1.74 $^{\beta}CH^{1}$ 1.69 $^{\beta}CH^{2}$	3.57	1.36	1.65	0.87-
Ala^{G}	5.79	7.23	3.41	2.65	4.05	1.01	-	-	-
Val^{U}	6.18 (*J* = 10.7)	6.31 (*J* = 9.6, 2.1)	3.60	2.31	3.59	1.59	0.85	-	-
Leu^{U}	5.81	6.62 (*J* = 10.2)	3.58	2.29	3.84	1.17	1.67	0.88	-
Ala^{U}	5.24 (*J* = 10.0)	5.71 (*J* = 9.6, 3.2)	3.55	2.35	3.81	1.02	-	-	-
Val^{U}	5.43 (*J* = 10.3)	5.54 (*J* = 6.8, 4.9)	3.58	2.54	3.47	1.64	0.86	-	-
NH-G	7.23	-	-	-	-	-	-	-	-
Boc	-	-	-	-	-	-	-	-	1.46

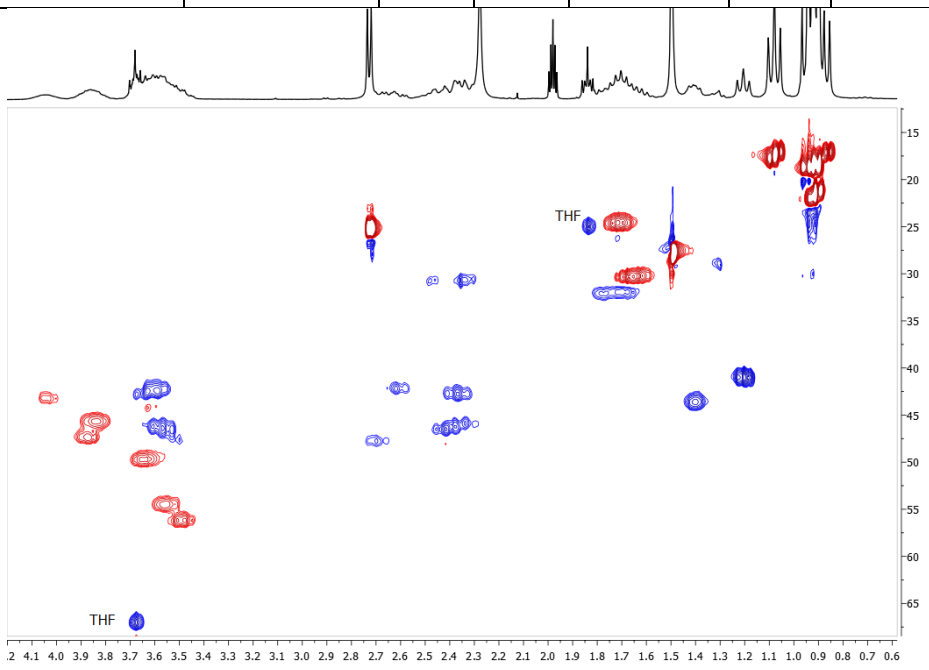

Figure S77. 2D-HSQC-NMR spectrum of **18** in CD_3CN (75 MHz)

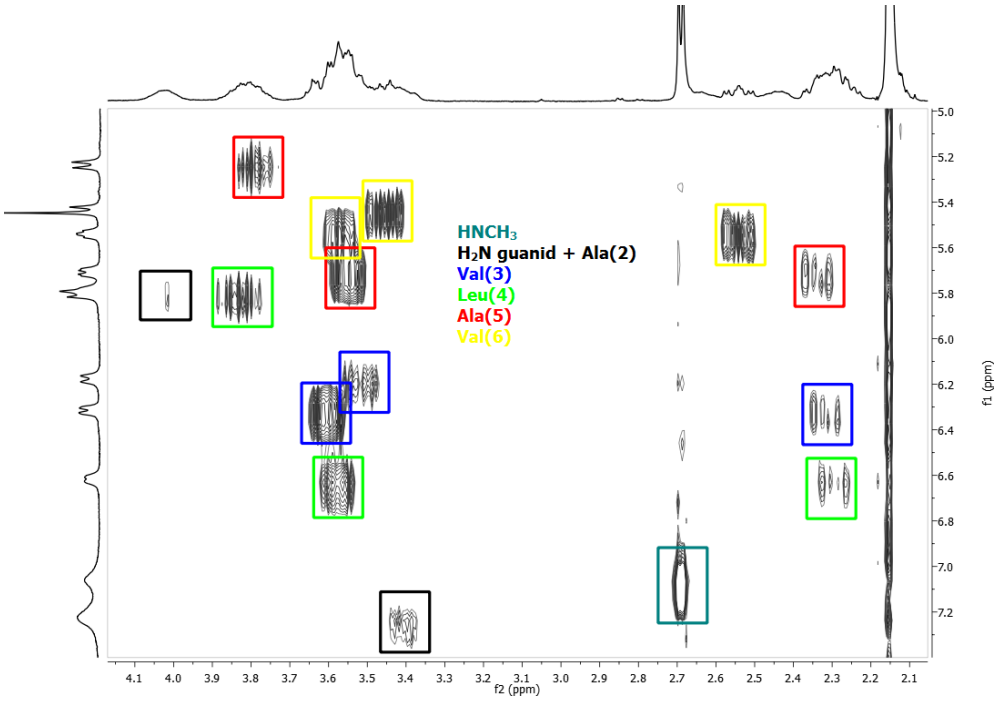

Figure S78. Zoom of the 2D-COSY NH/$^{\beta}$CH and N'H/$^{\alpha}$CH regions of **18** in CD_3CN (3mM, 400MHz)

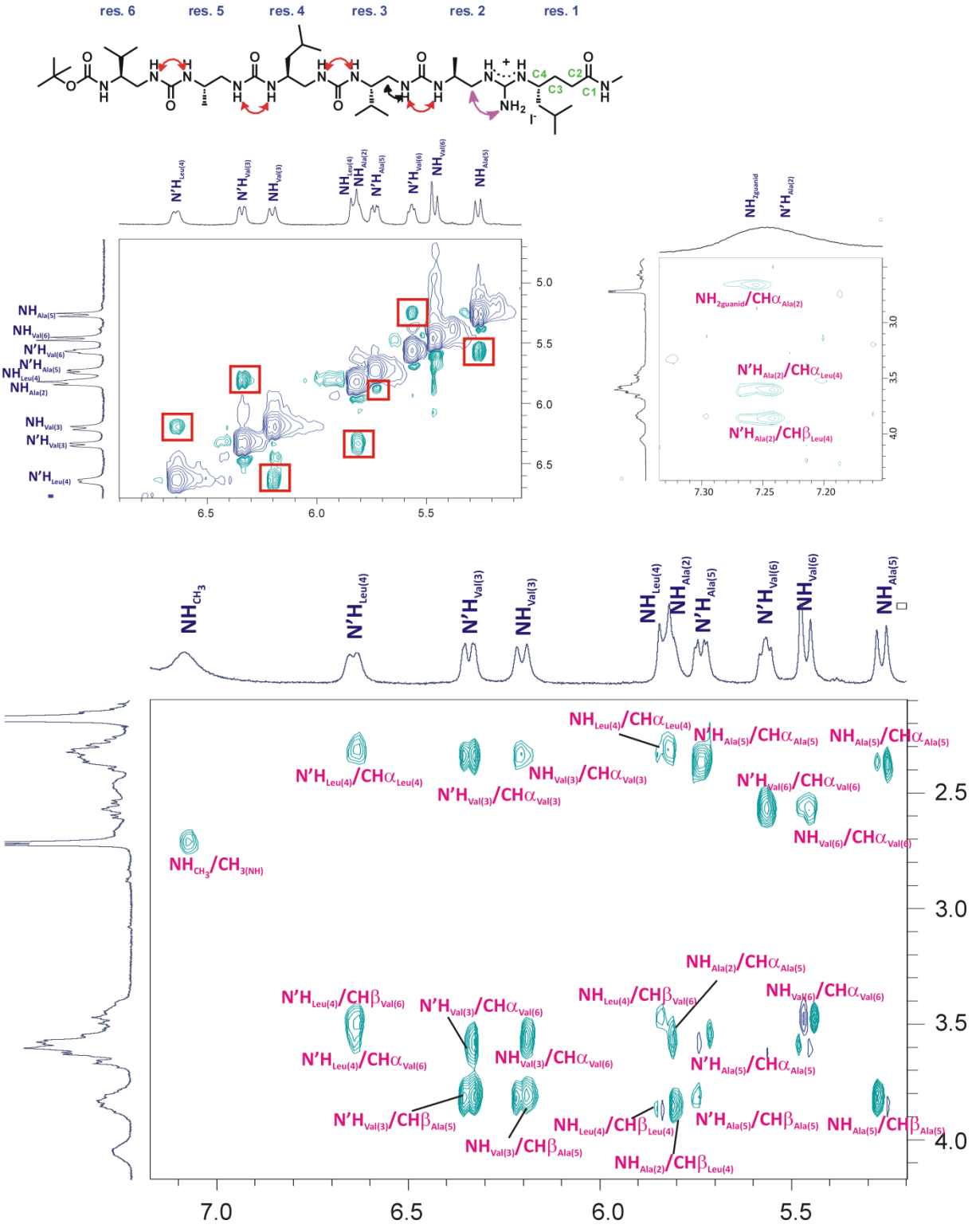

Figure S79. Zoom of 2D-ROESY NH/CH region of **18** in CD_3CN (300 MHz)

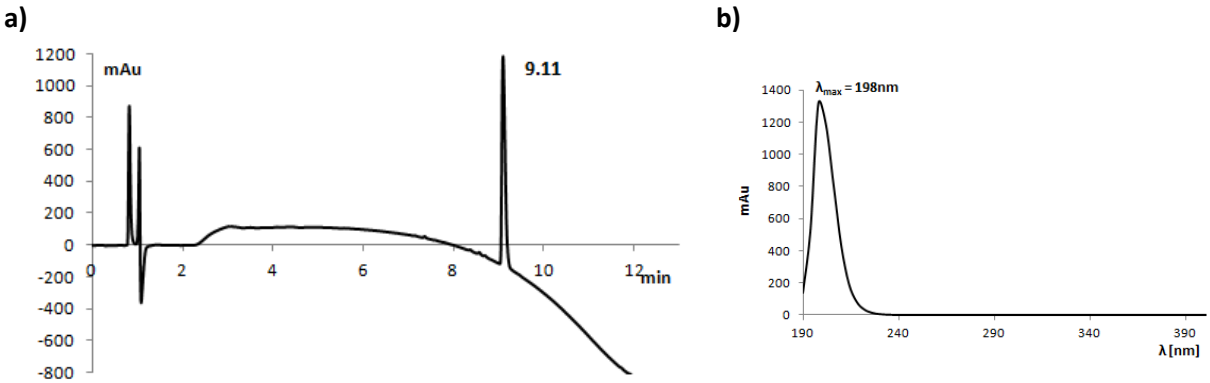

Figure S80. a) RP-HPLC chromatogram (λ = 200nm, 10−100% B in 10 min) and b) UV spectrum of **18**

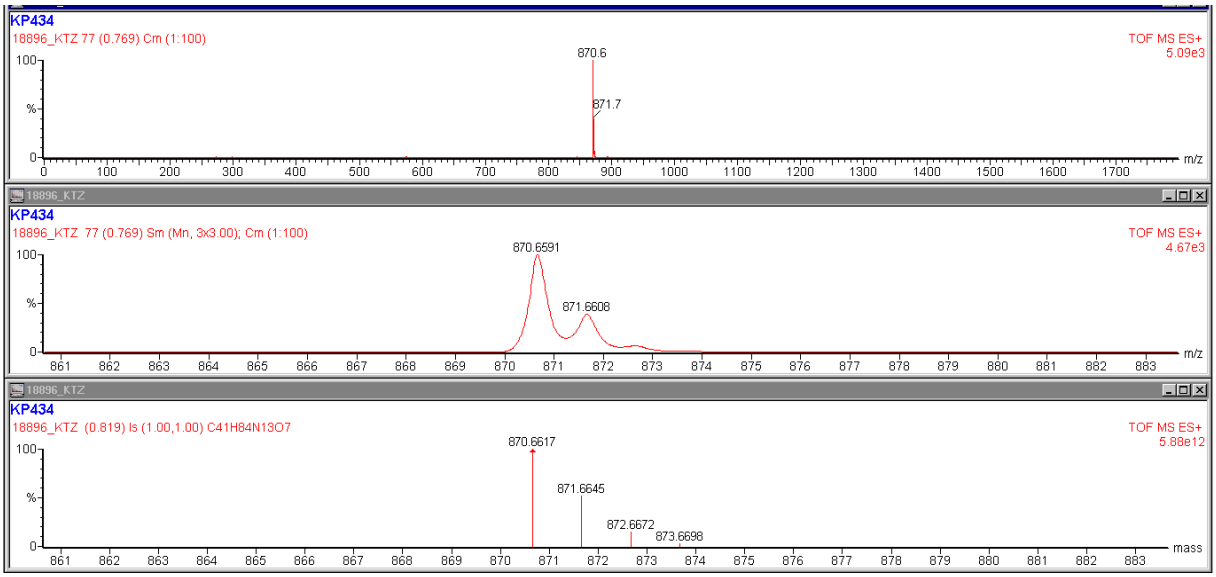

Figure S81. HRMS (ESI-TOF) spectra of compound **18**

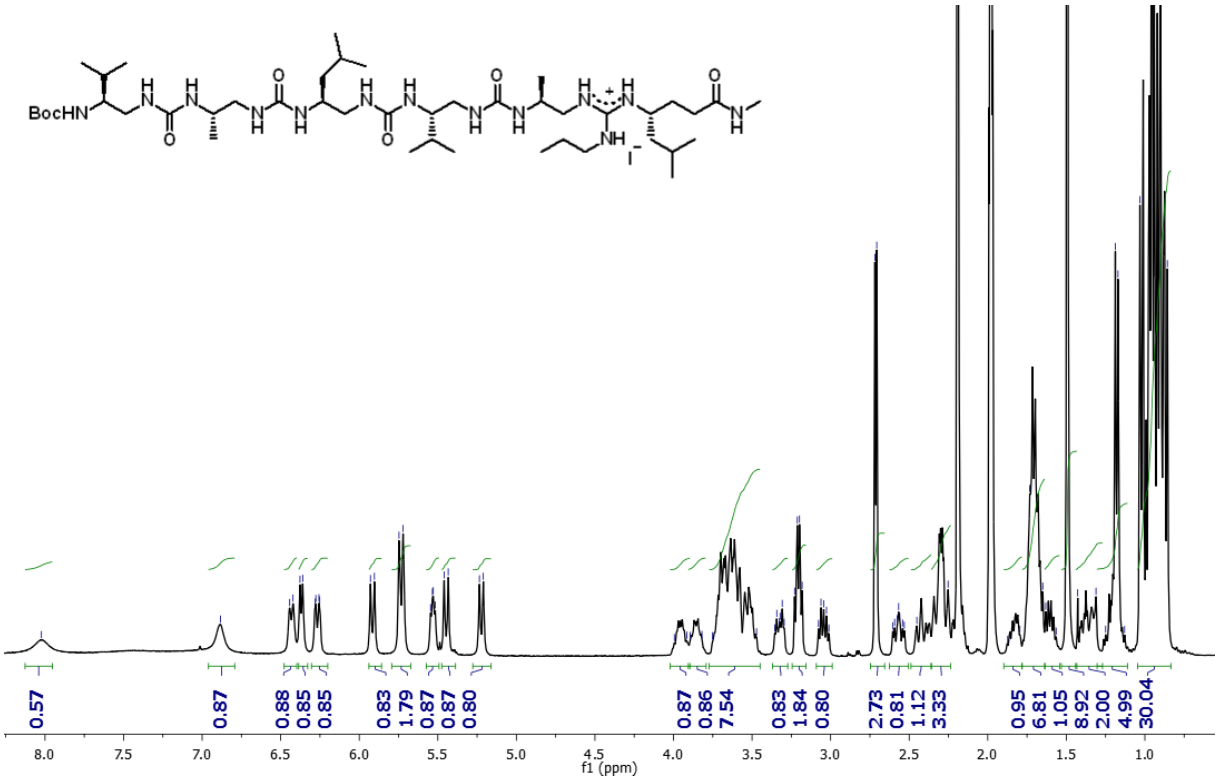

Figure S82. ^{1}H-NMR spectrum of **19** in CD_3CN (300 MHz)

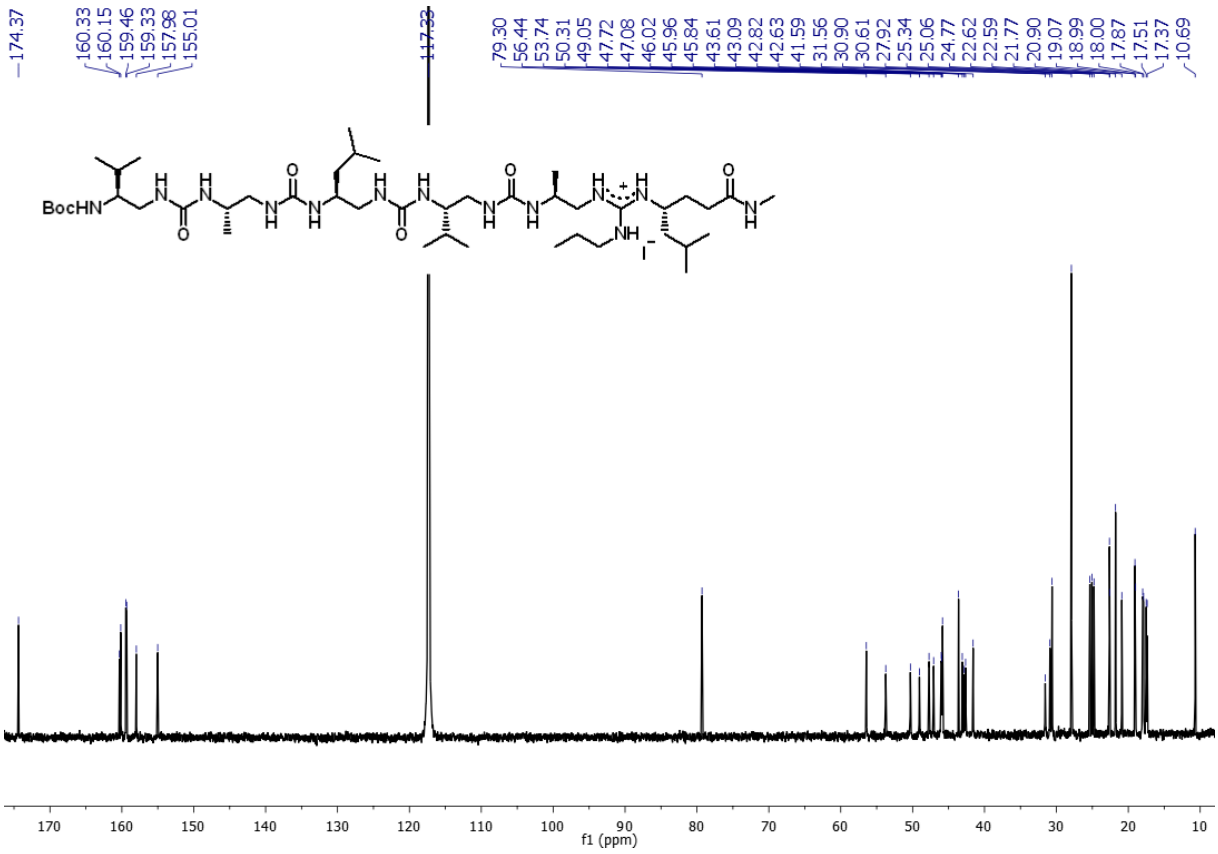

Figure S83. ^{13}C-NMR spectrum of **19** in CD_3CN (75 MHz)

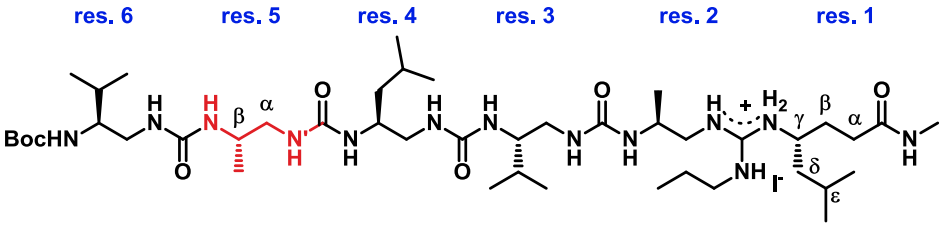

Table S7. ^{1}H-NMR chemical shifts (ppm) of **19** recorded in CD_3CN (3mM, 400MHz)

Residue	HN	HN'	$^{\alpha}CH^{1}$	$^{\alpha}CH^{2}$	$^{\beta}CH$	$^{\gamma}CH$	$^{\delta}CH$	$^{\varepsilon}CH$	other
HNMe	6.87	-	-	-	-	-	-	-	2.71
γLeu	Not visible		2.29	-	1.83 $^{\beta}CH^{1}$ 1.70 $^{\beta}CH^{2}$	3.62	1.46/1.74	1.75	0.9
Ala^{G}	6.37 (*J* = 7.0)	Not visible	3.31	3.03	3.67	1.18	-	-	-
Val^{U}	5.92 (*J* = 10.1)	6.43 (*J* = 8.5)	3.66	2.41	3.69	1.61	0.9/0.85	-	-
Leu^{U}	5.72	6.26 (*J* = 7.9)	3.60	2.25	3.95	1.18	1.01/0.93	1.72	-
Ala^{U}	5.11 (*J* = 10.0)	5.73	3.53	2.31	3.84	1.01	-	-	-
Val^{U}	5.44 (*J*=10.3)	5.53 (*J*=6.9, 4.8)	3.60	2.54	3.51	1.67	0.95/0.90		
***n*PrNH**	8.02								0.91 1.69 3.20
Boc	-	-	-	-	-	-	-	-	1.49

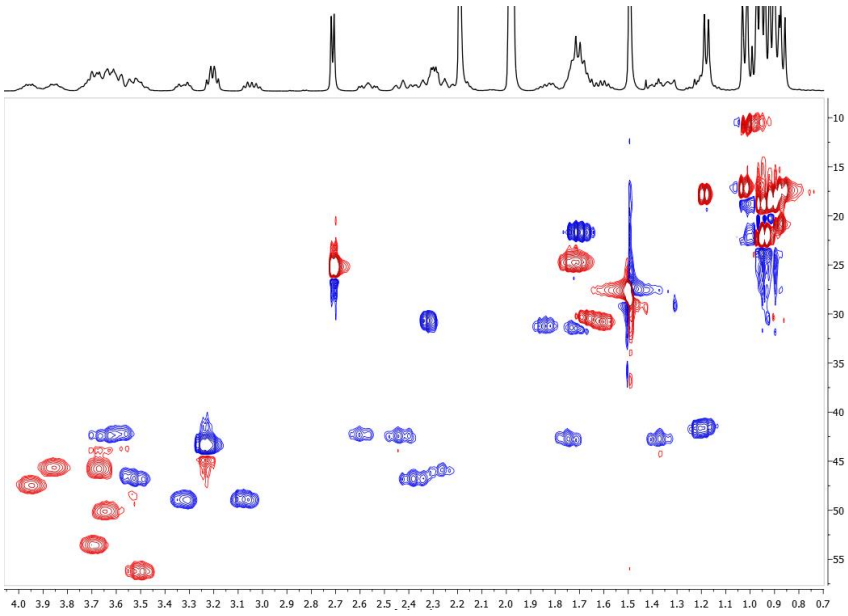

Figure S84. 2D-HSQC-NMR spectrum of **19** in CD_3CN (75 MHz)

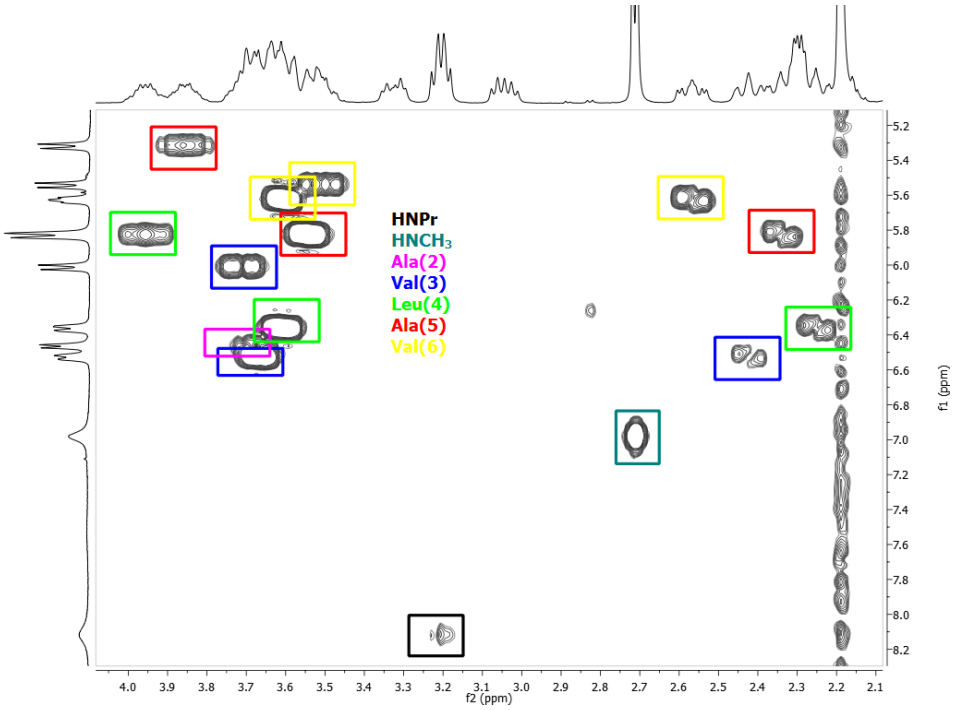

Figure S85. Zoom of the 2D-COSY NH/β-CH and N'H/α-CH regions of **19** in CD_3CN (3mM, 400MHz)

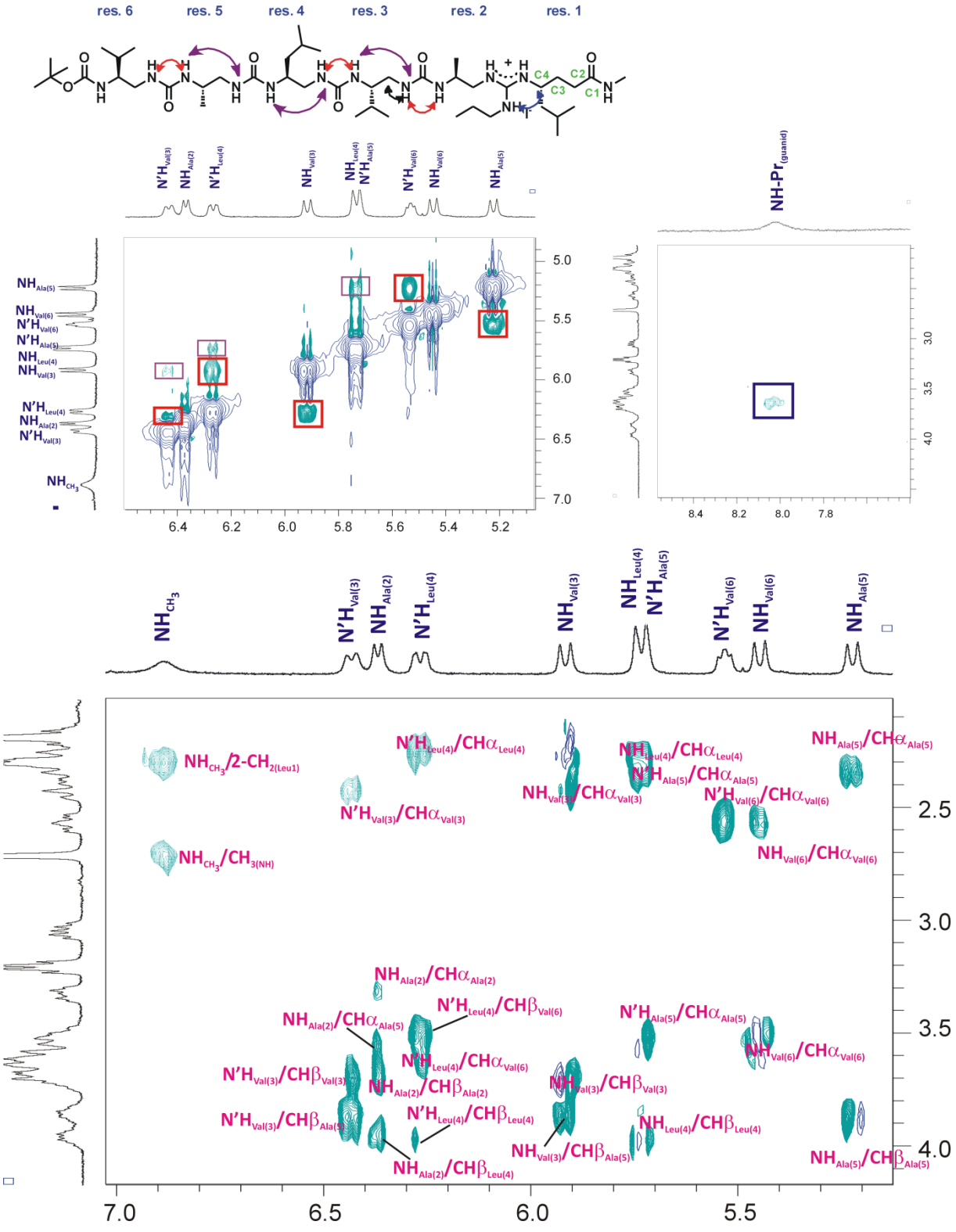

Figure S86. Zoom of the 2D-ROESY NH/CH region of **19** in CD_3CN (300 MHz)

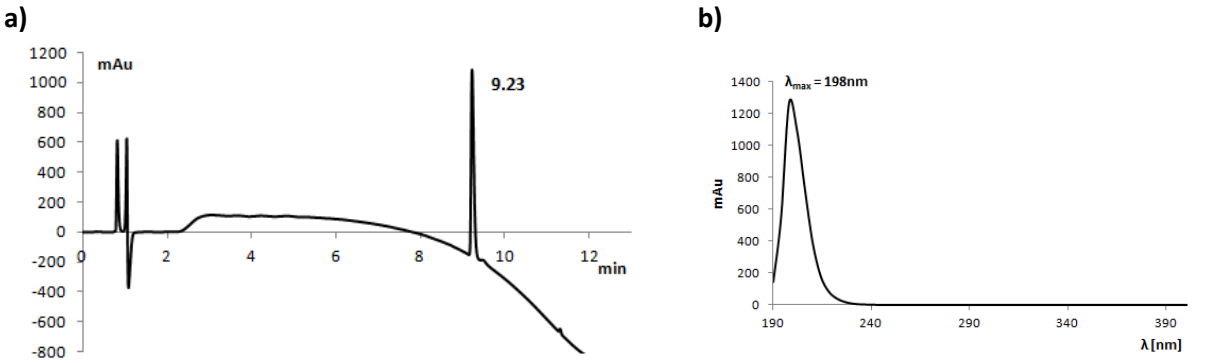

Figure S87. a) RP-HPLC chromatogram (λ = 200nm, 10−100% B in 10 min) and b) UV spectrum of **19**

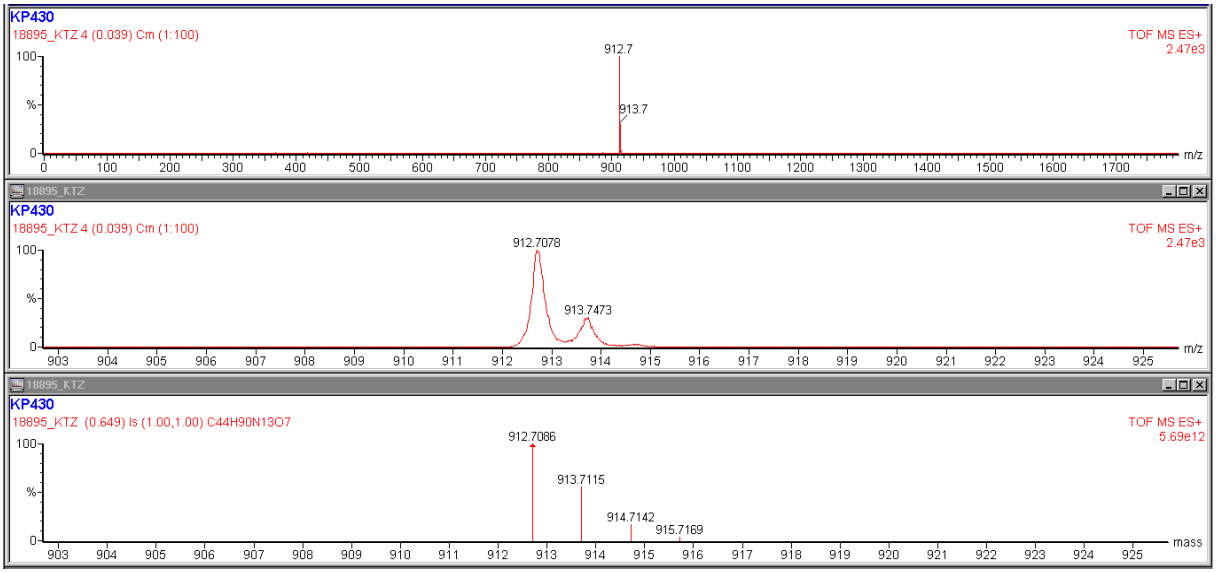

Figure S88. HRMS (ESI-TOF) spectra of **19**

5. *NMR characterizations, RP-HPLC chromatograms, ESI-MS analyses and CD spectra of oligomers 20 and 22*

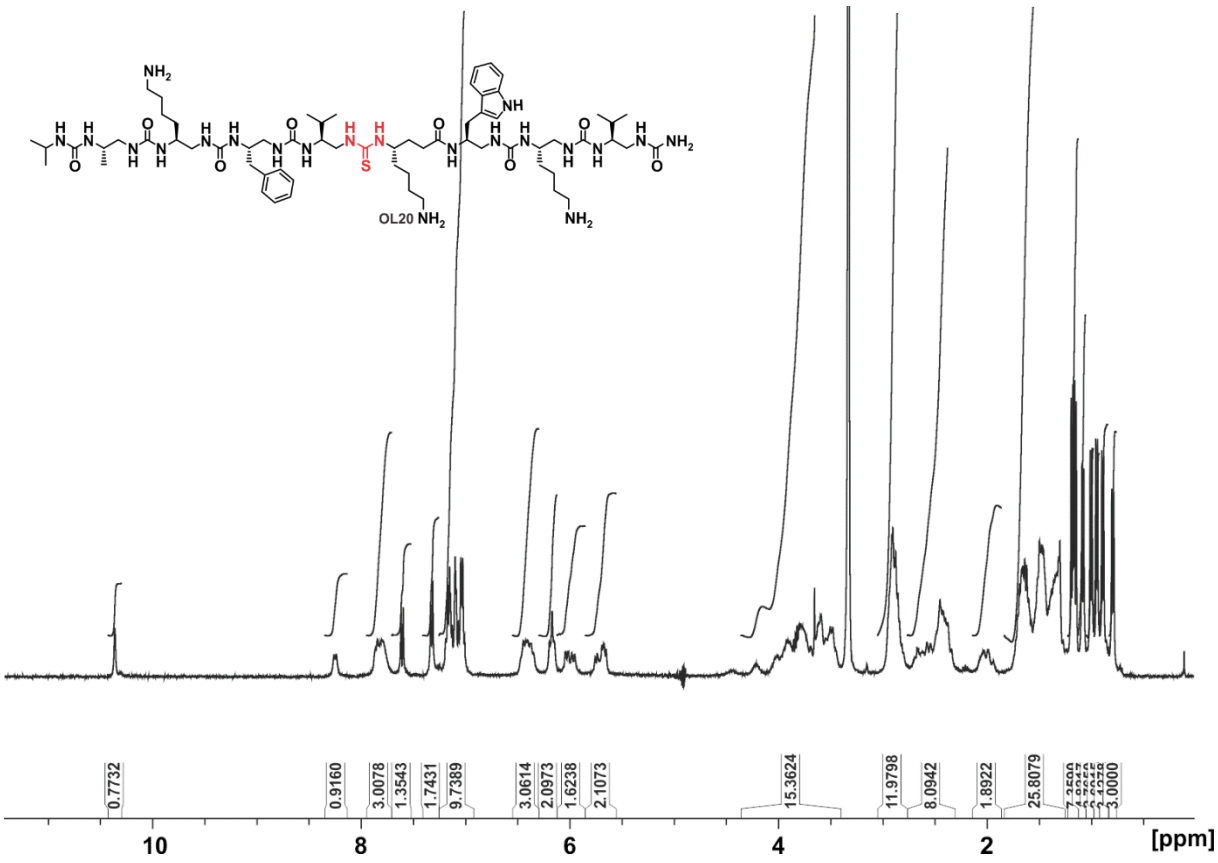

Figure S89. ^{1}H-NMR spectrum of oligo(thio)urea **20** in CD_3OH at 293K (2.5 mM).

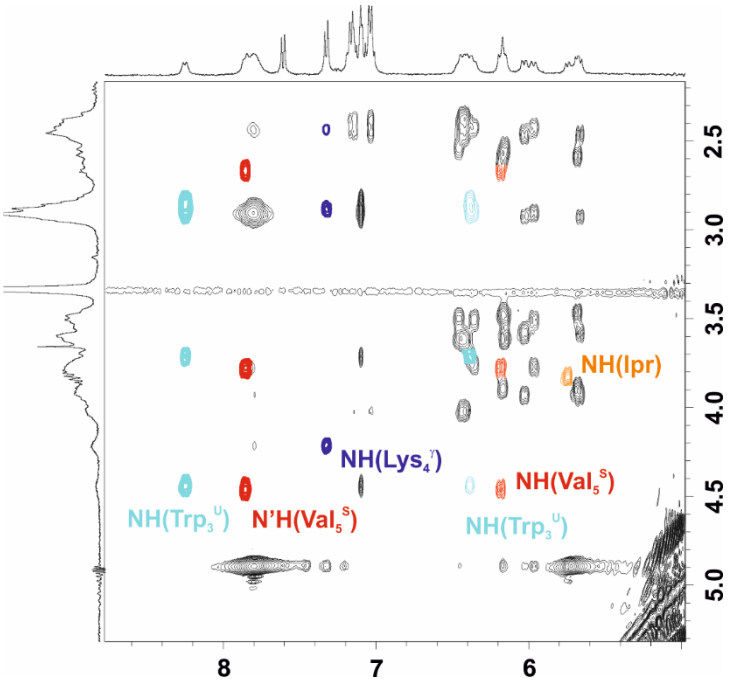

Figure S90. Zoom of the 2D-TOCSY NH/CH region of **20** showing the key residue signal assignments.

Table S8. ^{1}H-NMR Chemical Shifts (ppm) of **20** in CD_3OH at 293K (2.5 mM).

Residue		NH	N'H	$^{\alpha}CH^{1}$	CH_2	$^{\alpha}CH^{2}$	$^{\beta}CH$	$^{\gamma}CH$	$^{\delta}CH$	$^{\varepsilon}CH$	NH side chain	Arom	$\Delta\delta(^{\alpha}CH)$
Val^{u}	1	6.16	6.46	3.50		2.55	3.61	1.58	0.79 0.88				0.95
Lys^{u}	2	5.66	6.0	3.58		2.47	3.92	1.68 1.33	1.50 1.49	2.93	7.8		1.11
Trp^{u}	3	8.25	6.38	3.71		2.84	4.44	2.88			10.36	7.10/7.61 7.32/7.03	0.87
Lys^{γ}	4	7.32		1.46	2.43 1.98	1.25	4.21	1.63 1.38	1.64	2.88	7.8		0.22
Val^{s}	5	6.18	7.85	4.46		2.66	3.77	1.70	0.95 1.01				1.79
Phe	6	6.42	6.42	3.62		2.38	4.028	2.45			10.2	7.03/7.03 7.16	1.24
Lys	7	5.97	6.36	3.51		2.42	3.768	1.65 1.31	1.51 1.45	2.90	7.80		1.08
Ala^{u}	8	5.68	6.17	3.46		2.5	3.9	1.08					0.88
IprNH		5.74					3.83	1.17					

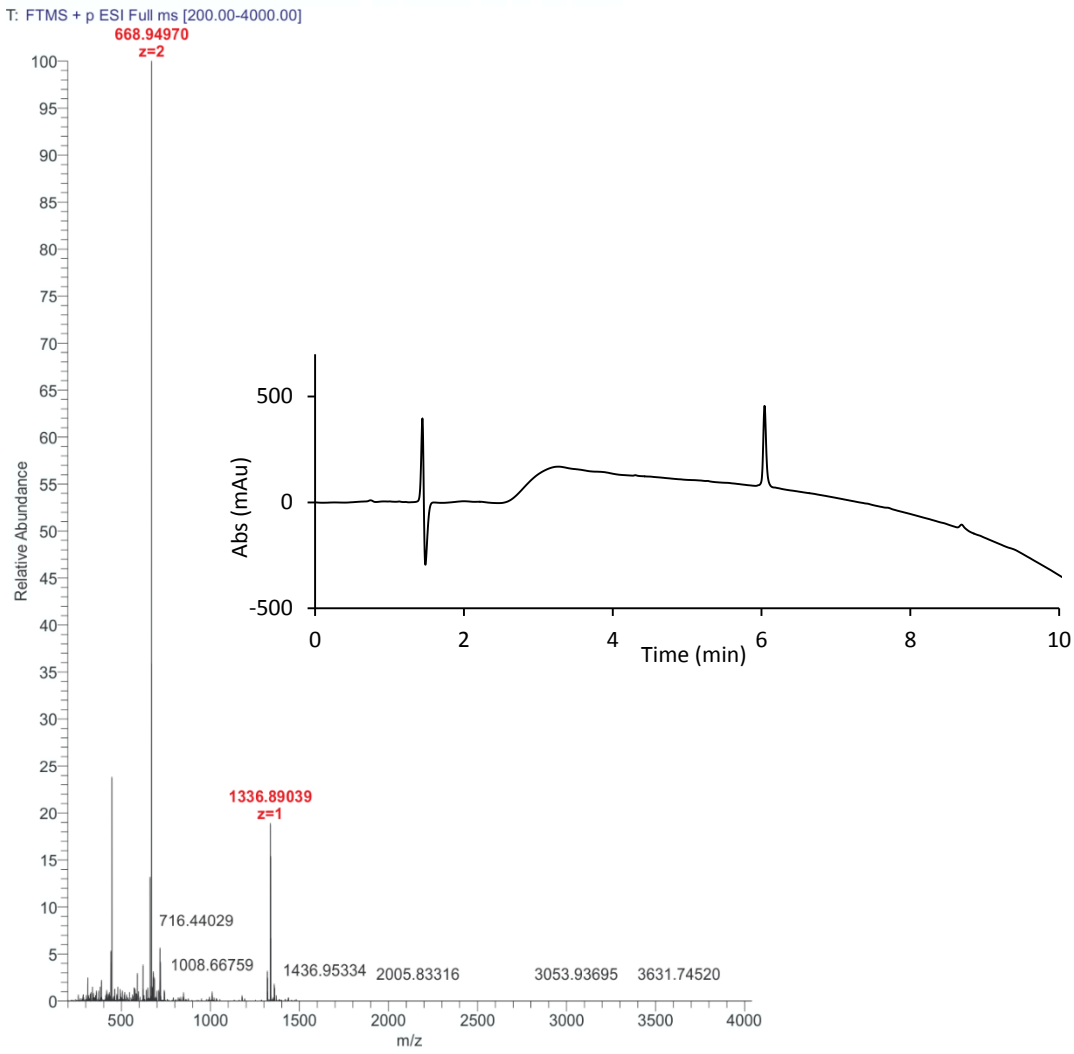

Figure S91. HRMS (ESI) spectrum and RP-HPLC chromatogram of **20** after purification (10-100% of B in 10 min, UV 200 nm).

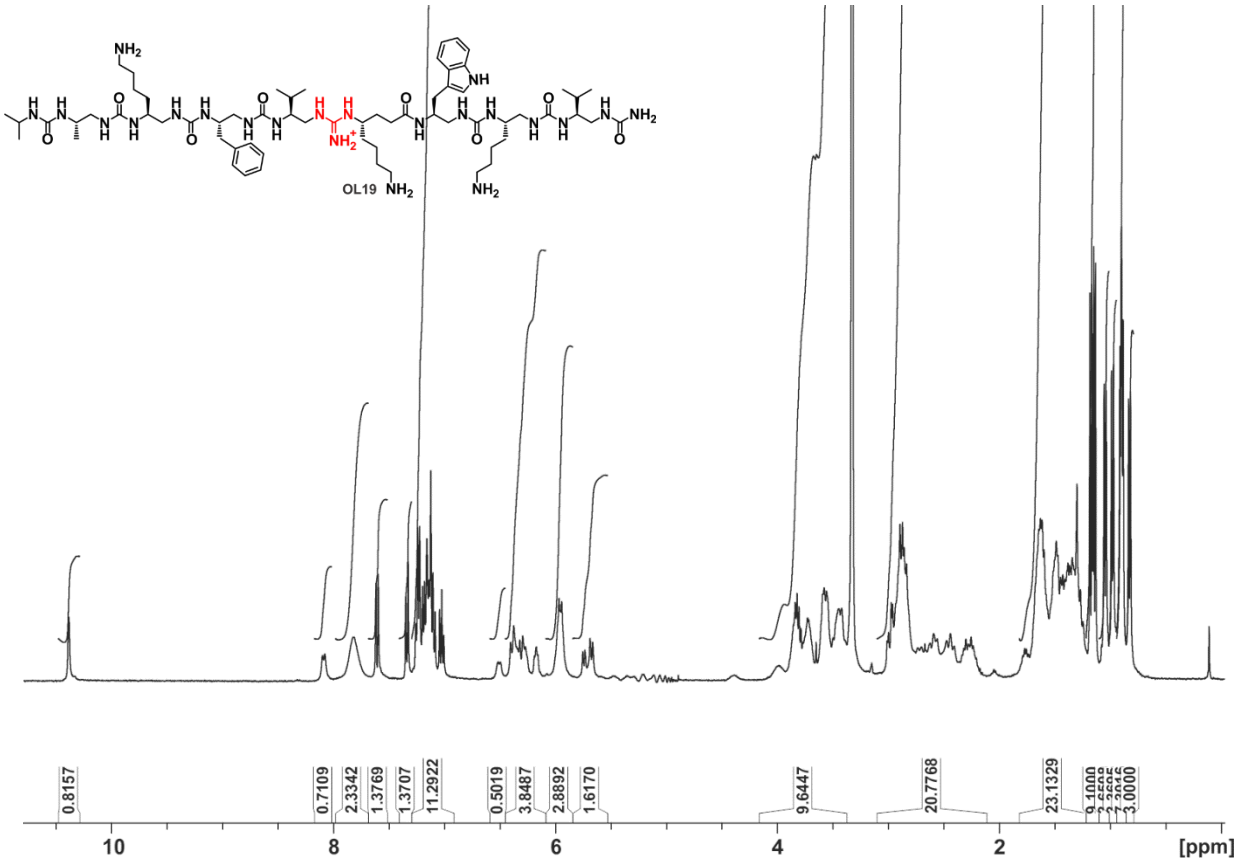

Figure S92. ^{1}H-NMR spectrum of hybrid octamer **22** in CD_3OH at 293K (2.5 mM).

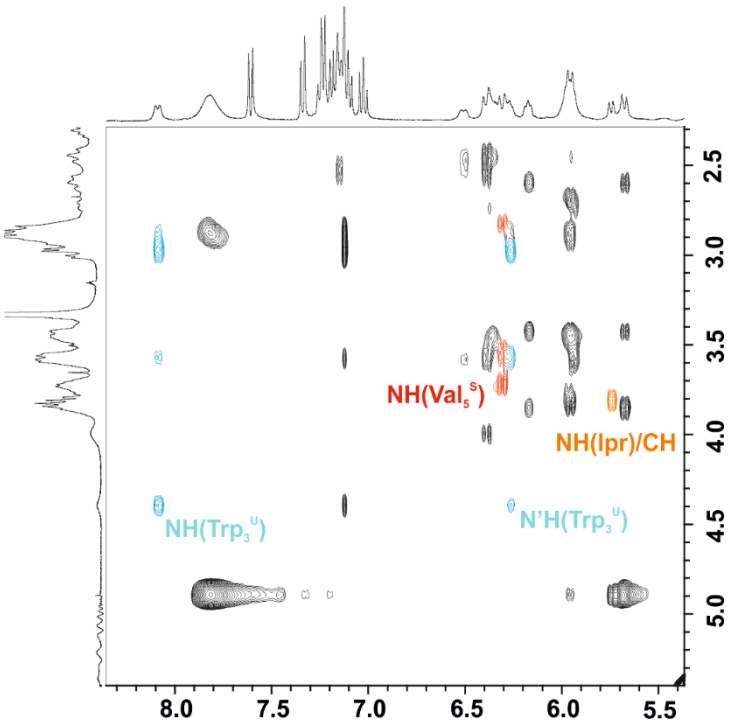

Figure S93. Zoom of the 2D-TOCSY NH/CH region of **22** showing the key residue signal assigments.

Table S9. ^{1}H-NMR Chemical Shifts (ppm) of **22** in CD_3OH at 293K (2.5 mM).

Residue		NH	N'H	CH_2	$^{\alpha}CH^{1}$	$^{\alpha}CH^{2}$	$^{\beta}CH$	$^{\gamma}CH$	$^{\delta}CH$	$^{\varepsilon}CH$	NH Side chain	Arom	Δδ ($^{\alpha}CH$)
Val^{u}	1	5.94	6.38		3.45	2.74	3.56	1.61	0.89 0.83				0.72
Lys^{u}	2	5.95	6.35		3.44	2.44	3.74	1.62 1.29	1.48 1.43	2.88	7.82		1.00
Trp^{u}	3	8.09	6.27		3.57	2.97	4.39	2.88			10.38	7.12/7.35 7.59	0.60
Lys$^{\gamma}$	4	*ND*		2.25 2.31	1.62	1.5	3.35	1,56, 1.26 overlapping signals		2.83			0.27
Val^{gua}	5	6.32	*ND*		3.55	2.84	3.72	1.76	0.90 0.98		7.82		0.71
Phe	6	6.39	6.51		3.57	2.47	3.99	2.56				7.15/7.18 7.23	1.14
Lys	7	5.95	5.99		3.45	2.68	3.86	1.65 1.37	1.49	2.90	7.81		0.76
Ala^{u}	8	5.67	6.17		3.41	2.59	3.85	1.04					0.82
IprNH		5.74					3.81	1.16					x

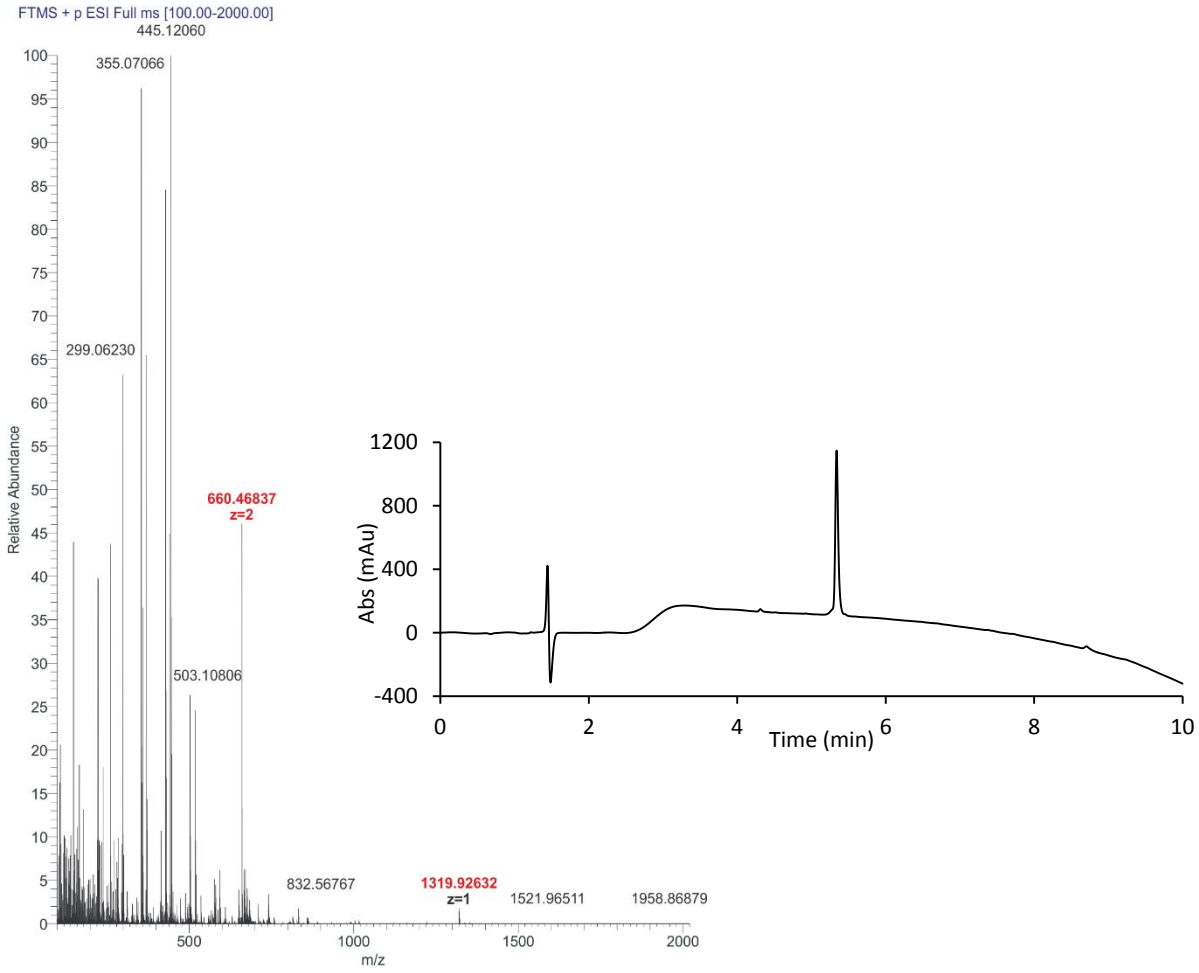

Figure S94. HRMS (ESI) spectrum and RP-HPLC chromatogram of **22** after purification (10-100% of B in 10 min, UV 200 nm).

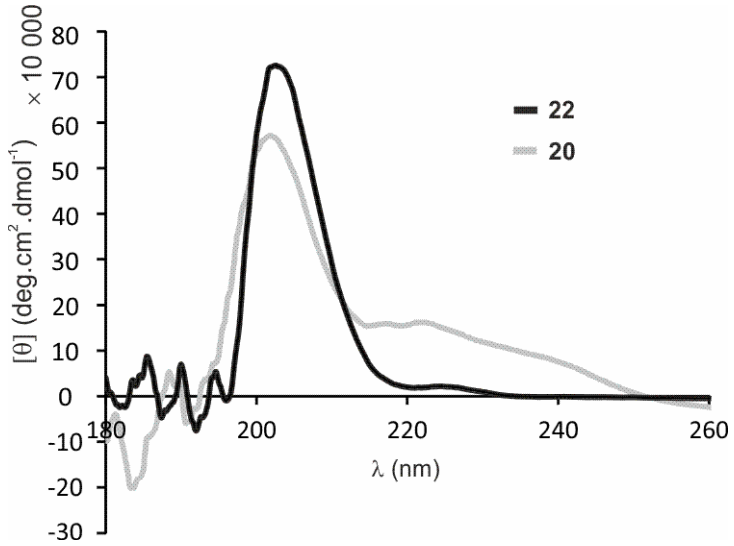

Figure S95. ECD spectra of oligomers **20** and **22** (spectra were recorded in TFE at 0.2 mM).

6. Study of backbone NH H/D exchange rates

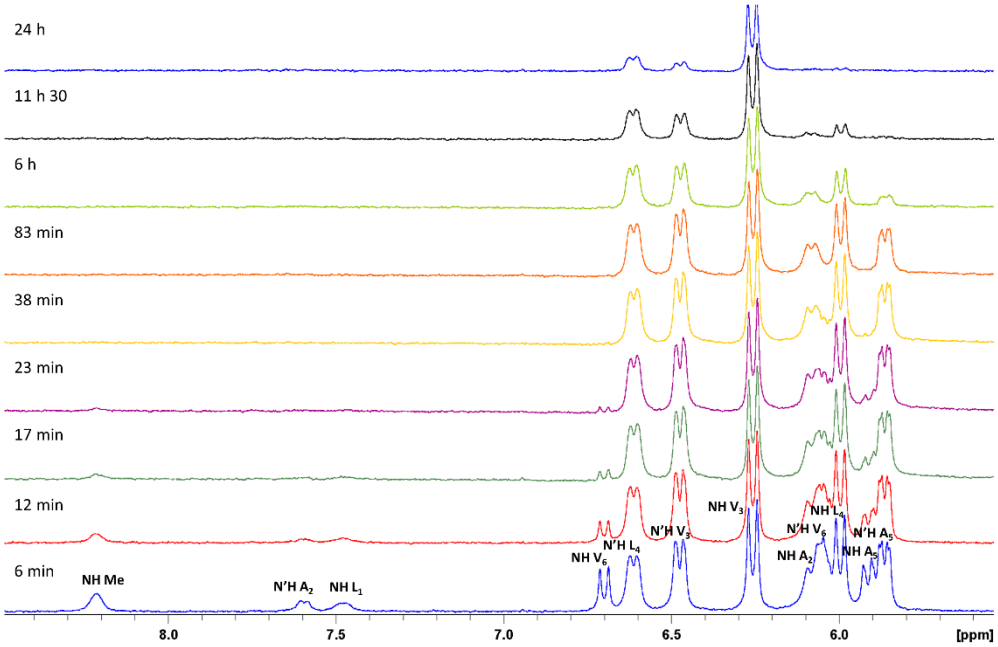

Figure S96. H/D exchange of backbone urea protons of hybrid oligo(thio)urea **4** (at 2.5 mM). The NMR spectra were recorded in CD_3OD (400 MHz) at 293 K.

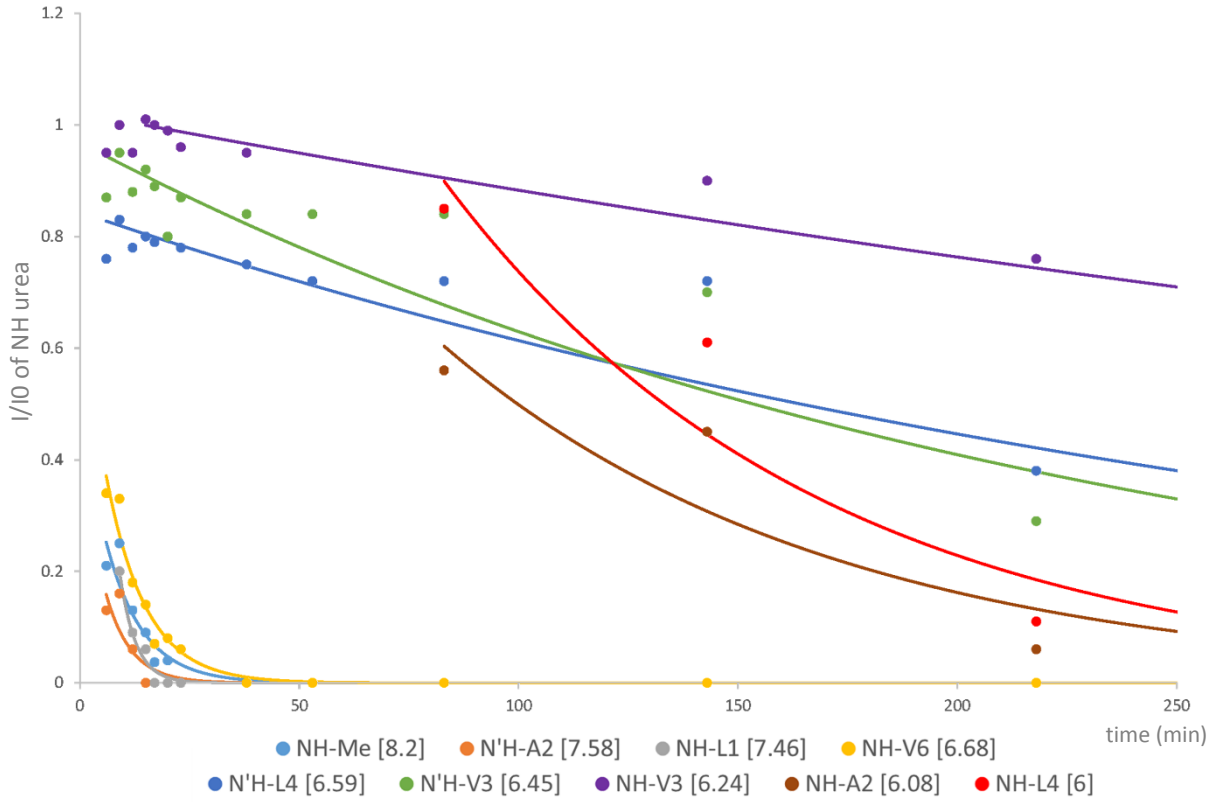

Figure S97. H/D **e**xchange curves of hybrid oligo(thio)urea **4** at 293K. The NMR spectra were recorded in CD_3OD (400 MHz) at 2.5 mM. Integration values (I) of NH peaks normalized over intensity of a non exchangeable proton (I0) were plotted as a function of time.

Table S10. Individual H/D exchange rate constants (k_{ex}) for urea/thiourea and amide NHs in hybrid oligomer **4** at 293K.

	δ (ppm)	k_{ex} x 10^{-3} (min^{-1})
NH-Me	8.20	120 ± 22
N'H-A2	7.58	173 ± 46
NH-L1	7.46	275 ± 27
NH-V6	6.68	111 ± 12
N'H-L4	6.59	3.2 ± 0.6
N'H-V3	6.45	4.3 ± 0.8
NH-V3	6.24	1.46 ± 0.19
NH-A2	6.08	11 ± 5
NH-L4	6.00	12 ± 4

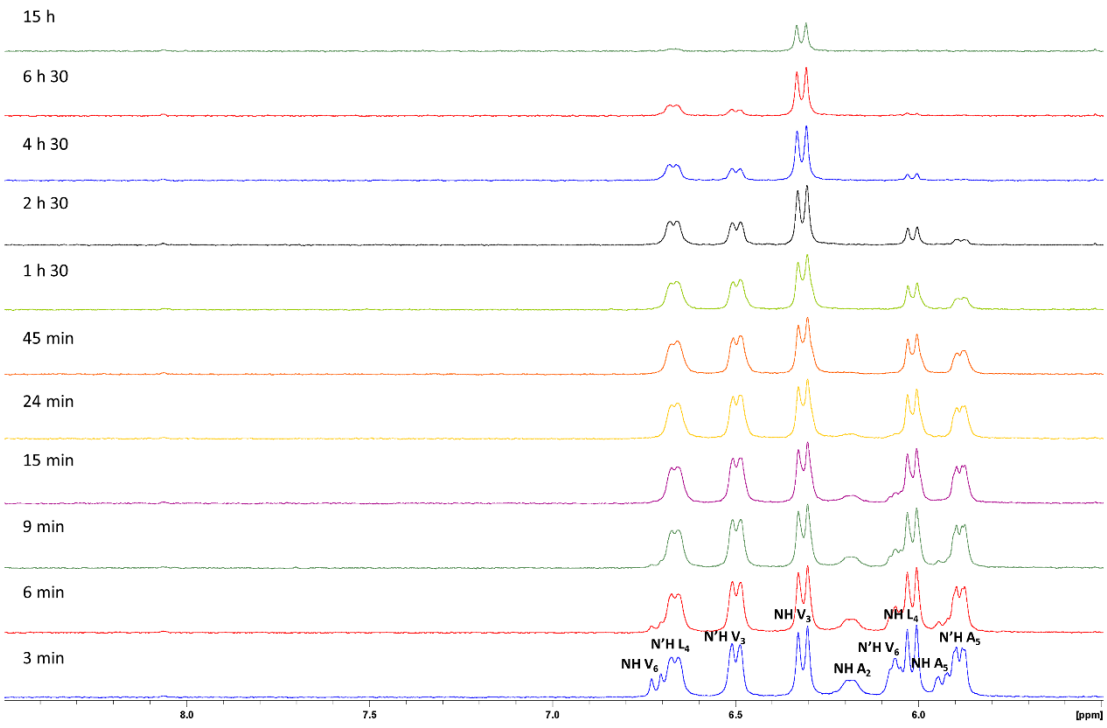

Figure S98. H/D exchange of backbone urea protons of oligomer **18** (at 2.5 mM). The NMR spectra were recorded in CD_3OD (400 MHz) at 293 K.

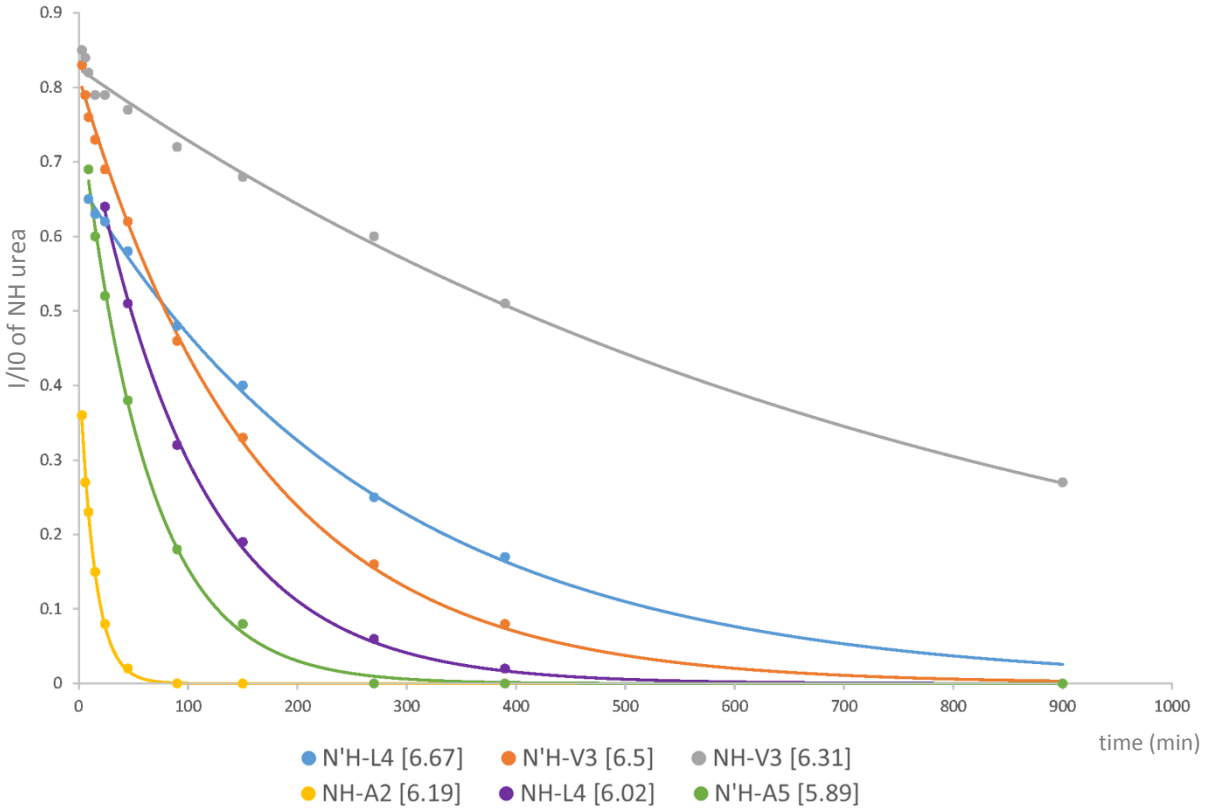

Figure S99. H/D exchange curves of oligomer **18** at 293K. The NMR spectra were recorded in CD_3OD (400 MHz) at 2.5 mM. Integration values (I) of NH peaks normalized over intensity of a non exchnageable proton (I0) were plotted as a function of time.

Table S11. Individual H/D exchange rate constants (k_{ex}) for urea NHs in oligomer **18** at 293K.

	δ (ppm)	k_{ex} x 10^{-3} (min^{-1})
N'H-L4	6.67	3.6 ± 0.12
N'H-V3	6.50	6.1 ± 0.17
NH-V3	6.31	1.25 ± 0.05
NH-A2	6.19	72 ± 2
NH-L4	6.02	9.9 ± 0.23
N'H-A5	5.89	16.2 ± 0.5